



Budapest University of Technology and Economics

Micromechanical deformation processes in polymer composites

Ph. D. Thesis

by

Károly Renner

Supervisor: Béla Pukánszky

Institute of Materials and Environmental Chemistry
Chemical Research Center
Hungarian Academy of Sciences

Laboratory of Plastics and Rubber Technology
Department of Physical Chemistry and Materials Science
Budapest University of Technology and Economics



2010



Contents

Chapter 1	5
INTRODUCTION	
1.1. Polymer composites	6
1.2.1. Modified polymers, types, benefits	6
1.2.2. Factors determining the properties of modified polymers	7
1.2.3. Mechanical properties	8
1.2.4. Layered silicate composites	10
1.2.5. Polymer/wood composites	12
1.3. Micromechanical deformation processes	14
1.3.1. Factors	14
1.3.2. Deformation mechanisms	15
1.3.3. Fiber related processes	18
1.3.4. Detection of micromechanical deformation processes	19
1.8. Scope	21
1.9. References	25
Chapter 2	29
ANALYSIS OF THE DEBONDING PROCESS IN POLYPROPYLENE MODEL COMPOSITES	
2.1. Introduction	29
2.2. Experimental	30
2.3. Results	30
2.3.1. Particle characteristics	30
2.3.2. Tensile characteristics	32
2.3.3. Acoustic emission	35
2.3.3. Debonding characteristics, process analysis	40
2.5. Conclusions	43
2.6. References	44
Chapter 3	45
MICROMECHANICAL DEFORMATION PROCESS IN PA/LAYERED SILICATE NANOCOMPOSITES: CORRELATION OF STRUCTURE AND PROPERTIES	
3.1. Introduction	45
3.2. Experimental	45
3.3. Results	47
3.3.1 Structure	47
3.3.2. Properties	52
3.3.3. Micromechanical deformations	54
3.3.4. Discussion, deformation mechanism	60

3.5. Conclusions	64
3.5. References	64

Chapter 4..... 67
DEFORMATION AND FAILURE OF WOOD FLOUR REINFORCED COMPOSITES; EFFECT OF INHERENT STRENGTH OF WOOD PARTICLES

4.1. Introduction	67
4.2. Experimental	67
4.3. Results and discussion.....	68
4.3.1. Particle characteristics	68
4.3.2. Composite properties, reinforcement.....	70
4.3.3. Micromechanical deformations	73
4.3.4. Discussion	79
4.5. Conclusions	81
4.6. References	81

Chapter 5..... 83
MICROMECHANICAL DEFORMATION PROCESSES IN PP/WOOD COMPOSITES: PARTICLE CHARACTERISTICS, ADHESION, MECHANISMS

5.1. Introduction	83
5.2. Experimental	83
5.3. Results.....	84
5.3.1. Particle characteristics	84
5.3.2. Properties, reinforcement.....	86
5.3.3. Micromechanical deformation processes.....	90
5.4. Consequences	96
5.5. Conclusions	98
5.6. References	98

Chapter 6..... 99
MICROMECHANICAL DEFORMATIONS IN PP/LIGNOCELLULOSIC FILLER COMPOSITES EFFECT OF MATRIX PROPERTIES

6.1. Introduction	99
6.2. Experimental	99
6.3. Results	100
6.3.1. Properties.....	100
6.3.2. Micromechanical deformations	103
6.3.3. Deformation and failure mechanisms	107
6.3.4. Consequences	111
6.4. Conclusions	112

6.6. References.....	113
Chapter 7	115
QUANTITATIVE DETERMINATION OF INTERFACIAL ADHESION IN COMPOSITES WITH STRONG BONDING	
7.1. Introduction.....	115
7.2. Experimental	115
7.3. Results and discussion.....	116
7.3.1. Approach	116
7.3.2. Determination of constants C_1, C_2	117
7.3.3. Strength of adhesion, surface modification	120
7.4. Conclusions.....	121
7.5. References.....	121
Chapter 8	123
SUMMARY	
LIST OF SYMBOLS	127
ACKNOWLEDGEMENT	128
PUBLICATIONS.....	129

Chapter 1

Introduction

In the past decades plastics became unnoticed an essential part of our everyday life. The number of application areas is increasing continuously and today it is almost impossible to design new products without plastic components. With the increasing number of applications the requirements for the raw materials increased as well. The aerospace industry is often mentioned as the most specific and demanding field, but similar, if not stricter conditions must be fulfilled by human implants, for example hip replacements. Because the number of industrially produced polymers is limited, progress would be impossible without modification. Modification usually improves some properties of the matrix polymer, but deteriorates others. Stiffness can be increased by the addition of particulate fillers, but tensile strength often decreases at the same time, which may create problems even in the case of such simple products as garden furniture. As a consequence, properties must be always optimized, that requires the thorough knowledge of structure-property correlation in all modified polymers.

Polymers can be modified in many ways. Copolymerization, grafting, or most polymer analogous reactions are usually complicated and economically not feasible for industrial applications. Another possibility of modification is offered by the addition of a second component to the matrix polymer. Depending on the type of modifier the heterogeneous polymers can be classified in several ways. Arbitrarily, we divide them into three categories: polymer blends, particulate filled polymers and fiber reinforced composites. Such modified polymers are typically used as structural materials. Commodity polymers are often modified with particulate fillers to achieve larger stiffness, while short or long fiber reinforcements are used when larger strength is needed. The introduction of a second component into the matrix polymer usually results in heterogeneous materials. As consequence, their structure is complicated; they consist of several phases and an interphase also forms between the phases. The behavior of modified polymers during loading is more complicated than that of homogeneous materials. In such composites stress concentration develops around the heterogeneities under the effect of external load. The induced actual stress distribution determines the local deformations around the inclusions and also the macroscopic properties of the composites. This Thesis discusses such micromechanical deformation processes in various heterogeneous polymers.

In the Department of Applied Polymer Chemistry and Physics at the Institute of Materials and Environmental Chemistry, HAS and the associated Laboratory of Plastics and Rubber Technology (LPRT) at the Budapest University of Technology and Economics heterogeneous polymer systems are investigated and developed for a long time. The group started with the study of particulate filled polymers and developed models describing various phenomena in these materials. A number of publications and industrial cooperations show the success of the group in this field. The investigated materials and problems changed considerably during the years. The focus of attention shifted towards multicomponent materials, carbon fiber reinforced thermosets and ther-

moplastics, and finally to layered silicate nanocomposites. Interfacial interactions are one of the most important factors determining the ultimate properties of composites. This Thesis is a further step in the line of research done in this area focusing on the factors determining deformation processes and their effect on the final properties of composites.

1.1. Polymer composites

As mentioned above, polymers are often modified to achieve new properties, to increase stiffness, strength, impact resistance or all at the same time. Creating new polymers through synthesis requires more time and larger investment than through physical modification, through the mixing of existing polymers with one or more other components. We discuss modified polymers according to the categories mentioned above, i.e. particulate filled polymers, polymer blends and fiber reinforced composites.

1.2.1 *Modified polymers, types, benefits*

In further discussion we do not mention polymer blends consisting of a matrix polymer and another polymer or an elastomer, but focus only on particulate filled and fiber reinforced polymers. Traditional particulate filled polymers are used in very large quantities in all kinds of applications in spite of the interest in new materials. The total consumption of fillers in Europe alone is currently estimated as 4.8 million tons (Table 1) [1], while GE used about 270 tons of nanocomposite material in 2004, which included the polymer as well [2]. In spite of the large quantities used, recently the interest shifted from traditional fillers towards new materials like nanocomposites, biomaterials and natural fiber reinforcements. One reason for the changing focus of interest and increased research activity lays in the changed role of fillers and reinforcements. In the early days fillers were added to the polymer to decrease price. However, the ever increasing technical and aesthetical requirements as well as soaring material and compounding costs require the utilization of all possible advantages of fillers, reinforcement and other modifiers. Fillers and reinforcements increase stiffness and heat deflection temperature, decrease shrinkage and improve the appearance of the composites [1,3,4]. Productivity can be also increased in most processing technologies due to decreased specific heat and increased heat conductivity [1,3,5,6]. Fillers are very often introduced into the polymer to create new functional properties not possessed by the matrix at all like flame retardancy or conductivity [7-9]. Another reason for the considerable research activity is that new fillers and reinforcements emerge continuously among others layered silicates [10-14], wood flour [15-19], sepiolite [20-24], etc. We must call the attention here to the fact that the transition between traditional, nearly spherical particulate fillers, fillers with platelet geometry and short as well as long fibers is continuous and properties are determined by the same factors and rules in all of their composites. In this thesis we focus our attention onto two of the new reinforcements, i.e. on layered silicates and natural fillers, or more exactly lignocellulosic fibers.

The properties of all heterogeneous polymer systems are determined by the same four factors: component properties, composition, structure and interfacial interactions [1, 25]. Although certain fillers and reinforcements including layered silicates,

other nanofillers, or natural fibers possess special characteristics, the effect of these four factors is universal and valid for all modified polymers. As a consequence, in this thesis we focus our attention on these factors and particularly on interfacial interactions and structure. Unlike many others, we believe that the general rules of heterogeneous materials apply also for nano- and wood reinforced composites, we use these general rules to interpret the phenomena encountered during our research and discuss composite properties according to them.

1.2.2. *Factors determining the properties of modified polymers*

All four factors mentioned in the previous section are equally important in influencing composite properties and they must be adjusted to achieve optimum performance and economics.

Component properties. The characteristics of the matrix strongly influence the effect of the filler or reinforcement on composite properties. The reinforcing effect of the filler increases with decreasing matrix stiffness. True reinforcement takes place in elastomers, both stiffness and strength increases [26]. In weak matrices the filler carries a significant part of the load, it reinforces the polymer. Numerous filler characteristics influence the properties of composites [27,28]. Chemical composition and purity, particle characteristics, surface free energy, hardness and other properties all affect composite properties in smaller or larger extent. Particle characteristics have increased significance in wood flour reinforced composites, they can modify the mechanism of deformation and failure thus determining the final properties of the composite.

Composition. Composition, i.e. the filler content of composites may change in a wide range. The range is very narrow in nanocomposites, maximum filler content is around 10 wt%, while the amount of reinforcement can be as large as 70 wt% in wood flour filled composites. The various factors determining composite properties are inter-related, the same property may change in a different direction as a function of matrix characteristics, or interfacial adhesion. The goal of the use of fillers and reinforcements is to improve properties, e.g. stiffness, dimensional stability, etc. These goals require the introduction of the largest possible amount of filler into the polymer, but the improvement of the targeted property may be accompanied by the deterioration of others. Since various properties depend in a different way on filler content, composite properties must be always determined as a function of composition.

Structure. The structure of particulate filled polymers seems to be simple, the homogeneous distribution of particles in the polymer matrix is assumed in most cases. This, however rarely occurs and often special, particle related structures develop in the composites. The most important of these are aggregation and the orientation of anisotropic filler particles. Structure is more complicated and its role is more important in nanocomposites. Several structural entities may prevail simultaneously in these materials and their relative amount affects properties significantly.

Interfacial interactions. Particle/particle interactions induce aggregation, while matrix/filler interaction leads to the development of an interphase with properties

different from those of both components. Secondary, van der Waals forces play a crucial role in the development of both kinds of interactions. They are usually modified by the surface treatment of the filler. Reactive treatment, i.e. coupling, is also used occasionally, although its importance is smaller in thermoplastics than in thermoset matrices. The reinforcements studied in this Thesis are very different in this respect. Wood has very low surface free energy and coupling is needed to achieve acceptable properties. On the other hand, the surface energy of layered silicates is large, but they are organophilized that decreases surface tension. Contradictory information is published in the literature about the effect of organophilization on interaction and properties, some sources claim improved “compatibility” [3, 29] while others say that interaction decreases as an effect of the treatment [30].

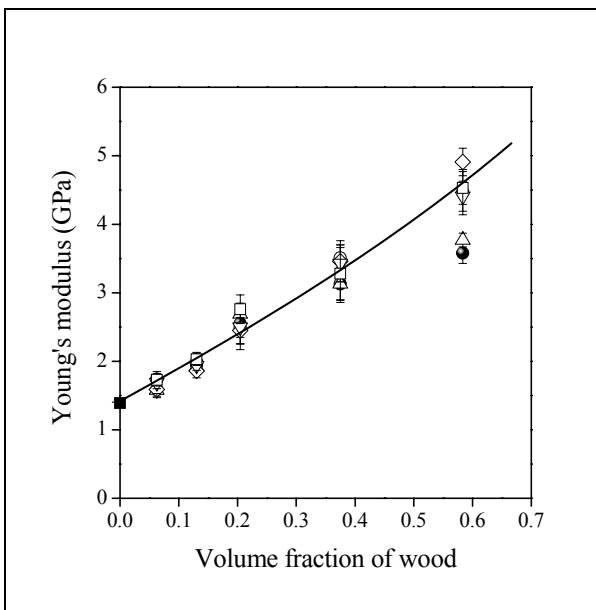


Fig. 1.1 Effect of wood content and the amount of MAPP on the stiffness of PP/wood composites. MAPP/wood ratio: (●) 0, (○) 0.05, (△) 0.10, (◇) 0.15, (▽) 0.20, (□) 0.25; (■) PP.

1.2.3. Mechanical properties

The focus of this thesis is on micromechanical deformations and their relationship with failure processes and final composite properties. Accordingly, mechanical properties and the factors influencing them are of utmost importance of us. Modulus is often the preferred property to study, since it is easy to measure and model. Unfortunately, modulus is not very sensitive to the factors listed above, it does not change much with interaction and even structure has limited influence on it. This statement is strongly supported by Fig. 1 showing the composition dependence of PP/wood composites con-

taining different amounts of maleated PP (MAPP) coupling agent¹. This functionalized polymer reacts chemically with the surface of wood particles and enhances stress transfer through interdiffusion with the matrix polymer. Modulus is practically the same independently of the presence or amount of the coupling agent.

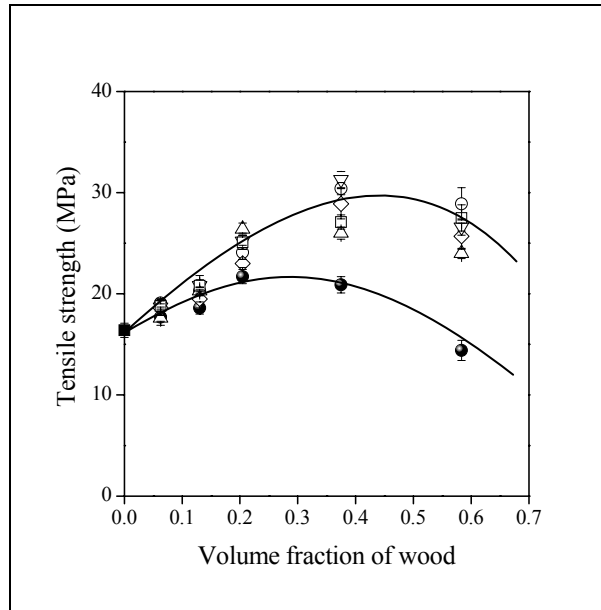


Fig. 1.2 *Dependence of the tensile strength of PP/wood composites on filler content and on the relative amount of MAPP and wood. Symbols are the same as in Fig. 1.1.*

On the other hand, properties measured at larger deformations, i.e. yield stress and tensile strength indicate changes in interaction very sensitively as proved by Fig. 1.2, in which the tensile strength of the same composites is plotted against composition. The effect of coupling is clearly seen in the figure, composites containing the functionalized polymer are stronger than those prepared without it. Moreover, the figure shows very well also the effect of structure, the decrease in strength at large wood content results from particle-particle interactions. In spite of the large size and low surface energy of wood particles, mere physical contact caused by their large amount leads to the deterioration of properties. Hardly any sign of this effect can be observed in Fig. 1.1. As a consequence, in this Thesis we pay our attention to properties measured at large deformations. Most of the experiments is done in tensile, but the traditional technique will be supplemented with methods which give further information about micromechanical deformation processes occurring around particles. Our attention is directed mainly to these processes; various fillers and reinforcements were used to study them. Because of

¹Dányádi, L., Renner, K., Szabó, Z., Nagy, G., Móczó, J., Pukánszky, B., *Polym Adv Technol* **17**(11-12), 967-974 (2006)

their novelty and the enhanced interest in them, we discuss layered silicates and wood flour somewhat more in detail in the next two sections.

1.2.4. Layered silicate composites

The interest in nanotechnology has been increasing continuously in recent years and it includes all kinds of polymer composites containing nano-sized fillers or reinforcements [3]. Layered silicate nanocomposites are one class of these materials containing finely dispersed silicate particles [3,21-24]. The original idea leading to the preparation of these composites assumes that clay particles break down, or exfoliate into individual silicate platelets thus creating very large interfaces and unique properties. The specific surface area of completely exfoliated montmorillonite is around 750 m²/g [31-33]. Accordingly, extensive exfoliation is a primary condition of the preparation of layered silicate nanocomposites with acceptable properties [34-39]. However, large degree of exfoliation is difficult to achieve and the structure formed is usually much more complicated than that of the traditional particulate filled microcomposites. Particle structure of the silicate, gallery structure, exfoliation and the formation of a silicate network must be considered in nanocomposites², but some of these structural formations, as well as their effect on properties are largely neglected in most studies.

The existence of original clay particles, either uncoated sodium montmorillonite (NaMMT), or organophilized silicate, is hardly ever mentioned in studies on nanocomposites. One may deduce from this fact that particles are not present in the composites; i.e. they break down to smaller units, into intercalated stacks or to individual platelets during mixing. This is not very surprising since mostly XRD and transmission electron microscopy (TEM) are used for the characterization of the composites and those do not necessarily detect large particles. However, SEM micrographs usually show the presence of large silicate particles in spite of the fact that the silicate reflection does not appear in the WAXS pattern of the composite. In the process of nanocomposite preparation solvated inorganic cations located in the galleries of layered silicates are exchanged to organic cations of long chain amines in order to separate the layers [30,40]. Increased gallery distance and decreased surface energy should lead to easier exfoliation. As a consequence, the amount of surfactants located in the galleries and the orientation of the molecules should influence significantly the structure and properties of layered silicate/polymer nanocomposites [41]. The gallery structure of organophilic silicate depends on the chemical structure and amount of the surfactant used for treatment and on the ion exchange capacity of the clay. Contradictory information published about the effect of surfactant structure on exfoliation clearly proves that unambiguous, general correlations have not been established yet among the gallery structure of the silicate, interactions and composite properties. The extent of exfoliation is usually studied by TEM, which is able to detect also individual silicate layers [42, 43]. However, usually intercalated stacks or particles with a range of gallery distances form in the composites and such particles appear in the micrographs as shown in Fig. 3. "Very good" composites with a high degree of dispersion may contain stacks of silicates with 3 to 10 layers [34, 44], but this can be achieved only with the proper selection of components and

² Dominkovics, Z., Renner, K., Pukánszky, B.Jr., Pukánszky, B., *Macromol Symp* **267**, 52-56 (2008)

processing conditions. Unfortunately, structures observed in the TEM micrographs depend on composition, but also on sampling, i.e. on the choice of location from which the slice is taken thus it is rather dangerous to draw general conclusions about the extent of exfoliation from TEM micrographs. At large silicate content and large extent of exfoliation silicate platelets may interact with each other. Face-to-face interaction leads to aggregation, while edge-to-face orientation results in the formation of a silicate network structure. The conditions of network formation and the effect of the network on composites properties are not known at the moment.

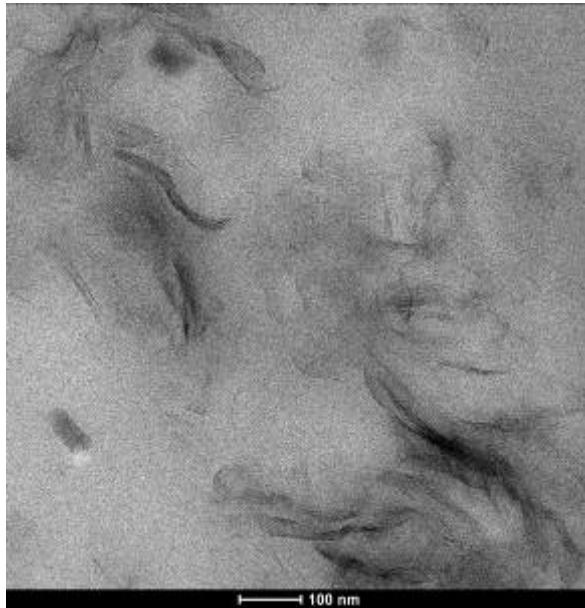


Fig. 1.3 *Various structural entities in a PA/layered silicate composite.*

One of the main benefits of layered silicate nanocomposites is claimed to be strong reinforcement at extremely small filler content. The basic conditions for reinforcement are a large extent of exfoliation and good interfacial adhesion between the components. Unfortunately both the extent of exfoliation and reinforcement are difficult to determine quantitatively and they are rarely discussed in publications. The use of a simple model developed for the prediction of the composition dependence of tensile yield stress and strength of particulate filled polymers allowed the determination of the load carried by the silicate, i.e. the extent of reinforcement [45, 46]. Rather surprisingly, an analysis of available data published in the open literature yielded relatively small extent of reinforcement even in PA composites, in spite of the fact that exfoliation is the easiest in this polymer. Using the parameter expressing reinforcement quantitatively and some simple assumptions, the extent of exfoliation was estimated to be approximately 12 % with the formation of stacks containing approximately 10 silicate layers in the average. This result agrees well with the experience that complete exfoliation is very difficult to achieve and nanocomposites always contain different structural formations

including individual silicate platelets, intercalated stacks, but sometimes even large particles. The question remains: which structural units determine final properties and in what extent. One of the goals of our study was to investigate this issue somewhat more in detail.

Table 1 *World production of natural fibers [47]*

Fiber	Source	Production (1000 t)
Wood	stem	1750000
Bamboo	stem	10000
Cotton lint	fruit	18450
Jute	stem	2300
Kenaf	stem	970
Flax	stem	830
Sisal	leaf	378
Hemp	stem	214
Coir	fruit	100
Ramie	stem	100
Abaca	leaf	70

1.2.5. Polymer/wood composites

The preparation and use of polymers containing natural fillers or reinforcements is not new in the plastic industry, but these materials went through a revival in recent years all over the world. Composites containing lignocellulosic components are known since the 1900-ies, especially in the building and furniture industry. Already in 1916 Rolls Royce used a phenol-formaldehyde resin/wood composite for the production of the knob of its gear lever. The various wood-fiber, laminated and MDF boards are prepared from phenol-formaldehyde, urea-formaldehyde and melamine-formaldehyde resins.

After recognizing the advantages of natural fillers and fibers, more and more research groups started to work on the replacement of glass and carbon fibers in composites and to study natural fiber reinforced unsaturated polyester, epoxy and novolac composites. In recent years, increasing quantities of thermoplastic polymers were used as matrix materials in wood/plastic composites (WPC). One of the main advantages of these materials is that products can be manufactured with traditional thermoplastic processing technologies for a wide range of applications. The production of various natural

fibers is shown in Table 1 [47]. The largest amount is produced from wood, more than 10000 species are known. Due to geographical conditions, i.e. large quantities of primary wood raw material as well as byproducts, wood composites are used in the building industry as decking mainly in North America. Europe is behind the US and Canada in the application of natural fiber reinforced plastics. Hemp, flax and jute are more often used here as natural reinforcements mostly in the automotive industry, since wood based raw materials, as well as wood waste are available in smaller quantities.

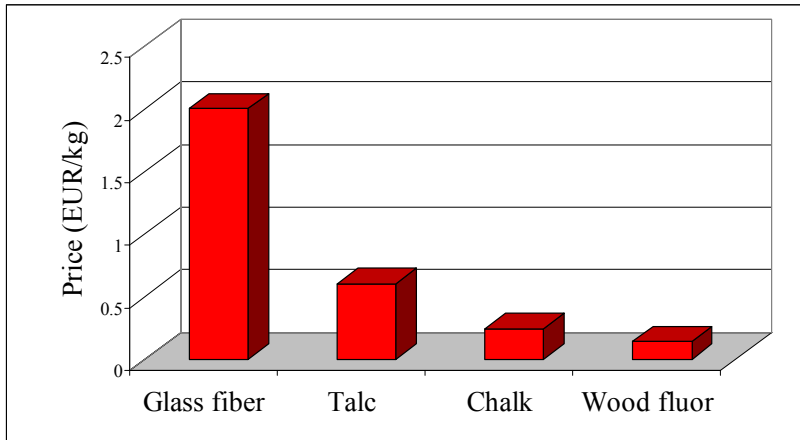


Fig. 1.4 Price of various fillers and reinforcements

Natural reinforcements possess numerous advantages. They are available in large quantities and their price is low compared to traditional reinforcements and competes even with mineral fillers (see Fig. 1.4.). They have large stiffness and strength, as well as low density. They are produced from renewable resources, often as byproducts. They can degrade biologically and the waste can be handled easily. The use of natural reinforcements may replace both plastics and wood. On the other hand, they have a few disadvantages as well. These reinforcements are sensitive to humidity and heat, they have poor transverse strength and very poor adhesion to the matrix due to their low surface energy. Some of these weaknesses will be addressed in this thesis in order to learn ways to produce better composites.

The largest part of polymer wood/composites is produced from commodity polymers. PP and PE are the cheapest polymers used in large quantities. On the other hand, their adhesion to other substances is extremely poor due to their small surface energy. Moreover, the usually large size of wood particles leads to poor properties as shown also by Fig. 1.2; coupling is needed to achieve reasonable strength. The study of the effect of matrix/filler adhesion in PP/wood composites indicated that the separation of the matrix and the filler, i.e. debonding was the dominating deformation mechanism in the absence of a coupling agent and this process led to the failure of the composites. On the other hand, the mechanism of deformation changed with increasing adhesion and the results indicated that depending on component properties and composition even the

fracture of the fibers may occur during failure³ (Fig. 1.5). The observations indicated that one way to improve composite properties is to increase its inherent strength or to decrease the probability of fiber fracture, which can be achieved in several ways. One of the goals of this thesis was to explore these possibilities, but in order to achieve these goals we needed more information about the processes leading to the failure of the composites. We hoped that the study of micromechanical deformation processes may supply this information thus we used acoustic emission measurements extensively for this purpose.

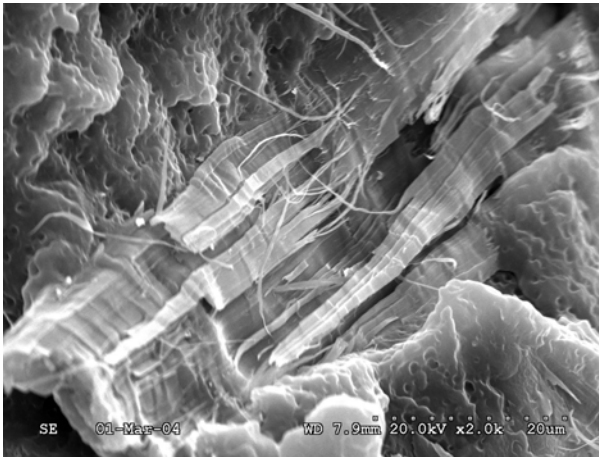


Fig. 1.5 *Fracture of a wood particle during the failure of a PP/wood composite with good adhesion between the fiber and the matrix.*

1.3. Micromechanical deformation processes

The introduction of fillers or reinforcements into a polymer matrix results in a heterogeneous system. Under the effect of external load heterogeneities induce stress concentration, the magnitude of which depends on the geometry of the inclusions, on the elastic properties of the components and on interfacial adhesion [48,49]. Heterogeneous stress distribution and local stress maximums initiate local micromechanical deformations, which determine the deformation and failure behavior, as well as the overall performance of the composites.

1.3.1. Factors

Stress concentration and local stress distribution can be estimated by the use of theoretical models or by finite element analysis [50-52]. The interacting stress fields of neighboring particles are very complicated and change with composition thus simplifying assumptions are used; Goodier [48] assumed the embedding of a single, spherical particle into an infinite matrix, as well as the continuity of stresses and displacements

³ Dányádi, L., Renner, K., Móczó, J., Pukánszky, B., *Polym Eng Sci* **47**(8), 1246-1255 (2007)

across the interface. The magnitude of stress concentration depends mainly on the elastic constants of the components. In the case of anisotropic particles significantly larger stress concentrations can be developed than in composites containing spherical particles. In tension, stresses about twice the average stress develop at the pole of hard spherical particles, while soft inclusions induce maximum stress concentration around their equator.

Micromechanical deformation processes initiated by local stress maxima around the particles are influenced also by thermal stresses induced by the different thermal expansion coefficients of the components, crystallization, or shrinkage during the curing of thermoset matrices [53,54]. Besides the thermal expansion coefficients of the components, the magnitude of thermal stresses depends also on their elastic properties and on the temperature range in which the stresses develop [51,55,56]. Thermal stresses decrease the radial stress component, but increase stress concentration in the tangential direction [56].

Another factor which must be taken into account during the analysis of micromechanical deformation processes is the interaction of the components [49,56-59]. Interactions can vary in a wide range both in character and strength. Adhesive interactions created by secondary forces are relatively weak and they can be expressed quantitatively by the reversible work of adhesion. Coupling may result in covalent bonding between the components. In such cases the quantitative prediction of the strength of interaction is difficult as well as for other interaction mechanisms like interdiffusion [60]. Although the importance of inhomogeneous stress distribution developing in particulate filled composites is pointed out in numerous publications, the exact role of stress concentration is not completely clear and contradictory information is published claiming either its beneficial [61], neutral [62] or detrimental effect on properties [63,64].

1.3.2. Deformation mechanisms

Micromechanical deformation mechanisms are competitive processes and the dominating one depends on material properties and loading conditions. Attempts were made to define the initiation conditions for most of them, but these attempts were not equally successful. One of the most frequent micromechanical deformation mechanism is **shear yielding**. It takes place both in amorphous and crystalline polymers and it includes the slipping of larger structural units. The most often used condition for this mechanism was defined by von Mises [52,65-67]. The analysis shows that in the case of stiff particles shear yielding is initiated at around 45° at the surface of the particle, a result corroborated also by experimental data at least in glassy, amorphous polymers [68,69]. **Crazing** was observed in a number of polymers including PS, PP and others. The most often used condition for crazing was given by Sternstein and Ongchin [70] who expressed the criterion in terms of a stress bias, and a similar approach was used by Oxborow and Bowden [52,65-67]. Another micromechanical deformation process occurring in impact modified polymers is **cavitation**. The large negative hydrostatic pressure developing during the deformation of polymers containing dispersed elastomeric particles tears these latter apart. The process results in the formation of voids and vol-

ume increase, and it was studied by Bucknall, who determined also the conditions of initiation [71].

The most frequent micromechanical deformation mechanism is **debonding** in particle filled polymers and sometimes also in polymer blends. If the adhesion between the polymer matrix and the filler is weak, the separation of the interface occurs under the effect of external load (see Fig. 1.6.). In tension, debonding occurs at the pole in composites containing hard particles, because stress concentration is the largest there. After reaching initiation stress the contact between the polymer and the particle is broken, a crack or void is formed, which proceeds towards the equator. Initiation stress is determined by thermal stresses, particle size and by the interfacial adhesion between the two components. Debonding stress decreases with increasing particle size, while strong interfacial adhesion prevents the separation of interfaces. Large particles and weak interaction result in debonding at very small external load. Large voids form by debonding in this case, which merge to cracks leading to rapid, catastrophic failure of the part.

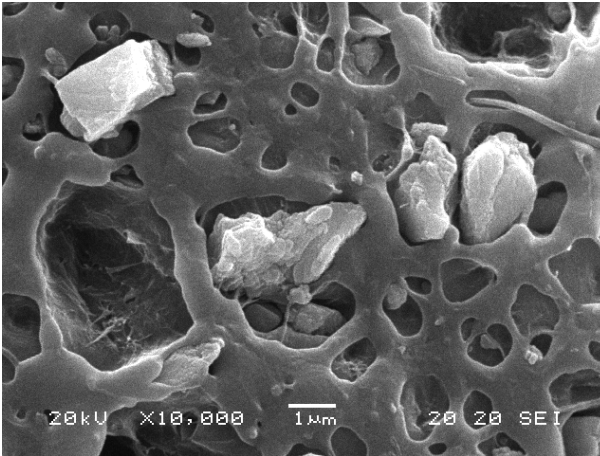


Fig. 1.6 *Debonding in CaCO_3 filled polypropylene [59].*

Because of the importance of debonding in particulate filled composites, several research groups studied its various aspects. In his early experiments Farris [72] investigated debonding in filled, cross-linked elastomers. He found that practically all particles debond at large deformations and that the volume increase caused by debonding is proportional to the volume fraction of the filler. He did not give any information about the factors influencing the stress necessary to initiate debonding.

Vollenberg and Heikens [51,73] studied debonding in PS and PP composites filled with glass beads by volume strain measurements. They created a model for debonding which relates debonding stress (s_d) to particle size and interfacial adhesion

$$s_d = \frac{s_T}{a} + \frac{K}{a} \left(\frac{AE}{r} \right)^{1/2} \quad (1.1)$$

where s_T is thermal stress, A is interfacial adhesion, E is the Young's modulus of the

matrix and r is the radius of the particles. In their equation a is a stress concentration factor, while the value of constant K depends on material properties, mainly on the elastic characteristics of the components. The authors assumed that constant stress acts at the pole of the particle down to a 25° area towards the equator and that debonding occurs instantaneously in this entire region. The first assumption is probably not valid, but the values of a and K are not known either, thus s_d cannot be predicted from the properties of the components. Using similar energy considerations as Vollenberg and Heikens [51,73], but without the assumptions made by those authors, Vörös and Pukánzsky [50] developed another model for the prediction of debonding stress with the following result

$$\sigma^D = -C_1 \sigma^T + C_2 \left(\frac{W_{AB} E}{R} \right)^{1/2} \quad (1.2)$$

where σ^D and σ^T are debonding and the thermal stresses, respectively, W_{AB} is the reversible work of adhesion and R denotes the radius of the particle. C_1 and C_2 are constants which have exact physical meaning; their values depend on the geometry of the debonding process and on the propagation of the crack along the surface of the particles. Although Eq. 1.2 was derived without the assumptions of Vollenberg and Heikens [51,73], the values of the geometric constants are not known and cannot be determined in a simple way, thus the absolute value of σ^D cannot be predicted with Eq. 1.2 either.

Because of the difficulties related to the determination of the constants of Eqs. 1.1 and 1.2, the critical stress or deformation initiating debonding cannot be determined on a theoretical basis. Based on volume strain measurements van Es et al. [58] claimed that debonding occurs at the maximum of the stress vs. strain curve, i.e. at yielding (σ_y). Several groups [74-77] criticized this statement and claimed that debonding occurs at a lower stress, before reaching σ_y . Their argument was based on the analysis of tensile stress vs. deformation traces and they assigned debonding to the deviation of the curves from linearity, similarly to Vollenberg and Heikens [51,73]. Unfortunately the exact identification of the stress, or deformation, which initiates debonding, is rather arbitrary and often very uncertain on this basis. Moreover, the references cited above [51,73,74-77] do not offer any additional evidence that debonding really occurs at the specific stress or strain selected on the stress vs. strain trace. The detection of debonding is further complicated by the fact that commercial fillers have a broad particle size distribution. If Eqs. 1.1 and 1.2 are correct, and some experimental evidence indicates that they are [51,58,73], debonding stress depends on the particle size of the filler. Particles with different sizes debond at dissimilar stresses covering a wide range, when fillers with a broad particle size distribution are used. The assignment of debonding to a definite stress or deformation is difficult and needs further attention.

1.3.3. Fiber related processes

The most frequent micromechanical deformation processes were discussed in the previous section. However, several additional, fiber related processes, like fiber breakage, pull-out, buckling, etc. may also take place in short and long fiber reinforced

composites. Quite a few of these can be observed also in wood fiber reinforced polymers or layered silicate nanocomposites as well. In order to prepare nanocomposites the polymer is usually homogenized with a silicate having a relatively large average particle size, usually in the range of 2 to 30 μm , or even larger. Depending on the conditions of mixing these particles may break down to individual platelets, but there is a good chance that several structural units with widely differing length scales are simultaneously present in the composite [78-80]. Besides platelets, intercalated structures or tactoids are observed occasionally, but original clay particles or their aggregates might be also present in the final product. Larger extent of exfoliation is often accompanied by the formation of a silicate network as observed in several polymer matrices [78,81-83]. Although the formation of a complex structure is seldom mentioned in relation with PA6 nanocomposites, we must assume the existence of various structural entities when we consider possible deformation mechanisms.

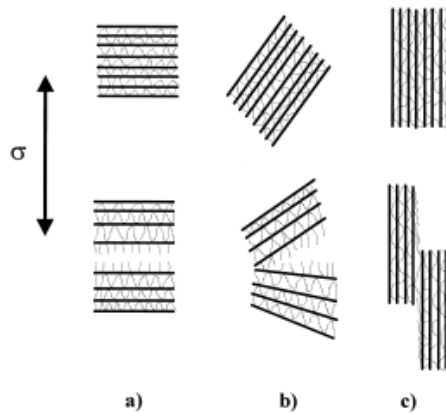


Fig. 1.7 Possible deformation of silicate layers: a) fracture of particles or tactoids; b) peeling off the layers; c) slipping of individual layers [85].

The deformation of such composites may be dominated either by that of the matrix or by processes related to the silicate reinforcement. The possibilities for the deformation of the matrix are relatively few and simple. The polymer may deform by shear yielding, but its cracking or fracture may also take place. Voiding was shown to occur during the deformation of neat polyamide [84]. Much larger is the number of possible deformation processes related to the silicate. According to Kim et al. [85] fracture or peeling off the silicate layers and the slipping of individual layers or stacks may occur during deformation depending on the direction of the load as indicated on Fig. 1.7.

If we allow also the presence of larger entities, and this is definitely the case when NaMMT is used as filler, debonding of the silicate and the matrix must be also considered as a possible deformation mechanism. Basically all silicate related processes

depend on interaction, both on the forces acting among the layers and on matrix/filler adhesion. As a consequence, the quality of organophilization, i.e. the type and amount of the surfactant used, is expected to influence the mechanism of deformation and the properties of the composites considerably.

Many attempts have been made to improve the properties of natural fiber reinforced polymers. As indicated before, numerous factors influence the mechanical properties of such composites. Several reports are available on the effect of wood type [86-88], but it is still unclear if the use of soft or hard wood results in composites with better properties. Increasing the aspect ratio of the fibers increases both stiffness and strength, and the role as well as importance of orientation becomes more pronounced as anisotropy increases. The extent of reinforcement increases with anisotropy, but the effect of coupling becomes less pronounced as the aspect ratio of the filler increases. While the effect of wood characteristics and interfacial adhesion on composite properties has been studied extensively [89-94], much less attention has been paid to the influence of matrix characteristics [26, 95]. Obviously all of these are important factors which influence mechanical properties by the modification of the mechanism of micromechanical deformation processes. Despite the importance of these questions the number of publication in this field is relatively small. Dogossy and Czigány [96] investigated maize hull filled polyethylene composites with acoustic emission and identified three different processes similarly to fiber reinforced polymers: matrix deformation, pull out of the maize hull and maize hull breakage. Romhány et al. [97,98] used the same method on flax fibers and their composites. They showed that an AE range of amplitudes can be assigned to identify three failure mechanisms of single fibers: longitudinal splitting of the pectin boundary layer among the elementary fibres; transverse cracking of the elementary fibre; fracture of elementary fibers and their microfibrils. They compared the deformation mechanism of a single fiber with that of the composite and showed similar processes to those observed in single fiber tests. Kocsis [99] analyzed the debonding process in wood flour filled polypropylenes, and showed different dominant mechanisms depending on composition. Debonding is accompanied by large number of acoustic signals at lower wood content. At higher wood fiber contents the slipping of the wood fiber aggregates and the debonding of fibers may appear simultaneously, and it is supposed to be the reason for the two local maxima in the acoustic emission count distribution.

1.3.4. Detection of micromechanical deformation processes

Relatively few methods are available for the detection and study of micromechanical deformation processes. Moreover, none of them is very easy to execute and/or only limited information is obtained by some methods. Probably that is one of the reasons but relatively few papers are published in the literature in this area. One of the oldest techniques used for the study of micromechanical deformations is the measurement of **volume strain**. Debonding, crazing and cavitation result in an increase of specimen volume during deformation. The separation of matrix/filler interface leads to the formation of voids which will grow during further elongation. The continuous measurement of sample volume makes possible to follow deformation processes accompanied by volume increase. The first solutions for the measurement of volume strain were

based on the determination of pressure changes in an isolated vessel containing the specimen, but perfect sealing was difficult to achieve with the simultaneous measurement of the load. The recording of changes in the thickness and width of the specimen during deformation made the determination of volume strain easier, but not always reliable. In this approach volume strain is determined by the measurement of the changes in one lateral dimension of the specimen by a strain transducer. The drawback of the method is that the transducer exerts additional stress on the sample, that influences neck formation and the yielding of the material. The use of optical extensometers eliminates this problem. Lefebvre [100,101] introduced this system for glass fiber reinforced polymers and G'Shel [102] extended the method to layered silicate composites.

Another approach to follow debonding is the **determination of the fraction of debonded particles** as a function of deformation. The model described by Eq. 1.2 was developed by using certain assumptions, which are not always fulfilled in practice. Debonding stress was derived for a single particle embedded in an infinite matrix. However, the particle size distribution of commercial fillers is relatively wide, large particles debond easily, while small ones remain strongly attached to the matrix, i.e. only a fraction of the particles separate from the matrix and create voids. The fraction of debonded particles can be estimated by the determination of the modulus of pretrained specimens as proposed by Hartingsveldt [103]. Móczó et al. [59] used this method to determine the extent of debonding in CaCO_3 filled polyethylene composites and found that the amount of debonded filler increases with increasing matrix modulus.

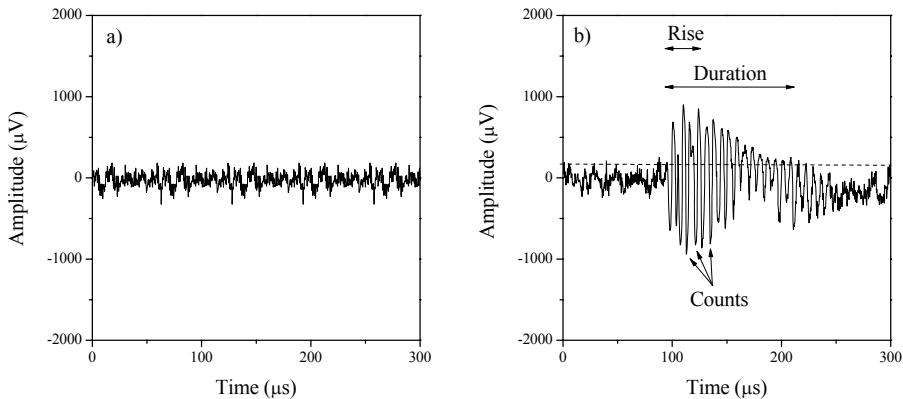


Fig. 1.8 Continuous (a) and burst-like (b) acoustic emission signals.

Acoustic emission (AE) is used to evaluate micromechanical deformation processes in heterogeneous polymers more and more frequently. The term acoustic emission describes both the technique and the phenomenon upon which the technique is based. The phenomenon is simple: if energy is released suddenly in the material, some of it is dissipated in the form of elastic waves. Basically two types of AE signals can be

distinguished: continuous and burst like emissions (Fig. 1.8). The source of the two types is different, continuous signals appear from dislocation motion or grinding. More important for us are burst like signals, which are emitted by sudden events like micro-mechanical deformations.

Several parameters of the burst event help to identify the source of acoustic emission. The events are usually characterized by a number of parameters: duration, rise time, amplitude, counts and frequency (counts/duration). In fiber reinforced polymers the frequency and the amplitude of the signal are used to identify consecutive processes [104-106]. This approach cannot be used in particle filled polymers, because the deformation processes emit signals with much lower amplitudes, thus even the detection of the event is complicated. Only a few groups investigated particulate filled polymers with acoustic emission [107-110]. Josef Kaiser [111] was the first who claimed that technical materials emit sound under loading. Recently the development of acoustic emission techniques allowed the investigation of not only metals and alloys, but also of polymeric materials. Czigány et al. [104,112] used acoustic emission on fiber reinforced composites. Their observations proved that many deformation processes may occur during the loading of these materials, which can be identified by the analysis of signal amplitudes. They found that signals with small amplitudes are emitted by the deformation of the matrix, somewhat larger amplitudes were assigned to debonding and large amplitudes to fiber pull-out and fiber fracture. Haselbach and Lauke [105] also used the amplitude and the frequency of the emitted sound for the identification of micromechanical deformation processes and arrived basically to the same conclusions as Czigány et al. [112].

Scanning electron microscopy (SEM) is a useful tool to confirm deformation processes detected by other methods. In the case of polymer composites the fracture surface of specimens failed during mechanical testing supply the most reliable information about the mechanism of deformation, since these initiate the catastrophic failure of the samples. Some authors [113,114] use in situ deformation measurements in the SEM apparatus. The advantage of this method is that the process is easy to follow. The main drawback of the approach is that stress distribution is different in films and on the surface of specimens than in the bulk material, which complicates the determination of the initiation stress of any process.

1.4 Scope

As the introductory part of this thesis proves, a large number of papers have been published on the mechanical properties of all kinds of polymer composites. However, very few of these concentrate on micromechanical deformation processes although the dominating process will determine the ultimate properties of the composites. In this Thesis we focus our attention onto these processes in order to obtain more information about the factors determining them, as well as to develop guidelines for the improvement of mechanical properties and to achieve better reinforcement. Our laboratory has been working on various heterogeneous polymer systems for a long time and the expertise developed helps considerably the identification and interpretation of these processes. The main motive of the Thesis is the study of micromechanical deformation proc-

esses and the factors influencing them, but the measurements were done on a wide variety of materials related to various projects. As a consequence, different sample preparation and experimental conditions, as well as methods were used during the years, which cannot be sensibly unified in a single experimental section. Although each chapter focuses on a well defined problem and seems to be more or less independent from the other, the interpretation of the results always required the observations made in former chapters. Occasionally one subproject was initiated by the results of another, just like in the case of Chapters 4 and 5. At beginning of the research we wanted to obtain more knowledge about and experience in the use of the acoustic emission technique, thus selected a simple system for study, i.e. polypropylene modified with spherical particles. Later we proceeded to more complicated materials, to layered silicate nanocomposites and to wood fiber reinforced composites. The knowledge gained in these studies allowed us to progress towards more complex problems and we could develop a unique technique for the determination of interfacial adhesion in strongly bonded composites as described in the last chapter. We summarize the main conclusion of the work in the final chapter of the Thesis.

Acoustic emission is a powerful technique to follow and indentify micromechanical deformation processes in composites as highlighted in the introductory part. It is widely used in fiber reinforced thermoset composites, because the detection of signals is easy, the deformation processes emit sound with high amplitudes. On the other hand, only a few attempts were made to measure acoustic emission in particle filled thermoplastic composites and most of them are confined to the investigation of model composites with very large filler particles. Large particles facilitate the detection of the emitted signals, but composites used in everyday practice contain fillers with much smaller particle sizes. Our laboratory has been studying particulate filled composites for some time quite intensively, and the results show that the dominating deformation process is usually debonding. The goal of the research reported in **Chapter 2** was to produce model composites from PP matrix and cross-linked PMMA particles of uniform size in order to obtain a better insight into the debonding process. The behavior of the model composites were compared to that of PP/CaCO₃ composites containing a commercial filler with a broad particle size distribution. These preliminary experiments served the purpose of getting acquainted with the acoustic emission technique, to explore its possibilities and limitations. An attempt was made to locate the initiation of debonding during deformation with acoustic emission experiments. The analysis of the AE signals offered valuable information about parameters influencing the debonding process.

The observations and the developed methodology reported in Chapter 2 formed a reliable basis for the investigation of more complex deformation mechanisms. Layered silicate nanocomposites are thought to be promising materials for structural applications, because in theory high level of reinforcement can be achieved with a small amount of filler. Polyamide nanocomposites seem to be the most successful among all polymer/layered silicate composites. In the last decade intensive research has been done in this field answering some question and also raising new ones. The modification of clay surface with ω -amino acid assists exfoliation and creates a strong bond with the matrix. The excellent properties of PA nanocomposites are explained with the complete or almost complete exfoliation of the silicate supported by X-ray diffraction measure-

ments and transmission electron microscopy. In spite of the general belief in extensive exfoliation and improved properties, widely differing modulus and strength values were reported in the literature even for composites composed of very similar ingredients. The dissimilar properties indicate differences either in structure and/or in interfacial interactions since mainly these factors determine composite properties. Although the knowledge of micromechanical deformation processes is crucial for the successful application of these materials, very few attempts have been made to study them in detail. In **Chapter 3** we report the results of experiments in which three different silicates were used to produce polyamide nanocomposites: sodium montmorillonite for reference, one organophilized with ω -amino acid to ensure good adhesion to the matrix and a clay treated with aliphatic amine. We investigated the effect of filler content and adhesion on the structure and properties of the composites. With the help of acoustic emission and volume strain measurements supplemented by microscopy we tried to obtain as much information about the mechanism of deformation as possible. Finally we wanted to relate the behavior of the composites to their structure.

Recently the interest in composite materials reinforced with wood flour and natural fibers increased considerably. The main application areas of these composites are the automotive and building industries in which they are used in structural applications as fencing, decking, outdoor furniture, window parts, roofline products, door panels, etc. In such applications the load bearing capacity of the dispersed component is crucial. Our laboratory started to study wood flour reinforced composites a few years ago, the work was and is still related to several national and international projects. The first results were summarized in a PhD thesis completed recently [115]. Previous studies on wood flour filled PP composites showed that four micromechanical processes occur during the deformation of such materials. The matrix polymer deforms mainly by shear yielding which does not emit much sound. The presence of wood flour initiates particle related processes, debonding dominates in the absence of coupling agent starting at very small deformations and stresses. The pull-out of fibers may follow the debonding of large particles at an intermediate stress level. The introduction of a functionalized polymer increases interfacial adhesion considerably and completely changes the deformation mechanism. Although debonding of very large particles may take place at intermediate stress levels, the dominating deformation process is the fracture of wood particles. We concluded from these results that further improvement in composite strength is possible only by the increase of the inherent strength of wood particles. One way to do that might be the decrease of their size. Accordingly, in **Chapter 4** we investigated the effect of interfacial adhesion and wood particle size on the deformation mechanism and failure of PP/wood composites to identify the main factors determining macroscopic properties and to find ways to improve composite performance, if possible. Two wood flours with different particle sizes were used in the project. Based on the conclusions obtained in the study described in Chapter 4 we extended our investigations to other natural fibers with a wider range of particle characteristics. In **Chapter 5** we report results obtained on composites prepared with three wood flours and one lignocellulosic fiber in a PP matrix with and without coupling agent. The characteristics of the natural fibers used were quite different, covering a range of size, size distribution, aspect ratio and chemical composition. The effect of these parameters on the mechanism of deformation was analyzed in detail and compiled into a failure map.

In the previous two chapters results obtained on PP/natural fiber composites were reported. The main variables were always particle characteristics and interfacial adhesion. As mentioned earlier, much less information is available on the influence of matrix characteristics on the deformation and failure of PP/natural fiber composites. In the experiments reported in **Chapter 6** three different polypropylenes, a homopolymer, a random and a heterophase copolymer were used as matrix, while corn cob was applied as filler. The goal of the study was to determine the effect of matrix properties on the deformation mechanism and finally on the properties of the composites.

The problem discussed in **Chapter 7** differs from those addressed in previous sections. In those studies we proved that debonding may occur in all composites if interfacial adhesion is weak. The strength of adhesion is proportional to the reversible work of adhesion if only secondary interactions act between the components. In the case of other mechanisms of adhesion, i.e. interdiffusion or covalent bonding, the strength of adhesion cannot be estimated by any model. Using a model developed earlier we made an attempt to estimate interfacial adhesion also in such cases. According to the model debonding stress depends on interfacial adhesion, thus the determination of debonding stress by acoustic emission allows us the calculation of adhesion. The approach is validated with known values of interfacial adhesion and the strength of adhesion is determined for composites containing various fillers and for different surface modifications.

In the final chapter of the Thesis, in **Chapter 8**, we briefly summarize the main results obtained during the work, but refrain from their detailed discussion, because the most important conclusions were drawn and reported at the end of each chapter. This chapter is basically restricted to the listing of the major thesis points of the work. The large number of experimental results obtained in the research supplied useful information and led to several conclusions, which can be used during further research and development related to the optimization of properties in particulate filled and fiber reinforced composites. Nevertheless, as usual, quite a few questions remained open in the various parts of the study, their explanation needs further experiments. Research continues in this field at the Laboratory and we hope to proceed successfully further along the way indicated by this Thesis.

1.5 References

1. Rothon, R. N.: in *Proc. High Performance Fillers 2007*, Paper 1, Hamburg, Germany (2007).
2. Hale, W. R., McGuire, J., Sand I. D., Dohrer, K. K.: *J Appl Polym Sci* **82**, 2454 (2001).
3. Alexandre, M., Dubois, P.: *Mater Sci Eng*, **28**, 1 (2000)
4. Stewart, R.: *Plast Eng*, **60**, 22 (2004).
5. Pukánszky, B.: in *Polypropylene. Structure, Blends and Composites*, J. Karger-Kocsis Ed., pp. 1-70, Chapman and Hall, London (1995).
6. Pukánszky, B.: in *Polypropylene. An A-Z reference*, J. Karger-Kocsis Ed., pp. 240-246, 574-580, Kluwer Academic, Dordrecht (1999).
7. Wypych, G.: *Handbook of fillers*. ChemTec Publishing, Toronto (1999)
8. Katz, H. S., Milewski, J. V.: *Handbook of Fillers and Reinforcements for Plastics*, Van Nostrand, New York (1978)
9. DeArmitt, C.: *Plast Additives Compound* **5**, 28 (2001)
10. Weidenfeller, B., Höfer, M., Schilling, F.: *Composites* **A33**, 1041 (2002)
11. Weidenfeller, B., Höfer, M., Schilling, F.: *Composites* **A35**, 423 (2004)
12. Wong, C. P., Bollampally, R. S.: *J Appl Polym Sci* **74**, 3396 (1999)
13. Weidenfeller, B., Höfer, M., Schilling, F.: *Composites* **A36**, 345 (2005)
14. Bertelli, G., Camino, G., Marchetti, E., Costa, L., Casorati, E., Locatelli, R.: *Polym Degrad Stabil* **25**, 277 (1989)
15. Acosta, J. L., Rodriguez, M., Linares, A., Jurado, J. R.: *Polym Bull* **24**, 87 (1990)
16. Almeras, X., Le Bras, M.: Poutch, F., Bourbigot, S., Marosi G., Anna, P.: *Macromol Symp* **198**, 435 (2003)
17. Almeras, X., Le Bras, M., Hornsby, P., Bourbigot, S., Marosi, Gy., Keszei, S., Poutch, F.: *Polym Degrad Stabil* **82**, 325 (2003)
18. Fukushima, Y., Inagaki, S.: *J Inclusion Phenom* **5**, 473 (1987)
19. Fukushima, Y., Okada, A., Kawasumi, M., Kurauchi, T., Kamigaito, O.: *Clay Minerals* **23**, 27 (1988)
20. Usuki, A., Kojima, Y., Kawasumi, M., Okada, A., Fukushima, Y., Kurauchi, T., Kamigaito, O.: *J Mater Res* **8**, 1179 (1993)
21. Ray, S. S., Okamoto, M.: *Prog Polym Sci* **28**, 1539 (2003)
22. Giannelis, E. P.: *Appl Organomet Chem* **12**, 675 (1998)
23. LeBaron, P. C., Wang, Z., Pinnavaia, T. J.: *Appl Clay Sci* **15**, 11 (1999)
24. Pinnavaia, T. J. G., Beall, W.: *Polymer-Clay Nanocomposites* Wiley, New York (2001)
25. Pukánszky, B.: in *Handbook of Polyolefins* C. Vasile Ed., pp. 689-722, Marcel Dekker, New York (2000).
26. Bledzki, A. K., Gassan, J.: *Prog Polym Sci* **24**, 221-274 (1999)
27. Markarian, J.: *Plast Additives Compound*, **4**, 18 (2002)
28. Pritchard, G.: *Plast Additives Compound*, **6**, 18 (2004)
29. Hári, J., Dominkovics, Z., Fekete, E., Pukánszky, B.: *Express Polym Lett* **3**, 692-702 (2009)

30. Kádár, F., Százdí, L., Fekete, E., Pukánszky, B.: *Langmuir* **22**, 7848-7854 (2006)
31. Santamarina, J. C., Klein, K. A., Wang, Y. H., Prencke, E.: *Can Geotech J* **39**, 233-241 (2002)
32. Theng, B. K. G.: *The chemistry of clay-organic reactions*, Hilger, London (1974)
33. LeBaron, P. C., Wang, Z., Pannavaia, T. J.: *Appl Clay Sci* **15**, 11-29 (1999)
34. Wang, H., Zeng, C. C., Elkovitch, M., Lee L. J., Koelling, K. W.: *Polym Eng Sci* **41**, 2036 (2001)
35. Osman, M. A., Rupp J. E. P., Suter, U. W.: *Polymer* **46**, 1653 (2005)
36. Ellis T. S., D'Angelo, J. S.: *J Appl Polym Sci* **90**, 1639 (2003)
37. Oya, A., Kurokawa, Y., Yasuda, H.: *J Mater Sci* **35**, 1045 (2000)
38. Kato, M., Okamoto, H., Hasegawa, N., Tsukigase A., Usuki, A.: *Polym Eng Sci* **43**, 1312 (2003)
39. Reichert, P., Nitz, H., Klinke, S., Brandsch, R., Thomann R., Mühlaupt, R.: *Macromol Mater Eng* **275**, 8 (2000)
40. Jordan, J. W.: *J Phys Colloid Chem* **53**, 294 (1949)
41. Hyun, Y. H., Lim, S. T., Choi H. J., Jhon, M. S.: *Macromolecules* **34**, 3804 (2001)
42. Lim, S. T., Yang, H. H., Choi H. J., Jhon, M. S.: *Chem Mater* **14**, 1839 (2002)
43. Monticelli, O., Musina, Z., Russo S., Bals, S.: *Mater Lett* **61**, 3446 (2007)
44. Manias, E., Touny, A., Wu, L., Strawhecker, K., Lu B., Chung, T. C.: *Chem Mater* **13**, 3516-3523 (2001)
45. Százdí, L., Pukánszky Jr, B., Vancsó, G. J., Pukánszky, B.: *Polymer* **47**, 4638-4648 (2006)
46. Százdí, L., Pozsgay, A., Pukánszky, B.: *Eur Polym Sci* **43**, 345-359 (2007)
47. Sperber, V.: in *Paper presented at Eurofillers '07*, Zalakaros, Hungary, August 26-30 (2007)
48. Goodier, J. N.: *J Appl Mech* **55**, 39 (1933)
49. Kowalewski, T., Galeski A., Kryszeński, M.: in *Polymer Blends. Processing, Morphology and Properties*, (ed.) Kryszeński, M., Galeski A., Martuscelli, E.: pp. 223-241, Plenum, New York, (1984)
50. Pukánszky, B., Vörös, G.: *Compos Interfaces* **1**, 411-427 (1993)
51. Vollenberg, P. H. T.: Ph.D. Thesis, Eindhoven University of Technology, Eindhoven, (1987)
52. Bucknall, C. B.: *Toughened Plastics*, Applied Sci Publ, London, (1977)
53. Stoklasa, K., Tomis, F., Navratil, Z.: *Thermochim Acta*, **93**, 221 (1985)
54. Kerch, G. M., Irgens, L.: *Thermochim Acta*, **93**, 155 (1985)
55. Nielsen, L. E.: *Mechanical properties of polymers and composites*, Marcel Dekker, New York (1974)
56. Beck, R. H., Gratch, S., Newman, S., Rausch, K. C.: *J Polym Sci, Polym Lett* **6**, 707 (1968)
57. Galeski, A., Kalinski, R.: in *Polymer Blends. Processing, Morphology and Properties*, (ed.) Martuscelli, E., Palumbo, R., Kryszeński, M., pp. 431-449, Plenum, New York (1980)
58. Pukánszky, B., van Es, M., Maurer, F. H. J., Vörös, G.: *J Mater Sci* **29**, 2350-2358 (1994)
59. Sudár, A., Móczó, J., Vörös, G., Pukánszky, B.: *Express Polym Lett* **1**, 763,

- (2007)
60. Pukánszky, B., Tüdös, F., Jancar, J., Kolarík, J.: *J Mater Sci Lett* **8**, 1040 (1989)
 61. Nakagawa, H., Sano, H.: *Polym Prepr* **26**, 249 (1985)
 62. Trantina, G. G.: *Polym Eng Sci* **24**, 1180 (1984)
 63. Riley, A. M., Paynter, C. D., McGenity, P. M., Adams, J. M.: *Plast Rubber Process Appl* **14**, 85 (1990)
 64. Maiti, S. N., Mahapatro, P. K.: *J Appl Polym Sci* **42**, 3101 (1991)
 65. Kinloch, A. J., Young, R. J.: *Fracture Behaviour of Polymers*, Elsevier, London (1983)
 66. Breuer, H.: *NATO ASI Ser, Ser E* **89**, 375 (1985).
 67. Breuer, H.: *NATO ASI Ser, Ser E* **89**, 383 (1985).
 68. Dekkers, M. E. J., Heikens, D.: *J Mater Sci* **20**, 3873 (1985)
 69. Dekkers, M. E. J., Heikens, D.: *J Mater Sci* **19**, 3271 (1984)
 70. Sternstein, S. S., Ongchin, L.: *ACS Polym Prepr* **10**, 1117 (1969)
 71. Lazzeri, A., Bucknall, C. B.: *J Mater Sci* **28**, 6799 (1993)
 72. Farris, R. J.: *Trans Soc Rheol* **12**, 315-334 (1968)
 73. Vollenberg, P., Heikens, D., Ladan, H. C. B.: *Polym Compos* **9**, 382-388 (1988)
 74. Dubnikova, I. L., Berezina, S. M., Antonov, A. V.: *J Appl Polym Sci* **85**, 1911-1928. (2002)
 75. Sjögren, B. A., Berglund, L. A.: *Polym Compos* **18**, 1-8 (1997)
 76. Asp, L. E., Sjögren, B. A., Berglund, L. A.: *Polym Compos* **18**, 9-15 (1997)
 77. Meddad, A., Fisa, B.: *J Appl Polym Sci* **64**, 653-665 (1997)
 78. Százdi, L., Ábrányi, Á., Pukánszky Jr., B., Vancso, J. G., Pukánszky, B.: *Macromol Mater Eng* **291**, 858-868 (2006)
 79. Dennis, H. R., Hunter, D. L., Chang, D., Kim, S., White, J. L., Cho, J. W., Paul, D. R.: *Polymer* **42**, 9513-9522 (2001)
 80. Rácz, L., Pukánszky Jr., B., Pozsgay, A., Pukánszky, B.: *Progr Colloid Polym Sci* **125**, 96-102 (2004)
 81. Ábrányi, Á., Százdi, L., Pukánszky, B., Vancso, G. J.: *Macromol Rapid Commun* **27**, 132-135 (2006)
 82. Lertwilmolnun, W., Vergnes, B.: *Polymer* **46**, 3462-3471 (2005)
 83. Okatmoto, M., Morita, S., Kim, Y. H., Kotaka, T., Tateyama, H.: *Polymer* **42**, 1201-1206 (2001)
 84. Galeski, A.: *Prog Polym Sci* **28**, 1643-1699 (2003)
 85. Kim, G. M., Lee, D. H., Hoffmann, B., Kressel, J., Stöppelmann, G.: *Polymer* **42**, 1095-1100 (2001)
 86. Bledzki, A. K., Letman, M., Viksne, A., Rence, L.: *Composites* **A36**, 789-97. (2005)
 87. Maldas, D., Kokta, B. V.: *Compos Interf* **1**, 87-108 (1993)
 88. Neagu, R.C., Gamstedt, E. K., Berthold, F.: *J Compos Mater* **40**, 663-699 (2000)
 89. Ichazo, M. N., Albano, C., Gonzalez, J., Perera, R., Candal, M. V.: *Compos Struct* **54**, 207-214 (2001)
 90. Cantero, G., Arbelaiz, A., Mugika, F., Valea, A., Mondragon, I.: *J Reinf Plast Compos* **22**, 37-50 (2003)

91. Demir, H., Atikler, U., Balköse, D., Tihminlioglu, F.: *Composites* **A37**, 447-456 (2006)
92. Zhang, C., Li, K., Simonsen, J.: *J Adhesion Sci Technol* **18**, 1603-1612 (2004)
93. Zhang, C., Li, K., Simonsen, J.: *Polym Eng Sci* **46**, 108-113 (2006)
94. Joly, C., Gauthier, R., Escoubes, M.: *J Appl Polym Sci* **61**, 57-69 (1996)
95. Doan, T. T. L., Gao, S. L., Mader, E.: *Compos Sci Technol* **66**, 952-963 (2006)
96. Dogossy, G., Czigány, T.: *Polym Test* **25**, 353-357 (2006)
97. Romhány, G., Karger-Kocsis, J., Czigány, T.: *J Appl Polym Sci* **90**, 3638-3645 (2003)
98. Romhány, G., Karger-Kocsis, J., Czigány, T.: *Macromol Mater Eng* **288**, 699-707 (2003)
99. Kocsis, Z., Czigány, T.: *Mater Sci Forum* **537-538**, 199-205 (2007)
100. Bouaziz, A., Zaïri, F., Naït-Abdelaziz, M., Gloaguen, J. M., Lefebvre, J.M.: *Compos Sci Technol* **67**, 3278-3285 (2007)
101. Gloaguen, J. M., Lefebvre, J. M.: *Polymer* **42**, 5841-5847 (2001)
102. Ahmadi, S. J., G'Sell, C., Huang, Y. D., Ren, N. Q., Mohaddespour, A., Hiver, J. M.: *Compos Sci Technol* **69**, 2566-2572 (2009)
103. van Hartingsveldt, E. A. A., van Aartsen, J. J.: *Polymer*, **30**, 1984 (1989)
104. Karger-Kocsis, J.; Harmia, T.; Czigány, T.: *Compos Sci Technol* **54**, 287-298 (1995)
105. Haselbach, W.; Lauke, B.: *Compos Sci Technol* **63**, 2155-2162 (2003)
106. Bohse, J.: *Compos Sci Technol* **60**, 1213-1226 (2000)
107. Kraus, J.; Wilke, W.; Zhuk, A.; Luzinov, I.; Minko, S.; Voronov, A.: *J Mater Sci* **32**, 4397-4403 (1997)
108. Kraus, J.; Wilke, W.; Zhuk, A.; Luzinov, I.; Minko, S.; Voronov, A.: *J Mater Sci* **32**, 4405-4410 (1997)
109. Minko, S.; Karl, A.; Voronov, A.; Senkovskij, V.; Pomper, T.; Wilke, W.; Malz, H.; Pionteck, J.: *J Adhes Sci Technol* **14**, 999-1019 (2000)
110. Ou, Y.-C.; Yu, Z.-Z.; *Polym Int* **37**, 113-117 (1995)
111. Kaiser, J.: Ph.D.Thesis, München Technische Hochschule, 1950
112. Czigány, T.; Marosfalvi, J.; Karger-Kocsis, J.: *Compos Sci Technol* **60**, 1203-1212 (2000)
113. Kim, G. M., Michler, G. H., Gahleitner, M., Fiebig, J.: *J Appl Polym Sci* **60**, 1391-1403 (1996)
114. Kim, G. M., Lee, D. H.: *J Appl Polym Sci* **82**, 785-789 (2001)
115. Dányádi, L. Ph.S Thesis, Budapest, Budapest University of Technology and Economics, 2007

Chapter 2

Analysis of the debonding process in polypropylene model composites⁴

2.1. Introduction

In particulate filled polymers debonding is the dominating deformation mechanism and if a large number of particles separate from the matrix under the effect of external load, the yield stress and tensile strength of the composite decrease with increasing filler content. This is the usual case when commercial fillers are used and the decrease of strength is often associated with the normal behavior of particulate filled polymers. However, the value of the debonding stress depends on particle size and interfacial interaction thus certain combinations of these parameters may lead to increasing yield stress and strength with increasing filler content [1,2]. The control of the debonding process raises some theoretical questions and it has great practical importance, as well. Easy debonding and the formation of large voids lead to premature failure [2]. On the other hand, the production technology of breathable films is based on the debonding process. PE films containing a large amount of CaCO₃ particles are stretched to form voids in a specified size range, which let vapor pass through, but prevent the permeation of liquids [3]. The size and number of voids determine the properties of the films, thus the control of the debonding process is of the utmost technological importance. Although the phenomenon of debonding is well known, it cannot be controlled in the desired extent yet.

The goal of the present research was to produce model composites from PP matrix and cross-linked PMMA particles of uniform size in order to obtain a better insight into the debonding process. The behavior of the model composites were compared to that of PP/CaCO₃ composites containing a commercial filler with a broad particle size distribution. An attempt was made to locate the initiation of debonding during deformation with acoustic emission (AE) experiments. An analysis of the AE signals gave valuable information about parameters influencing the debonding process.

2.2. Experimental

Tipplén H 543 polypropylene homopolymer produced by TVK, Hungary was used as matrix. The preparation of the cross-linked PMMA particles was described elsewhere [4-9]. Omycarb 15 GU CaCO₃ was used as reference filler. It is a commercial product with a broad particle size distribution. The characteristics of the fillers are discussed in more detail in the next section. The filler loading of the composites was changed from 0 to 0.3 volume fraction in 0.05 volume fraction steps. The components

⁴Renner, K., Yang, M-S., Móczó J., Choi, H-J., Pukánszky, B.: *Eur Polym J* **41**, 2520-2529 (2005)

were homogenized in a Brabender W 50 EH internal mixer at 190 °C, 50 rpm for 10 min, and then the melt was compression molded into 1 mm thick plates at the same temperature.

The mechanical properties were characterized by tensile testing using an Instron 5566 apparatus with 10 mm/min cross-head speed and 80 mm gauge length. Acoustic emission signals were recorded with a Sensophone AED 40/4 apparatus. After deformation and debonding, the structure of the composites was studied by SEM. Micrographs were taken from fracture surfaces using a JEOL 5500 LV equipment. Specimens were removed from the tensile testing machine after a given deformation, notched, immersed into liquid nitrogen and broken in order to create the fracture surfaces.

2.3. Results

The results of this study are discussed in several sections. The particle characteristics of the fillers are presented first, and then the tensile properties of the two sets of composites are compared to each other. The evaluation of the acoustic emission signals detected during the deformation of the composites is followed by a general section analyzing the debonding process and the characteristics related to it.

2.3.1. Particle characteristics

Our basic assumption was that a very narrow particle size distribution would help us to follow debonding and the deformation of the composites generally, thus the preparation of particles with uniform size was an essential part of the project. A SEM micrograph of the PMMA particles used is presented in Fig. 2.1. Although they appear to be of rather uniform size, smaller and larger particles can be also observed in the micrograph.

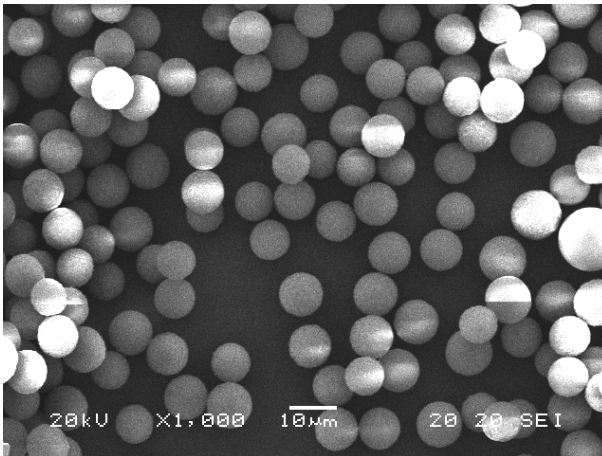


Fig. 2.1 SEM micrograph of the cross-linked PMMA model filler used in the experiments.

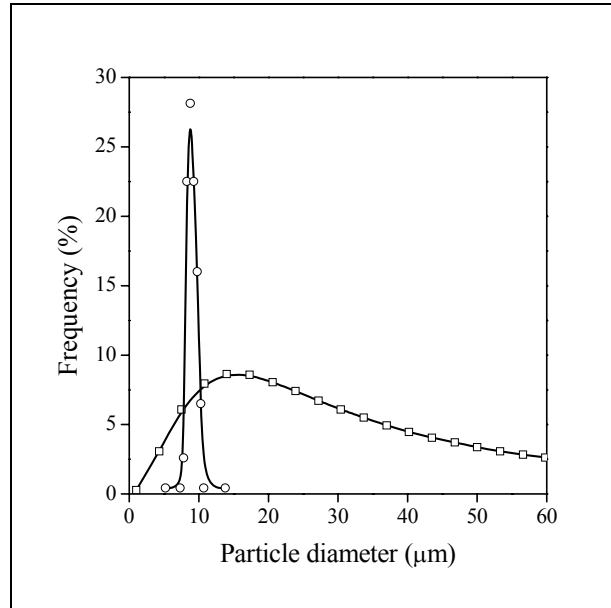


Fig. 2.2 Particle size distribution of the PMMA model filler (○) determined by image analysis and that of the reference CaCO₃ (□).

The actual distribution of particle size was determined by image analysis (Fig. 2.2). The figure clearly demonstrates that apart of a few exceptions the diameter of most particles falls in a very narrow range, between 7.6 and 10.4 μm. The average size of the particles is 8.8 ± 0.7 μm. The particle size distribution of the reference CaCO₃ filler is also shown in Fig. 2.2. In this latter case the maximum of the distribution is around 14 μm and the average particle size is 12 μm.

Although this difference in the average particle size of the fillers might not influence debonding and the mechanical properties of the composites considerably, the broad particle size distribution certainly does. Based on these results we can state that the particle size distribution of our model PMMA filler is very narrow, especially if we compare it to that of the commercial CaCO₃.

2.3.2. Tensile characteristics

The tensile characteristics of particulate filled polymer composites may offer considerable information about the dominating deformation processes and the interaction of the components. Debonding was identified by the deviation from linearity of the stress vs. strain curve by some authors [10-15], while others [16] found that the debonding stress and the yield stress are almost identical. The first part of the stress vs. strain trace of the matrix PP and its composites containing 10 vol% PMMA or CaCO₃ particles, respectively, are presented in Fig. 2.3.

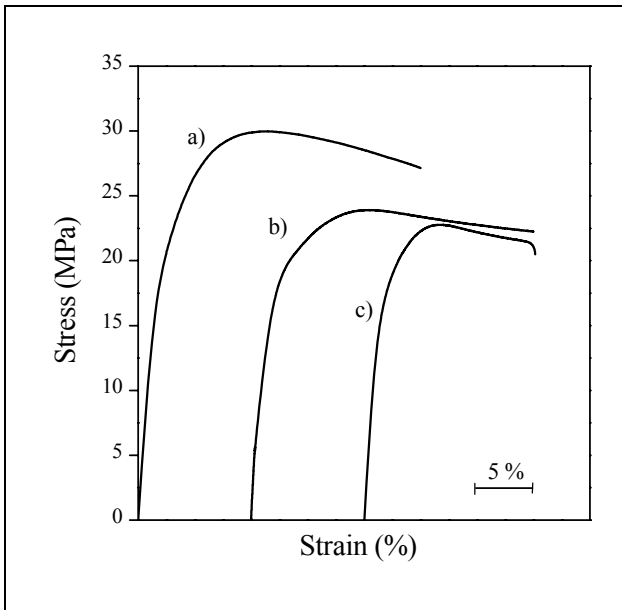


Fig. 2.3 Stress vs. strain curves of PP (a), PP/PMMA (b) and PP/CaCO₃ (c) composites in the small deformation range. Filler content: 0.1 volume fraction.

The traces are very similar and a closer scrutiny shows that they do not possess a linear section at all. As a consequence, it is impossible to determine the point where the correlations deviate from linearity, which was claimed to indicate debonding [10-15]. In the case of the PP/PMMA composite we might say that the curvature of the trace changes suddenly at around 18-20 MPa stress, i.e. the slope suddenly decreases, but the exact location of this point cannot be determined unambiguously. Moreover, we do not have any proof that debonding really occurs at this stress value. We would encounter even more serious difficulties, if we wanted to find such a point on the stress vs. strain curve of the PP/CaCO₃ composite.

The composition dependence of yield stress gives some indication about the dominating deformation process. Decreasing yield stress is associated with debonding, but the slope of the curve depends also on the particle size of the filler and on the strength of interaction. Usually only a part of the particles debond, the rest carries some load. In PP composites debonding is frequently accompanied by shear yielding. The composition dependence of the yield stress of the composites studied is compared in Fig. 2.4. The functions are very similar, they run very close to each other. The larger particle size of the CaCO₃ filler results in smaller yield stresses compared to the composite containing the 9 μm large PMMA particles.

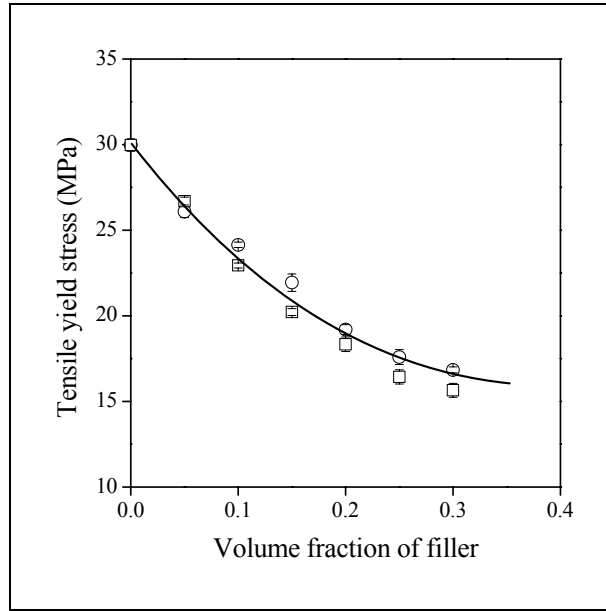


Fig. 2.4 Composition dependence of the tensile yield stress of PP composites. Filler: (○) PMMA, (□) CaCO₃.

The load carried by the dispersed component can be determined by a simple model developed earlier [1,2]. According to this approach composite yield stress consists of three terms, the yield stress of the matrix (σ_{y0}), its effective load bearing cross-section, $(1-\varphi)/(1+2.5\varphi)$, where φ is the volume fraction of the filler, and a term related to interaction, i.e. to the load-bearing capacity of the filler [$\exp(B\varphi)$]. Plotting the logarithm of reduced yield stress

$$\ln \sigma_{yred} = \ln \frac{\sigma_y (1 + 2.5 \varphi)}{1 - \varphi} = \ln \sigma_{y0} + B \varphi \quad (2.1)$$

against filler content should result in a straight line, the slope of which gives information about interfacial interactions, i.e. about the load carried by the dispersed filler. The yield stress values of the two sets of composites are plotted according to Eq. 2.1 in Fig. 2.5.

We obtain relatively good straight lines in both cases. The somewhat larger scatter of the PP/CaCO₃ composites can be explained with the broader size distribution of the filler, a larger fraction of smaller particles and the presence of aggregates or other inhomogeneities. The smaller size of the PMMA particles results in a steeper slope in spite of their lower surface tension, which indicates the combined effect of particle size and adhesion on composite properties [17-19]. The characteristic values of the lines of Fig. 2.5 (slope, intersection, fit) are compiled in Table 2.1. The relatively large B values

indicate that only a certain fraction of the particles debond during deformation, a part of the load is carried by the filler. The overall performance of the two sets of composites is very similar to each other. The extent of debonding cannot be estimated from these results and we cannot locate the occurrence of debonding unambiguously during deformation. These results do not offer any information about the value of debonding stress (σ^D) either.

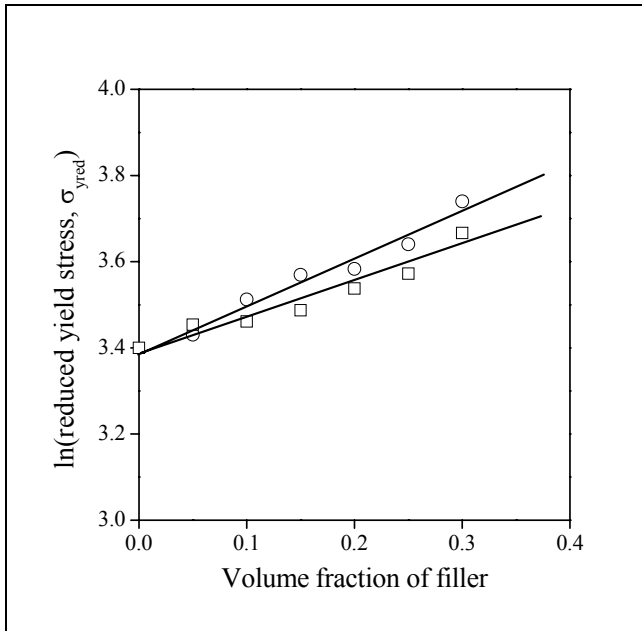


Fig. 2.5 Linearized plot of the reduced tensile yield stress of the studied composites. Filler: (○) PMMA, (□) CaCO₃.

Table 2.1 Load-bearing capacity of the filler used in the study and other characteristic values derived from Eq. 2.1

Filler	Particle size (μm)	σ_0 (MPa)	σ_{0c}^a (MPa)	B	R
PMMA	8.9	29.5	29.5	1.11	0.9875
CaCO ₃	12.0		29.7	0.79	0.9672

^amatrix yield stress calculated from the intersection

2.3.3. Acoustic emission

The stress vs. strain correlation of the PP matrix polymer is plotted in Fig. 2.6 together with the cumulative number of events, which emit sound signals and are detected during deformation. The correlations are presented only up to the yield point, or somewhat beyond that, because the PP used in these experiments has a very large elongation at the deformation rate applied. The total number of detected signals (or hits) increases continuously and almost linearly with increasing deformation, which indicates a very low level of acoustic activity. A large part of the recorded events is caused by noise and not by the deformation of the sample. We cannot distinguish any characteristic point on the AE trace, which could be assigned to yielding.

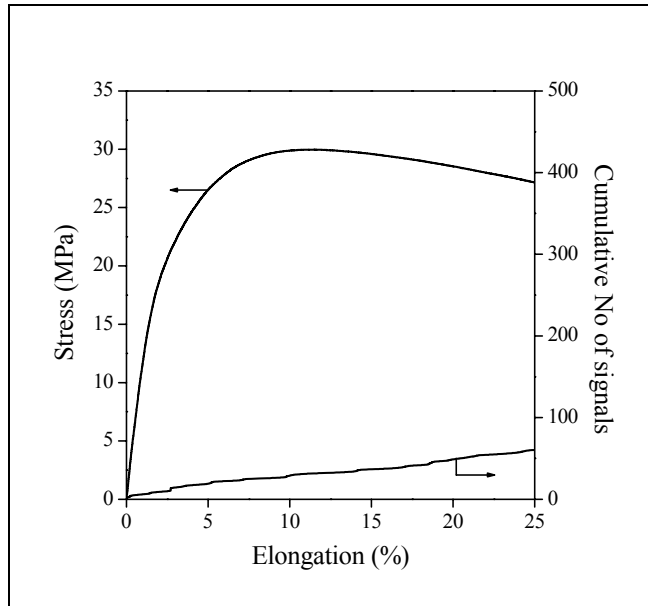


Figure 2.6 Stress and cumulative acoustic activity plotted against deformation for the matrix PP.

The model composite containing only 5 vol% PMMA particles behaves differently (Fig. 2.7). Although the stress vs. strain correlation is similar to the one presented in Fig. 2.6, the cumulative number of signals increases very steeply after a critical deformation. Above a certain deformation value, the rate of increase in the number of hits decreases drastically. We may assume that the larger number of events occurring at small deformations is caused by debonding and the change in the slope may be related to the completion of this process. After all the particles, which are able to separate from the matrix, debonded, the plastic deformation of the matrix begins. This latter process is not accompanied by significant acoustic activity.

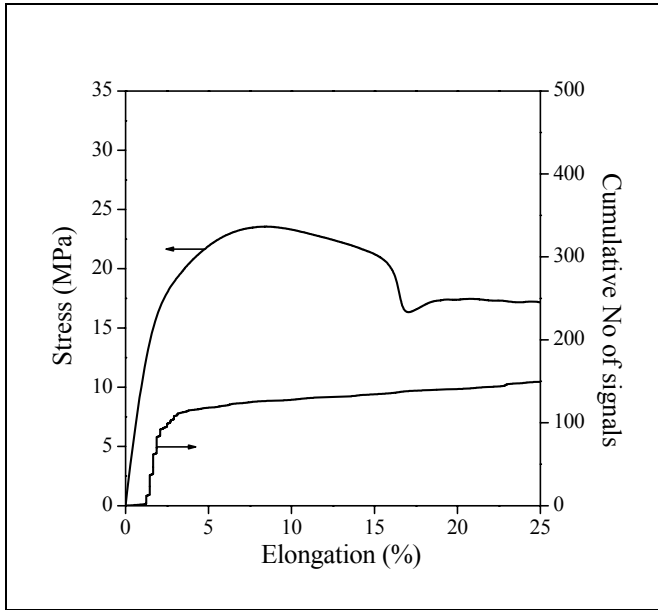


Fig. 2.7 *Stress and cumulative acoustic activity plotted against deformation for PP/PMMA composite containing 5 vol% filler.*

The same behavior was observed practically for all PP/PMMA composites. The stress vs. strain and cumulative hit vs. strain correlation of the composites containing 20 vol% PMMA filler are shown in Fig. 2.8. The general feature of the correlations is very similar to those seen in the previous figure. We can see again that no acoustic activity is detected at very small deformations and most events are located inside a very narrow deformation range. If the sudden increase in acoustic activity belongs to debonding, indeed, this deformation process has an initiation stress or deformation. Moreover, the process is completed within a narrow deformation range for the model filler used in these experiments.

The results obtained for the composites containing 10 vol% CaCO_3 filler are plotted in Fig. 2.9 for comparison. We cannot see any characteristic change in the stress vs. strain trace and the increase in the number of acoustic events is much more continuous than in the PP/PMMA model composites. Both the threshold deformation and the change in the slope of the cumulative hit vs. elongation function are difficult to identify exactly. We are convinced that the slower transition is related to the particle size distribution of the filler. Large particles debond very easily as predicted by Eqs. 1.1 and 1.2, while small particles do not separate from the matrix at all. The debonding process takes place in a much wider deformation range than in PP/PMMA composites and the transition from elastic deformation to debonding and then to the plastic deformation of the matrix is more or less continuous.

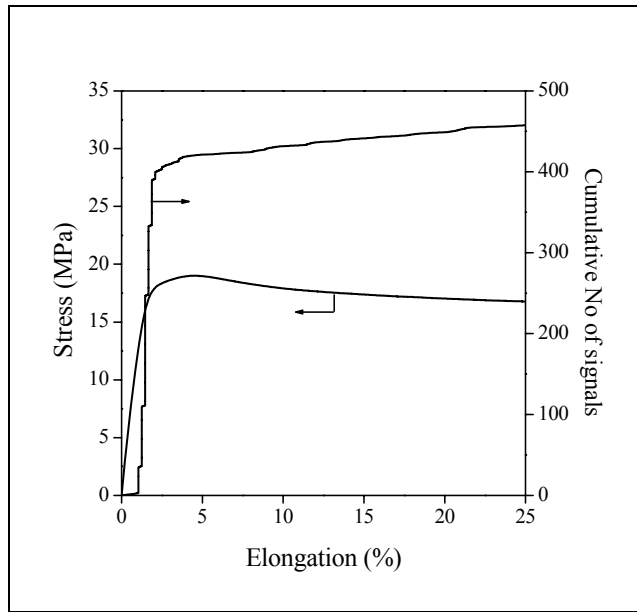


Fig. 2.8 Stress and cumulative acoustic activity plotted against deformation for PP/PMMA composite containing 20 vol% filler.

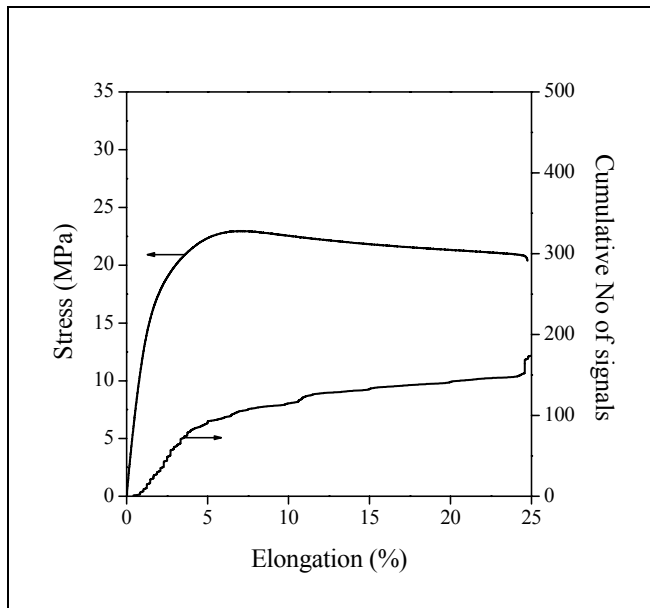


Fig. 2.9 Stress and cumulative acoustic activity plotted against deformation for PP/CaCO₃ composite containing 10 vol% filler.

In spite of the fact that the increase in acoustic activity can be seen clearly on the cumulative event vs. deformation traces, the exact stress or strain value at which it occurs cannot be defined unambiguously. From a closer scrutiny of Figs. 2.7 and 2.8 we can only say that debonding starts before reaching the maximum of the stress vs. strain curve, i.e. it is completed before significant yielding starts, as it was claimed by several groups [10-15]. To facilitate the determination of the deformation (or stress) values which can be assigned to maximum acoustic activity, i.e. to debonding, we calculated the derivative of the cumulative hit function similarly to Kraus et al. [20,21]. Three sets of curves are plotted in Fig. 2.10 for PP, PP/PMMA and PP/CaCO₃ composites. The latter two were prepared with 10 vol% of the respective fillers.

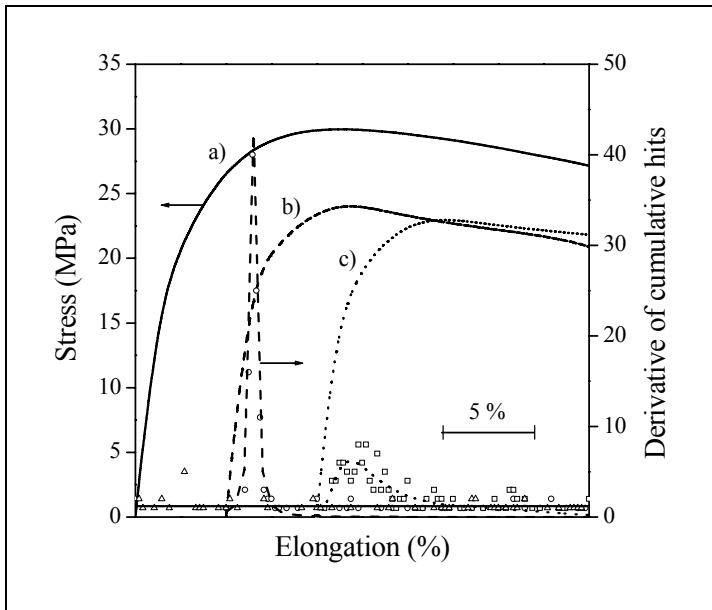


Fig.2.10 Changes in the stress and derivative cumulative hit number correlations as a function of deformation for PP (a), PP/PMMA (b), and PP/CaCO₃ (c) composites. Filler content: 10 vol%.

The correlations are shifted along the deformation axis, but they are plotted in the same scale to facilitate comparison. The maximum of the derivative acoustic event curve shows well the range of the deformation in which debonding takes place. In the matrix polymer the intensity of emission is very low, almost negligible shown by the horizontal solid line, which represents the derivative of the cumulative hit curve. Very few events are detected in the material represented by the triangles in the plot. Shear yielding is the dominating process in PP, which does not emit much sound. On the other hand the presence of PMMA particles of uniform size results in a very sharp and strong

maximum in the derivative function (see circles and the broken line representing a fitted average function). Obviously a different process takes place in the composites, which generates more and stronger acoustic signals. This process, which must be debonding, occurs in a very narrow range of deformation. Both the intensity and the width of the maximum are different for the PP/CaCO₃ composite (see squares and dotted line), but we can clearly establish that the majority of particles debond before reaching the maximum in the stress vs. strain curve. The analysis of the acoustic emission signals and the plotting of derivative cumulative hit functions proved that in the investigated PP composites elastic deformation is followed by debonding. This latter is practically completed before significant plastic deformation of the matrix polymer starts, at least at small filler contents.

2.3.3. *Debonding characteristics, process analysis*

The total number of acoustic events detected is plotted against filler content in Fig. 2.11. The correlation can be divided into three parts. The total number of events detected in the matrix polymer is extremely small; obviously the shear yielding of the matrix does not generate any sound. Cracks may develop occasionally in the crystalline phase of PP [22], which might result in the few signals detected. More acoustic signals are generated in the composites and the dissimilar mechanism of deformation is clearly indicated by the difference between the intersection of this second part of the correlation and the value obtained for the matrix material. The significant increase in the number of acoustic events at 0.2 volume fraction filler content is difficult to explain; only further study may reveal its reason. The subsequent decrease of acoustic emission events might be related to the interaction of the particles. The association of two particles may lead to easier debonding and/or to the decrease of events; simultaneous debonding of two particles might not be distinguished by the detector. Interesting to note that the increase in the number of events at higher filler contents is absent in the PP/CaCO₃ composites, but above 0.2 volume fraction filler content the total number of hits decreases here, too. Decreasing particle distance or aggregation may lead to this change in the deformation of the composites.

The difference in the deformation mechanism of the matrix and the composites, respectively, is supported also by the average amplitude of the detected acoustic signals (Fig 2.12). Although the difference is not large, the average intensity of the signals in the composite is about 2-3 dB larger than in the matrix. This small difference makes the separation of the processes very difficult in particulate filled polymers and only the complete analysis of all available data allows us to draw valid conclusions about the prevailing deformation mechanism.

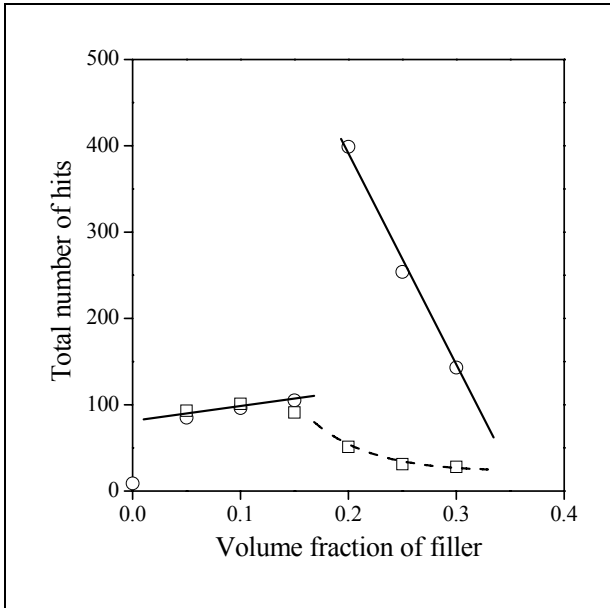


Fig. 2.11 Dependence of the total number of hits on filler content. Filler: (○) PMMA, (□) CaCO₃.

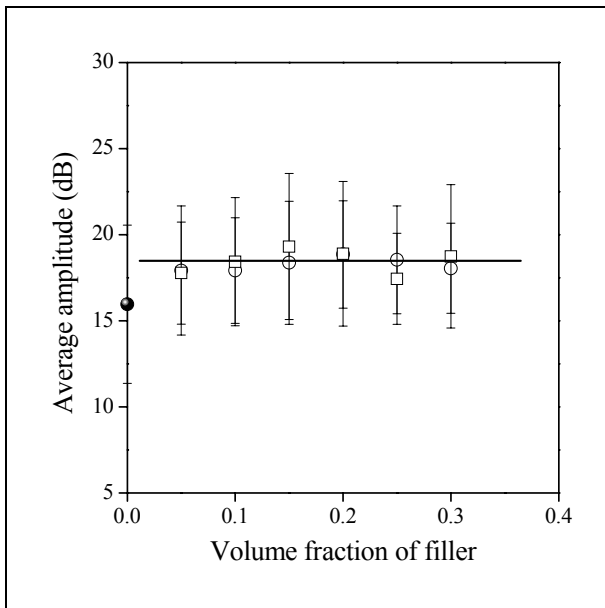


Fig. 2.12 Effect of filler content on the average amplitude of hits detected by AE. Symbols: (●) PP, (○) PP/PMMA, (□) PP/CaCO₃.

It is the subject of continuing debate if debonding occurs at a critical stress or at a critical strain. The deformation at which the maximum of the cumulative event function is detected does not depend on filler content. However, local deformation must change considerably with increasing filler content, thus we cannot state that debonding occurs at a critical strain. The stress at which debonding occurs is plotted against filler content in Fig. 2.13. The critical stress increases up to 0.2 volume fraction and decreases afterwards. The increase of debonding stress can be explained with the interaction of the stress fields of neighboring particles, which leads to smaller local stresses with increasing filler content [23,24]. At large filler loading the association of particles leads to decreasing debonding stress in accordance with the prediction of Eqs. 1.1 and 1.2. The debonding stress derived from AE signals is almost constant for the PP/CaCO₃ composites, which can be explained by the wide particle size distribution of the commercial filler. We plotted also the yield stress of the composites in Fig. 2.13. It is very interesting to note that debonding and yield stress are practically identical above 0.2 volume fraction filler content, as suggested by us earlier [16]. Obviously, the number of debonded particles is very large at this filler loading, thus debonding and plastic deformation proceed practically simultaneously. Volume strain measurements can identify debonding only when voids already increase, i.e. large plastic deformation starts, while AE detects the actual separation of the interfaces.

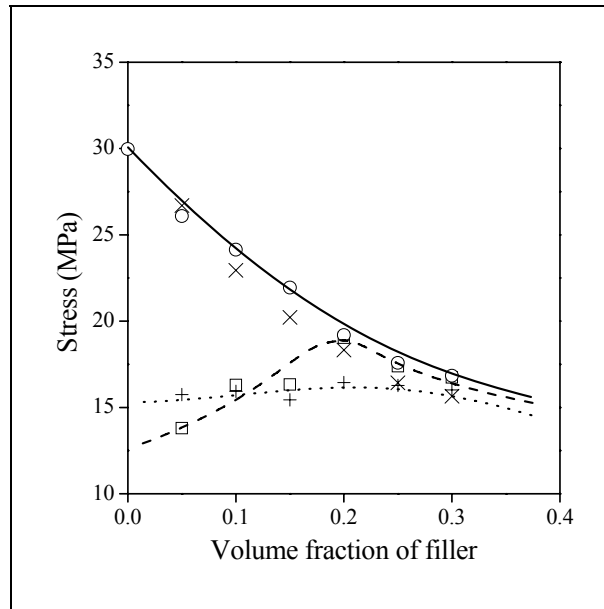


Fig. 2.13 Composition dependence of debonding stress determined from acoustic emission measurements. Symbols: (○) σ_y , PMMA; (□) AE, PMMA; (×) σ_y , CaCO₃; (+) AE, CaCO₃.

We attempted to follow the deformation of the composites also by taking SEM micrographs from samples deformed to different extents. We present only one example

in Fig. 2.14. The fact of debonding can be clearly established in the micrograph; practically all the particles are separated and smaller or larger voids formed around them. It is interesting to note that we could not detect voids on fracture surfaces, if the samples were deformed to smaller deformation than the yield strain. We may conclude that voids can be detected only after the yield point, deformation below that level relaxes and the bond between the filler and the matrix reforms. This explains also the fact that according to volume strain measurements debonding and yield stresses are identical. Debonding in itself does not lead to the significant increase of volume, void formation starts with the plastic deformation of the matrix after reaching the yield point.

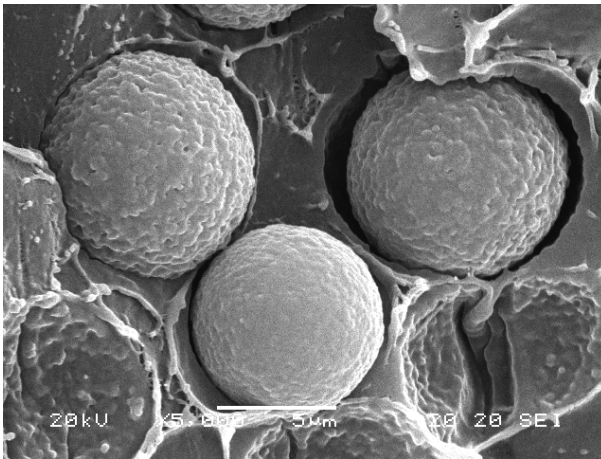


Fig. 2.14 Void formation in PP/PMMA model composites at large deformation ($2\varepsilon_y$).
Filler content: 20 vol%

2.4. Conclusions

Measurements of acoustic emission signals during the elongation of PP/PMMA model composites containing particles with a narrow particle size distribution allowed us to assign the debonding process, including its initiation, unambiguously to a well defined range of the stress vs. strain curve. The number and intensity of the signals detected in the matrix and the composite, respectively, differed considerably, which made possible the separation of the various micromechanical deformation processes occurring in them. At low extensions the composite is deformed elastically, then debonding takes place in a very narrow deformation range, followed by the plastic deformation of the matrix. At small particle content debonding occurs at relatively low stresses, which differ considerably from yield stress. Significant plastic deformation of the matrix starts at the yield point. At larger filler content debonding and shear yielding occur simultaneously. Micromechanical deformation processes cannot be separated as clearly in composites prepared from the commercial CaCO_3 filler with a broad particle size distribution. The debonding of particles with different size occurs in a wide deformation range because of the particle size dependence of debonding stress. The analysis

of characteristic values derived from acoustic emission experiments proved that the interacting stress fields of neighboring particles influence deformation and that even large particles may aggregate or at least associate at large filler content. Further study must be carried out to explore all the consequences of the results.

2.5. References

1. Pukánszky, B., Turcsányi, B., Tüdös, F., in: *Interfaces in polymer, ceramic, and metal matrix composites*. Ishida, H. (ed.), New York, Elsevier, 1988, pp. 467-477.
2. Pukánszky, B.: *Composites* **21**, 255-262 (1990)
3. Moreiras, G.: *Ind Minerals* **6**, 29-33 (2001)
4. Kim, J. W., Kim, J. Y., Suh, K. D.: *Polym Bull* **36**, 141-148 (1996)
5. Han, S., Moon, T. J., Suh, K. D., Noh, S. T., Bae, Y. C.: *J Appl Polym Sci* **61**, 1985-1989 (1996)
6. Kim, J. W., Suh, K. D.: *Macromol Chem Phys* **202**, 621-627 (2001)
7. Park, J. G., Kim, J. W., Suh, K. D.: *Colloid Polym Sci* **279**, 638-645 (2001)
8. Lee, S. S., Park, K. Y., Kim, J. Y., Suh, K. D.: *J Appl Polym Sci* **81**, 1206-1212 (2001)
9. Lee, I. S., Cho, M. S., Choi, H.J.: *Polymer* **46**, 1317-1321 (2005)
10. Vollenberg P. PhD Thesis, Eindhoven University of Technology, Eindhoven, 1987
11. Vollenberg, P., Heikens, D., Ladan, HCB.: *Polym Compos* **9**, 382-388 (1988)
12. Dubnikova, I. L., Berezina, S. M., Antonov, A. V.: *J Appl Polym Sci* **85**, 1911-1928 (2002)
13. Sjögren, B. A., Berglund, L. A.: *Polym Compos* **18**, 1-8 (1997)
14. Asp, L. E., Sjögren, B. A., Berglund, L. A.: *Polym Compos* **18**, 9-15 (1997)
15. Meddad, A., Fisa, B.: *J Appl Polym Sci* **64**, 653-665 (1997)
16. Pukánszky, B., van Es, M., Maurer, F. H. J., Vörös, G.: *J Mater Sci* **29**, 2350-2358 (1994)
17. Pukánszky, B., Fekete, E., Tüdös, F.: *Makromol Chem, Macromol Symp* **28**, 165-186 (1989)
18. Vörös, G., Fekete, E., Pukánszky, B.: *J Adhesion* **64**, 229-250 (1997)
19. Pukánszky, B., Fekete, E.: *Adv Polym Sci* **139**, 109-153 (1999)
20. Kraus, R., Wilke, W., Zhuk, A., Luzinov, I., Minko, S., Voronov, A.: *J Mater Sci* **32**, 4397-4403 (1997)
21. Kraus, R., Wilke, W., Zhuk, A., Luzinov, I., Minko, S., Voronov, A.: *J Mater Sci* **32**, 4405-4410 (1997)
22. Henning, S., Michler, G. H., Ania, F., Balta-Calleja, F. J.: *Colloid Polym Sci* **283**, 486-495 (2005)
23. Vörös, G., Pukánszky, B.: *J Mater Sci* **30**, 4171-4178 (1995)
24. Pukánszky, B., Vörös, Gy.: *Polym Compos* **17**, 384-392 (1996)

Chapter 3

Micromechanical deformation process in PA/layered silicate nanocomposites: Correlation of structure and properties⁵

3.1. Introduction

Although the knowledge of micromechanical deformation processes is crucial for the successful application of polymer nanocomposites, very few attempts have been made to study them in detail. Kim et al. [1] investigated the deformation behavior of PA/layered silicate nanocomposites and based on TEM microscopy, they proposed a scheme of the deformation and failure mechanism (see Fig. 1.7). The model of the authors consists of several processes including the deformation and fracture of clay particles or tactoids, which indicates that intercalation was not complete in their case. LeFebvre et al. [2] measured the volume strain of PA nanocomposite samples during deformation. They determined the various components of strain by a detailed analysis and concluded that besides elastic deformation, considerable debonding and plastic flow also takes place during the elongation of the samples. These experiments [1,2] indicate that both the structure and the deformation mechanism of PA nanocomposites might be more complex than often indicated in the literature.

In the present study three different silicates were used, a sodium montmorillonite (NaMMT) for reference, one organophilized with ω -amino acid (N784) to ensure good adhesion to the matrix and a clay treated with aliphatic amine (N948). The application of this latter surfactant results in weak interaction between the matrix polymer and the silicate [3]. The goal of the study was to investigate the effect of filler content and adhesion on the structure and properties of the composites. With the help of acoustic emission and volume strain measurements supplemented by microscopy we tried to obtain as much information about the mechanism of deformation as possible. Finally we wanted to relate the behavior of the composites to their structure.

3.2. Experimental

Two organophilic silicates (OMMT) were selected for the study with different organophilization. The ω -amino acid was expected to form chemical bond with the matrix polymer resulting in strong adhesion, while the use of an aliphatic amine surfactant was assumed to lead to weak interaction. The Nanofil silicates were supplied by Süd Chemie AG, Germany. Sodium montmorillonite was used as reference filler. The

⁵Renner, K., Henning, S., Móczó, J., Yang, M-S., Choi, H-J., Pukánszky, B: *Polym Eng Sci* (47) 1235-1245 (2007)

most important characteristics of the fillers are listed in Table 3.1. Danamid E grade polycaprolactame produced by Zoltek Rt., Hungary was used as matrix material. The filler content of the composites varied in a relatively wide range, they contained 0, 0.5, 1, 1.5, 2, 3, 5, 7 and 10 vol% silicate. The components were homogenized by extruding them twice on a Rheomex S 3/4" single screw extruder driven by a Haake Rheocord EU 10V unit. Set temperatures of the extruder were 220-240-250 °C, while screw speed was 50 rpm. The pellets produced were injection molded to dog-bone type tensile specimens using a Battenfeld BA 200 CD machine at 220-230-250-260 °C set temperatures; the temperature of the mold was kept at 60 °C.

Table 3.1. *The most important characteristics of the silicates used in the study*

Name	Abbrev.	Surfactant		Gallery distance (nm)	Specific surface (m ² /g)	Particle size (μm)	Surface tension, γ_s^d (mJ/m ²)
		Type	Amount (wt%)				
NaMMT	NaMMT	–	0	1.0	26.0	75.0	257
Nanofil 784	N784	12-amino-dodecanoic acid	20	1.7	33.0	3.0	48
Nanofil 948	N948	Distearyl-dimethyl-ammonium chloride	45	3.5	13.0	36.0	31

The gallery structure of the fillers was studied by X-ray diffraction (XRD) using a Phillips PW 1830/PW 1050 equipment with CuK_α radiation at 40 kV and 35 mA excitation current. Exfoliation and structure of the nanocomposites in the nanoscale were qualitatively verified by transmission electron microscopy using a Phillips CM200, EDS DX-4 apparatus. The presence of larger particles was checked by scanning electron microscopy (Jeol JSM 6300). The micrographs were taken from fracture surfaces created at liquid nitrogen temperature. Micrographs were taken also from selected samples broken during tensile testing. Stiffness (E) was determined on injection molded specimens in tensile loading at 0.5 mm/min cross-head speed and 80 mm gauge length. Tensile yield stress (σ_y), yield strain (ϵ_y), tensile strength (σ), and elongation-at-break (ϵ) were calculated from force vs. deformation traces recorded on the same specimens at 5 mm/min cross-head speed. Specimens were conditioned at 23 °C and 50 % relative humidity for 48 hours before mechanical testing. Acoustic emission signals were recorded with a Sensophone AED 40/4 apparatus. Volume strain was determined by measuring also the change in one lateral dimension of the specimen by a strain transducer. The measurements were carried out at 5 mm/min cross-head speed. We assumed that dimensional changes are the same in both lateral directions. Five parallel specimens were measured in all mechanical and micromechanical experiments.

3.3. Results and discussion

The results of the experiments are presented in several sections. First the structure of the nanocomposites in question is analyzed using results derived by various techniques. Subsequently the tensile properties of the composites are presented briefly, then deformation processes are discussed in detail based mainly on the results of acoustic emission measurements. The deformation behavior of the composites is related to their structure in the final section.

3.3.1. Structure

The usual techniques used for the characterization of the structure of layered silicate polymer nanocomposites are XRD and TEM [4-8]. The XRD traces of the two organophilic silicates used and some of their composites are presented in Fig. 3.1. The comparison of the silicates shows that their gallery structure is completely different. Their initial layer distance differs considerably, 1.7 nm for the one coated with the amino acid, while 3.5 nm for that treated with the aliphatic amine (see Table 3.1). The arrangement or regularity of the layers is also dissimilar shown by the overtones appearing in the XRD trace of the clay organophilized with the aliphatic amine, which are absent from the trace of the N784 clay.

Much less difference is observed in the XRD patterns of composites containing the silicates in 1 vol%. The characteristic reflection of the silicate is absent in both traces, which can have two reasons. Either the silicate is completely exfoliated as some groups claim [4-6,10-16] or the intensity of the reflection is below detection level. It has been proven several times that the disappearance of the silicate reflection is not an unambiguous proof of complete exfoliation [17]. The traces recorded on composites with 5 vol% silicate loading indicate the presence of ordered clay entities. Moreover, although the reflection of the silicate shifts slightly, at least in the case of the amino acid coated clay, we cannot exclude completely the presence of some original silicate particles either. Further information is supplied about the exfoliation of the silicates by the integrated peak area of their characteristic reflection, which is plotted in Fig. 3.2 as a function of silicate content. Since besides the amount of reflecting species intensity depends also on the regularity of the stacks and their orientation, this quantitative evaluation must be treated with caution. Nevertheless, the figure indicates the continuous increase in the amount of non-exfoliated silicate with increasing filler loading. Based on these results we might draw also the conclusion that the silicate treated with the aliphatic amine exfoliates more than the one covered with ω -amino acid.

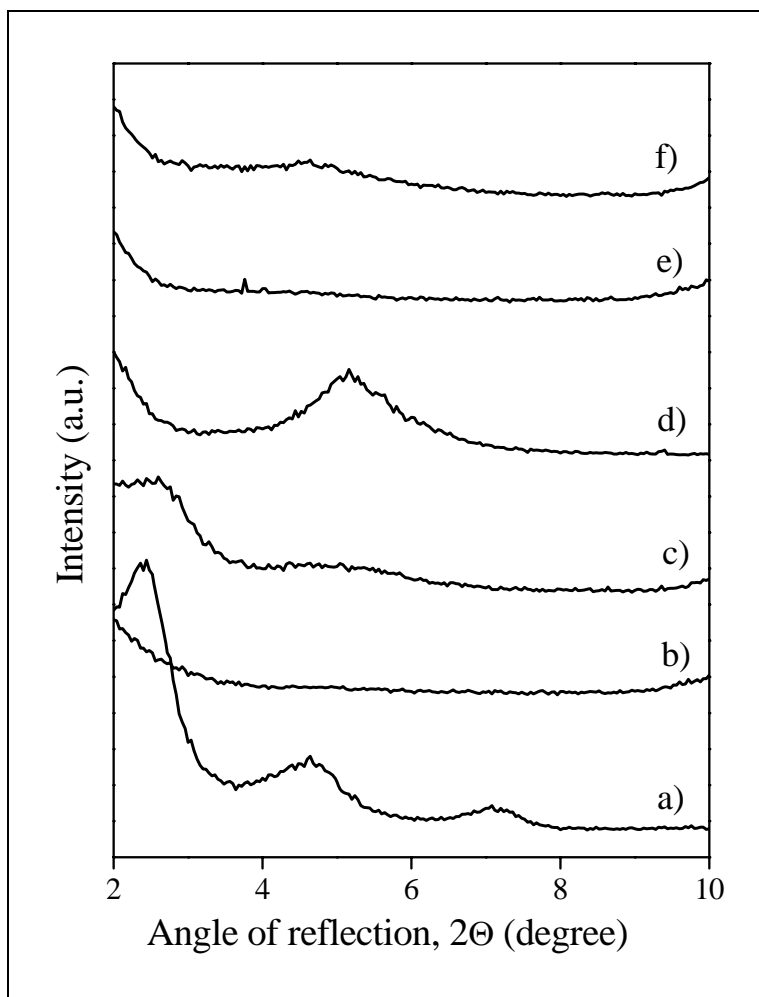


Fig. 3.1 XRD traces recorded on the organophilic silicates used in the study and on some of their composites. a) OMMT coated with hexadecylamine (N948), b) PA6/1 vol% N948, c) PA6/5 vol% N948, d) OMMT coated with ω -amino acid (N784), e) PA6/1 vol% N784, f) PA6/5 vol% N784.

XRD measurements are often supported by TEM micrographs to characterize the structure of nanocomposites [4-8,18]. Such a micrograph is presented in Fig. 3.3a for the composite containing the amino acid treated silicate in 0.5 vol%. Several individual platelets and stacks containing only a few layers are seen in the micrograph as expected, but also a larger particle, which supports the results of XRD measurements indicating the presence of non-exfoliated silicate. At small silicate content TEM micrographs taken from the silicate covered with the aliphatic amine are very similar to that presented in Fig. 3.3a. With increasing silicate content the number of larger structural

units increases in both types of composites. In Fig. 3.3b a partially exfoliated/intercalated tactoid is shown with very different gallery distances along its length. Further increase in silicate content leads to the appearance of more tactoids or even large particles, similar to those present in the composite prepared with NaMMT (Fig. 3.3c). The results clearly indicate that various structural units are present in our composites and structure changes continuously with composition.

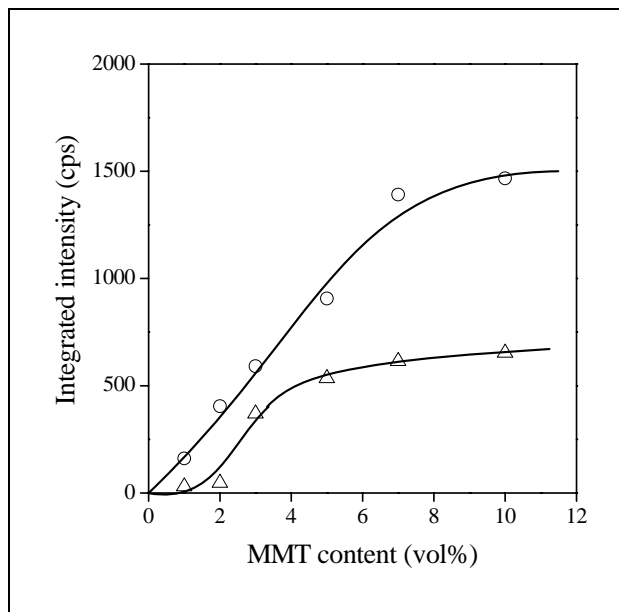


Fig. 3.2 *Integrated intensity of the silicate reflection in PP/OMMT composites plotted against silicate content. (O) amino acid (N784), (Δ) aliphatic amine (N948).*

Large particles are usually not detected in layered silicate nanocomposites because they are rarely looked for. A SEM micrograph is presented in Fig. 3.4 taken from the fracture surface of a composite sample, which contains 5 vol% of the silicate treated with the amino acid. A large particle with a diameter of 30-40 μm is seen in the middle of the micrograph. The particle has very diffuse boundaries and seems to adhere strongly to the matrix. The internal part of the particle appears to be a looser aggregate of smaller units probably formed during processing, since the average particle size of this silicate was 3 μm before composite preparation (see Table 3.1). Thin ribbons peel off the particle, which might be exfoliating stacks of the silicate. Such formations are present in composites containing both organophilic silicates. These and the previous results clearly prove that the structure of our PA nanocomposites is complex; it contains various structural entities in unknown proportions. Deformation mechanism must reflect the complexity of the structure, and we expect the simultaneous occurrence of various deformation processes.

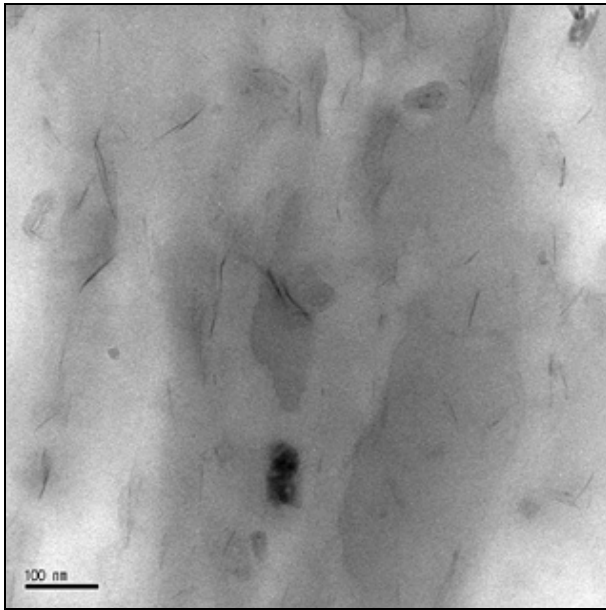


Fig. 3.3a

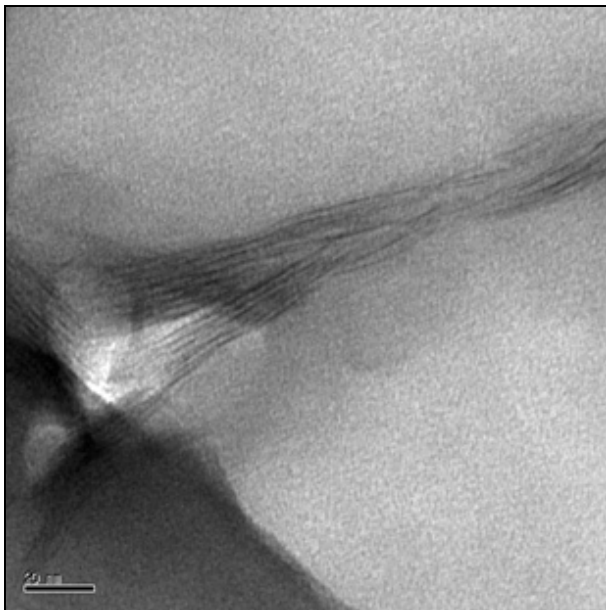


Fig. 3.3b

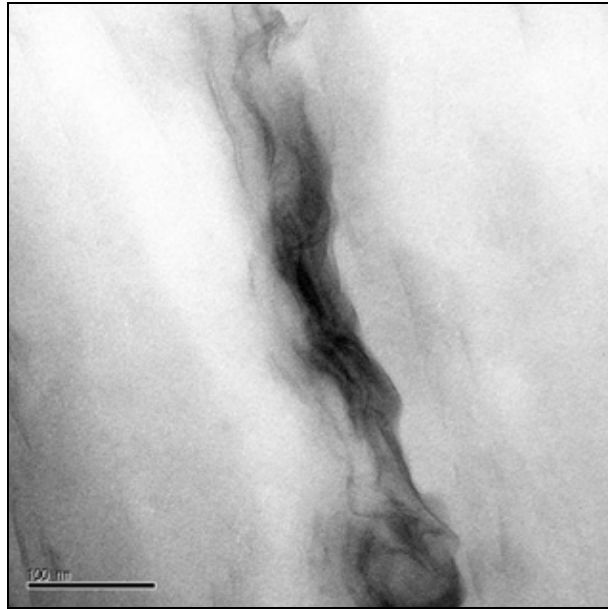


Fig. 3.3c

Fig. 3.3 TEM micrographs of PA6 nanocomposites. a) 0.5 vol% N784, b) 2.0 vol% N948, c) 2.0 vol% NaMMT.

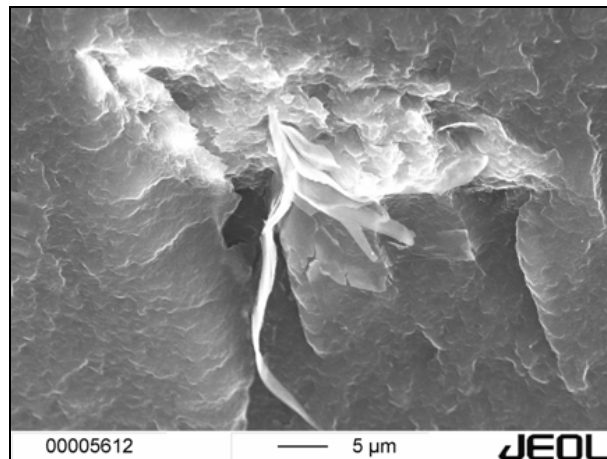


Fig. 3.4 SEM micrograph taken from the fracture surface of a PA6 nanocomposite with 5 vol% N784 (amino acid).

3.3.2. Properties

Stiffness is used the most often for the characterization of the reinforcing effect of silicates in nanocomposites [17]. Sometimes even attempts are made to estimate the extent of exfoliation from changes in modulus [19-21]. The composition dependence of the Young's modulus of our PA composites containing the three different silicates is presented in Fig. 3.5. The stiffness of the composite increases in all three cases, which is not very surprising if we consider the significantly larger modulus of the clay compared to that of the matrix. We can make two interesting observations in relation with Fig. 3.5. The modulus of the composites containing NaMMT and the OMMT treated with the aliphatic amine is practically the same. This similarity may result either from the low extent of exfoliation of this OMMT, since we must assume that NaMMT does not exfoliate at all, or from differences in interfacial interactions.

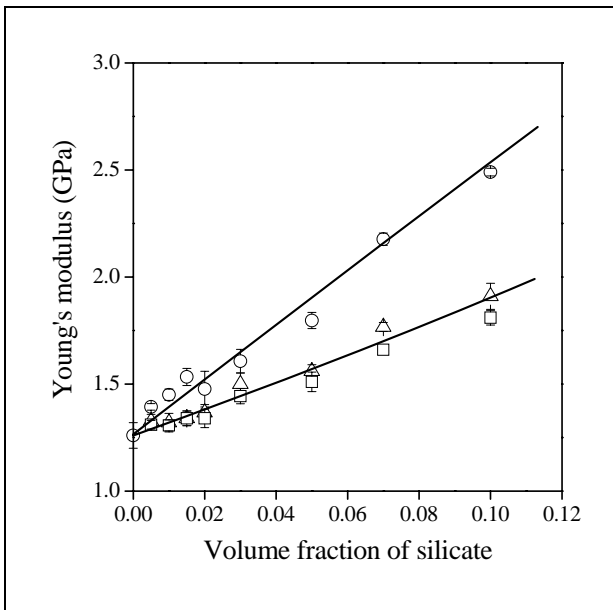


Fig. 3.5 Dependence of the stiffness of PA6 composites on silicate content and on the strength of interaction. (○) amino acid (N784), (△) aliphatic amine (N948), (□) NaMMT.

According to the results of XRD measurements (see Fig. 3.2), the silicate modified with the aliphatic amine exfoliates in a larger extent than the one organophilized with the amino acid and TEM micrographs also indicate considerable exfoliation. On the other hand, the surface free energy of NaMMT is much larger than that of the two organophilized silicates [21], which leads to stronger matrix/filler adhesion, and a

larger modulus. This explanation and the role of interfacial adhesion are further confirmed by the performance of the composites containing the silicate organophilized with the amino acid. The stiffness of these composites is considerably larger than that of the other two, which may be explained by the decreased deformability of the polymer due to the larger extent of exfoliation and strong interaction.

Rather surprisingly, the yield stress of the composites changes much less with filler content than their stiffness (Fig. 3.6), which might be the result of changing deformation mechanism with increasing elongation. On the other hand, a maximum is observed in the yield stress of the two nanocomposites containing the organophilic silicates. The increase in yield stress at small silicate content indicates exfoliation and reinforcement, while the decrease after the maximum suggests changing structure and deformation mechanism. No maximum appears in the yield stress of PA6/NaMMT composites, since the neat silicate does not exfoliate and the structure of these composites does not change with composition. The composition dependence of the mechanical properties of our PA6/silicate composites confirms the results of structural investigations and indicates the change of structure with composition. The results also prove that interfacial interactions play a significant role in the determination of composite properties.

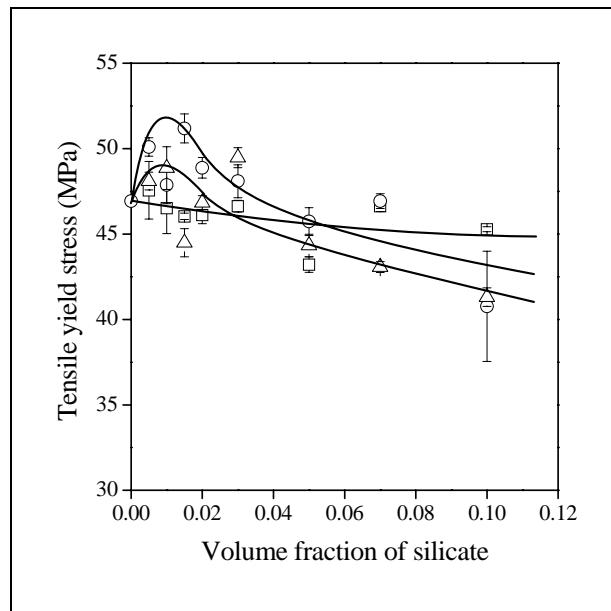


Fig. 3.6 Effect of surface modification and filler content on the tensile yield stress of PA6/layered silicate nanocomposites. Symbols are the same as in Fig. 3.5.

3.3.3. Micromechanical deformations

As indicated in one of the previous sections, several micromechanical deformation processes may take place in our layered silicate composites. The presence of various structural entities increases further the number of possible processes. However, these processes are competitive and we may assume that one or two dominates during deformation and thus determines the properties of the composites. Some local deformations may be accompanied by the emission of sound and its detection may reveal the mechanism of the process. The stress vs. strain trace of a PA6 nanocomposite containing 5 vol% silicate coated with the amino acid is presented in Fig. 3.7. The individual acoustic events detected during the deformation of the sample are also plotted; they are indicated by circles. We can see that the majority of sound emitting events occur before the maximum in the stress vs. elongation correlation is reached. The events might be related to any of the processes listed earlier.

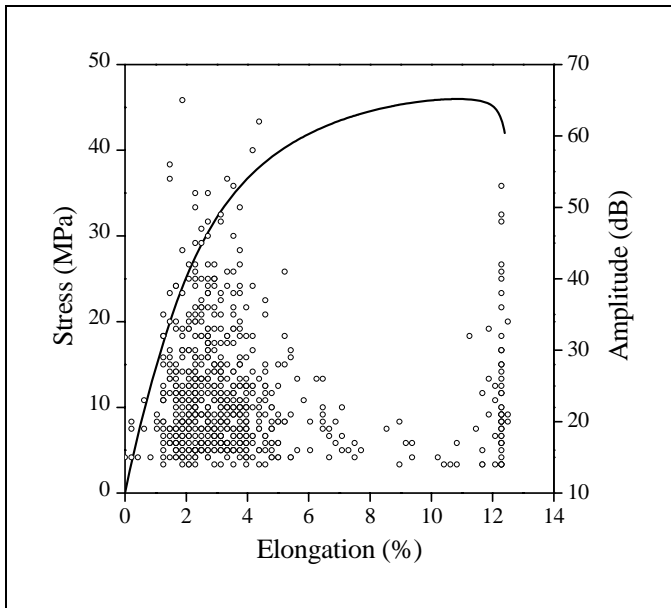


Fig.3.7 *Development of acoustic emission signals during the deformation of a PA6 nanocomposite. Silicate: 5 vol% N784. (○) individual acoustic events, — stress vs. strain trace.*

The evaluation of the individual acoustic signals is difficult. Their number is large and their amplitude changes in a wide range. Various quantities are derived from the primary signals to facilitate evaluation. One of these is the cumulative total number of events (or hits) detected during the deformation of the specimen. The stress vs. strain curve of the matrix polymer is compared to that of the composite containing the amino

acid treated silicate in 5 vol% in Fig. 3.8. The corresponding acoustic emission traces are also shown in the figure. Acoustic signals are detected also in the matrix polymer, but in much smaller number than in the composite. They might be caused by the cavitation of the polymer as proposed by Galeski et al. [22]. We must mention here that the deformability of the neat PA6 polymer is much larger than that of the composites and all analysis is done only up to the maximum of the stress vs. strain curves.

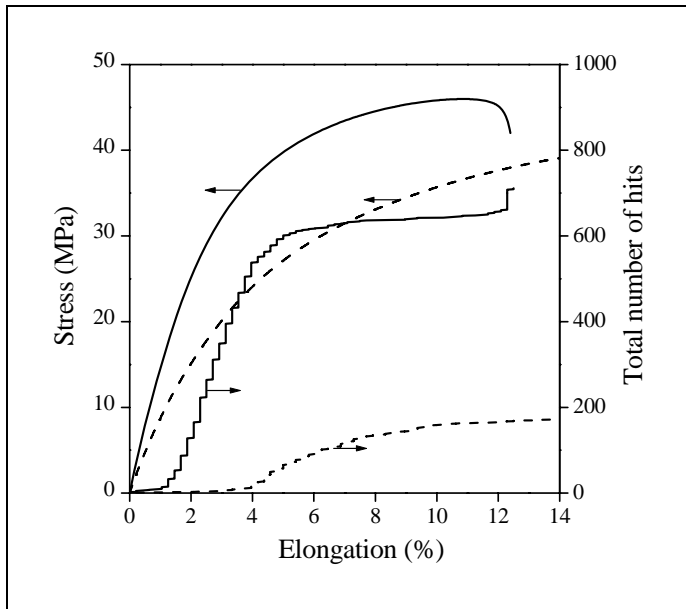


Fig. 3.8 Differences in the acoustic activity of the PA6 matrix polymer (----) and a composite containing 5 vol% N784 silicate (——). Acoustic activity is characterized by the cumulative total number of hits.

The larger number of acoustic events detected in the composite must be related to the silicate. Events start to occur after a certain deformation and most of them are completed before yield stress is reached. The initiation deformation is much smaller in the composite than in the neat matrix polymer which suggests the occurrence of silicate related processes again. These acoustic events might be caused by the fracture of tactoids or particles, or by their debonding. We do not believe that slipping of the layers or the shear yielding of the matrix initiate detectable signals.

The effect of surface modification on the occurrence of acoustic events is demonstrated in Fig. 3.9 for composites containing the three silicates in 5 vol %. Instead of the cumulative total number of hits, we plotted the derivative of this value, because this representation facilitates the identification of the deformation range, in which the majority of the events occur. The stress vs. strain traces of the composites are also plotted in the figure as usual. The generation of signals is the fastest in the composite containing

the silicate treated with the aliphatic amine and the slowest in the PA6/NaMMT composite. We believe that the faster development and earlier completion of events are the result of weaker attraction forces acting in the composite containing the silicate treated with the aliphatic amine surfactant.

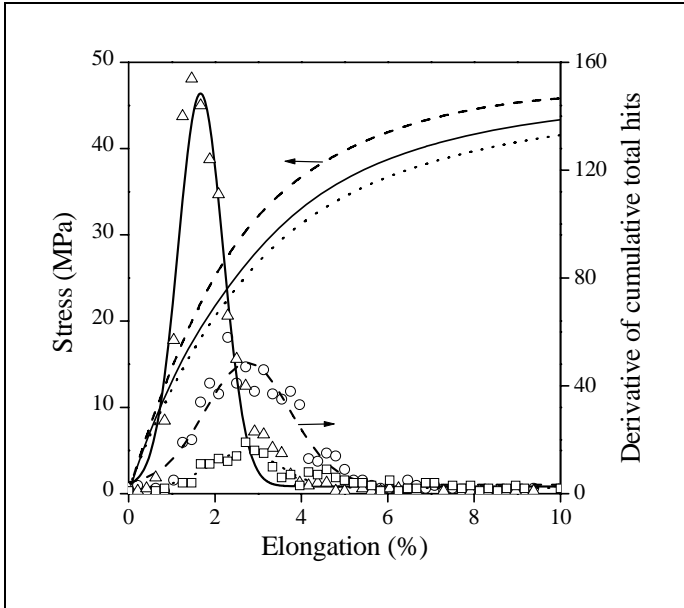


Fig. 3.9. Comparison of the acoustic activity of PA6 composites containing the three different silicates; (O) amino acid (N784), (Δ) aliphatic amine (N948), (\square) NaMMT. The derivative of cumulative total hits shows the maximum rate of acoustic activity.

Further characteristic values might be also derived by the proper evaluation of the acoustic signals detected during the deformation of the samples. The average amplitude of the signals is plotted against silicate content in Fig. 3.10. Various deformation processes were identified by the amplitude of the signals in fiber reinforced composites [23,24]. As a consequence, we may assume that the amplitude of the signal is related to the process emitting it in our composites, too. Somewhat higher amplitudes are detected in the neat polymer than in the composites at small silicate content, what indicates the occurrence of different processes. The amplitude of the signals does not depend on composition in the PA6/NaMMT composites showing constant structure and deformation mechanism. Signals with very low amplitudes are detected in nanocomposites with small silicate content; amplitudes become higher as silicate loading increases. The much stronger signals detected in the composite containing N784 are probably caused by the stronger interaction of this silicate with the matrix.

The total number of hits detected up to yield stress is plotted against filler content in Fig. 3.11. The number of hits is very low in composites containing only a small amount of the silicate. Moreover, fewer signals are developed in these materials than in the neat matrix, which indicates that new processes are initiated in the presence of the silicate and these dominate in all composites. The number of signals increases with increasing silicate content. The total number of hits must be determined by the number of structural units initiating the event and we believe that interaction also plays a role. If debonding of larger units is the dominating process, it definitely must be influenced by the strength of interaction between the silicate and the matrix. Even if tactoids or particles break, the interaction among the layers or parts of the units must depend on the type and extent of organophilization.

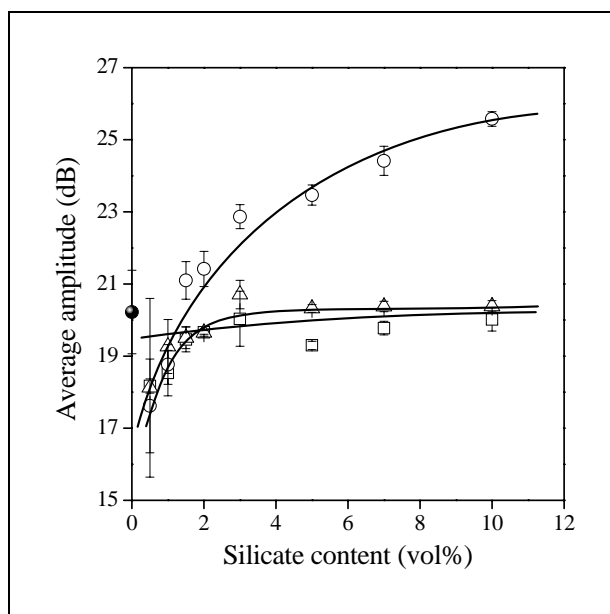


Fig. 3.10 Dependence of the average amplitude of acoustic signals on silicate content. Symbols are the same as in Fig. 3.9; (●) neat PA.

We determined also the stress at the maximum rate of sound generation (see maximums in Fig. 3.9). The values are plotted as a function of silicate content in Fig. 3.12. The stresses related to the sound emitting processes differ for the three silicates. The observed differences might indicate the occurrence of different processes, but we think that they are related mainly to the strength of interaction between the silicates and the matrix polymer. The characteristic stress is much smaller in composites containing the silicate treated with the aliphatic amine as a consequence of weaker interaction. NaMMT adheres to the polymer strongly because of its larger surface free energy (see Table 3.1), but we expect that the strongest bond develops between the amino acid

treated silicate and PA. The minimum observed in the composition dependence of the characteristic stress for the composites containing the N784 silicate is very difficult to understand, its explanation needs further study and considerations.

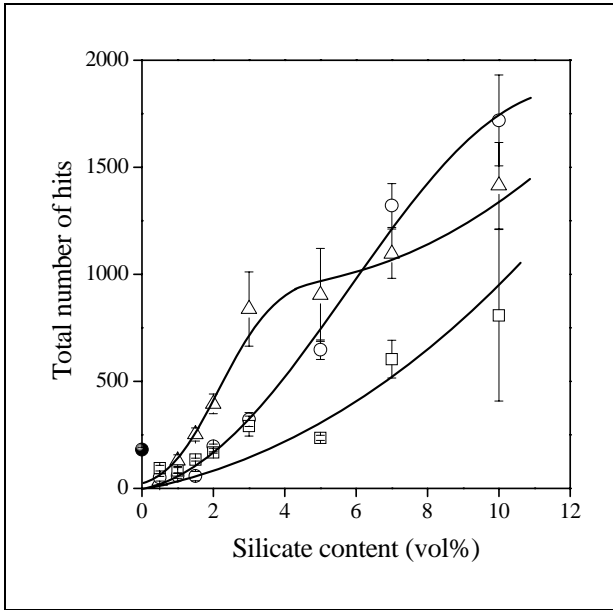


Fig. 3.11 *The effect of interfacial adhesion and silicate content on the total number of hits occurring during the deformation of PA6 nanocomposites. Symbols are the same as in Fig. 3.10.*

Quite a few of the possible micromechanical deformation processes is accompanied by void formation, by the increase of the volume of the specimen during deformation. We hoped that the comparison of volume strain traces to stress vs. strain curves and to the occurrence of acoustic events might supply further information about the deformation mechanism of our composites. We observed strong similarities in the behavior of all composites. Very small volume increase was observed practically in all cases. The largest increase in volume was detected in the composite containing the amino acid treated silicate, while the volume strain of the composite containing the clay organophilized with the aliphatic amine was almost negligible. Analysis of the deformation process and the calculation of strain components showed, that elastic and shear deformation dominate, and considerable volume strain occurs only at larger elongations.

Another very important observation of these measurements is that the majority of acoustic emission events occur before the start of volume increase. This statement is demonstrated by Fig. 3.13 comparing the elongation dependence of volume strain to that of the development of acoustic signals for the composite containing 5 vol% NaMMT. Very similar correlations were obtained for practically all composites containing NaMMT and N784; volume did not increase basically at all in the presence of N948, as mentioned above. According to Fig. 3.13 the process related to the development of acoustic signals is either independent of volume increase or the process results in the acoustic signal lead to void formation and initiates volume strain. We must emphasize here again that the increase of volume is rather small in these composites and elastic deformation and shear yielding dominate during elongation.

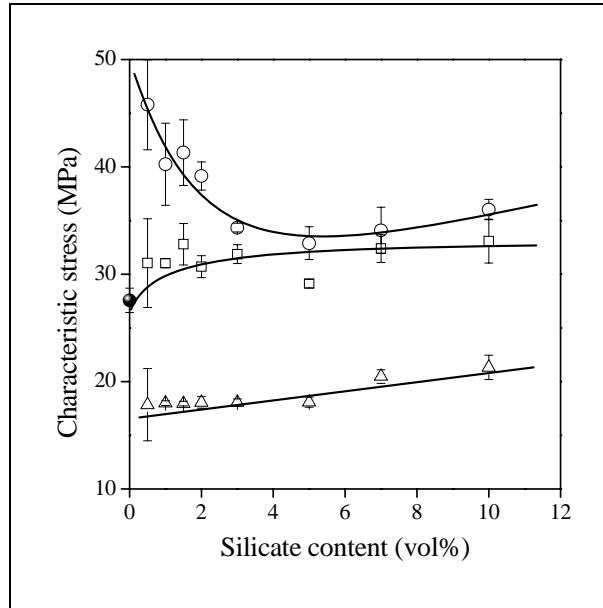


Fig. 3.12 *Dependence of the characteristics stress measured at maximum acoustic activity on organophilization and silicate content. Symbols are the same as in Fig. 3.10.*

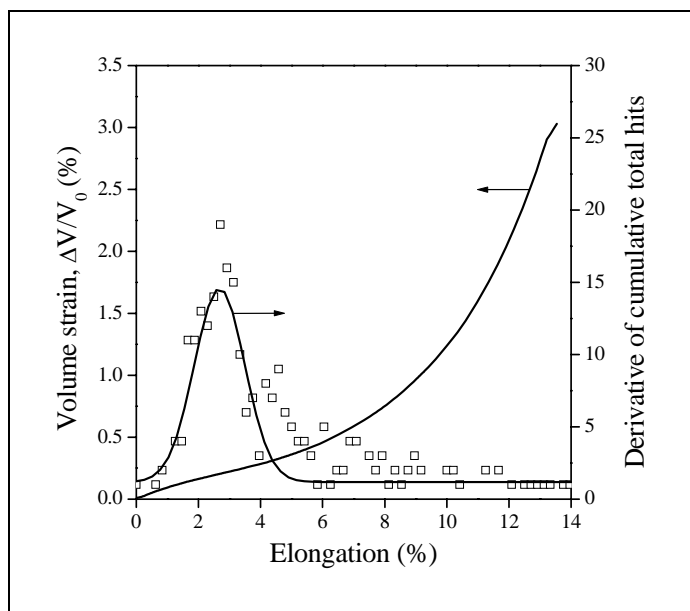


Fig. 3.13 Relationship between the acoustic activity of a composite sample and its volume increase during deformation. Silicate: 5 vol% NaMMT.

3.3.4. Discussion, deformation mechanism

The analysis of volume strain traces and acoustic emission events indicated that the two processes might be related, but acoustic emission events precede volume increase, the extent of which is relatively small. Slipping of silicate layers on each other may occur, as well as the plastic deformation of the matrix, but we do not expect these to generate sound and they are not accompanied by volume increase. The cavitation of the matrix, and particle or tactoid related events may generate most of the sound detected during deformation. Additionally, several of the correlations indicated that different micromechanical processes take place in the matrix and in the composites.

In order to check the relationship of exfoliation, or more exactly the lack of it, and acoustic events, we plotted the total number of hits against the integrated area of clay reflection in Fig. 3.14. Since the characteristic reflection of the silicate disappears in the case of complete exfoliation, it must be related to the amount of non- or only partially exfoliated clay. Two very close correlations were obtained for the organophilized silicates. Composites containing NaMMT could not be analyzed in the same way, since the silicate reflection could not be detected or was extremely weak in their XRD traces. The close correlations indicate that practically all acoustic events are related to non-exfoliated, reflecting entities in the composites. The figure clearly shows also the effect of interfacial interaction. The silicate treated with the aliphatic amine adheres very weakly to the polymer, but also the adhesion among the platelets must be weak. The strong adhesion of the amino acid coated silicate, on the other hand, hinders the

deformation process accompanied by the acoustic events. At small silicate content the distribution of the clay is homogeneous and the extent of exfoliation is large. Even larger tactoids may remain intact during deformation thus sound emission starts only at larger silicate content, when more and larger silicate units are also present in the composite. Several results indicated the change of structure and properties with increasing silicate content and the results of Fig. 3.14 are in line with them.

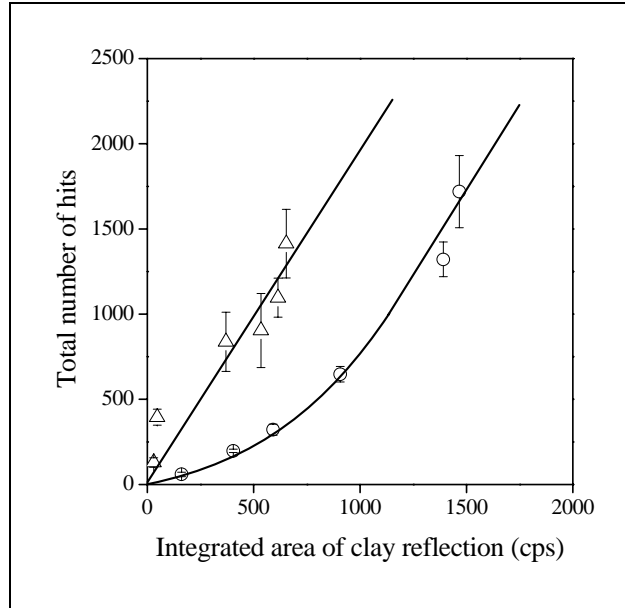


Fig. 3.14 Correlation between the structure characterized by the integrated area of silicate reflection and the total number of acoustic events during deformation. Acoustic events are related to the amount of non-exfoliated silicate; (○) amino acid (N784), (△) aliphatic amine (N948).

The only question which remains to be answered is the process emitting sound and then leading to limited volume increase. The scanning electron microscopic study of deformed samples may help to answer it. Such a micrograph is presented in Fig. 3.15a. A larger and several smaller NaMMT particles can be seen in the micrograph, according to which extensive particle fracture and some debonding takes place during the deformation of the composite. We must emphasize that the composite presented in the figure contained NaMMT without any organophilization, i.e. also the neat silicate fractures during deformation. The process is demonstrated even better in Fig. 3.15b, where the fracture of a NaMMT particle is shown in larger magnification. A part of the particle clearly splits off during the deformation of the composite. It is interesting to note that the adhesion of the filler to the matrix seems to be rather good and debonding is only a secondary process, indeed, as indicated by volume strain measurements.

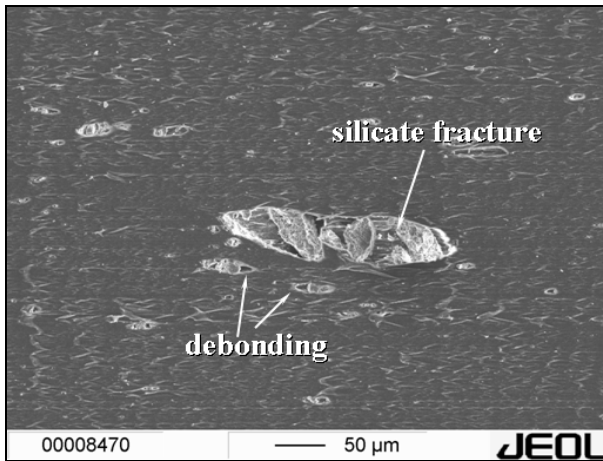


Fig. 3.15a

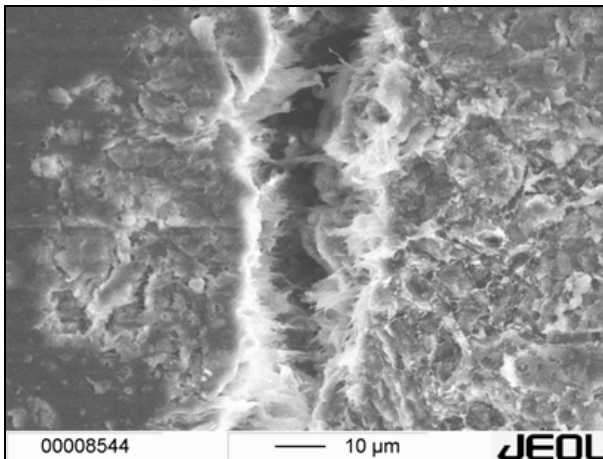


Fig. 3.15b

Fig. 3.15 *Mechanism of micromechanical deformations in PA6/NaMMT composites. a) 1 vol% NaMMT, b) 5 vol% NaMMT.*

We might expect a very different deformation mechanism in the composites containing the organophilic clays. However, according to Fig. 3.16 they deform in a very similar manner, the fracture of larger particles is the dominating failure process also in these composites. The deformation of the composite containing the amino acid treated silicate is shown in Fig. 3.16a, while that of the one prepared with the N948 silicate (aliphatic amine) can be seen in Fig. 3.16b. The micrographs are very similar; the only difference might be in the adhesion of the particles to the matrix. No separation of the interfaces can be detected in Fig. 3.16a, while some voids seem to appear at the surface of the particle in Fig. 3.16b, but the evidence is rather ambiguous. The easier

deformation of the composite containing the aliphatic amine treated silicate is probably the result of the larger amount of surfactant (see Table 3.1) used and the weaker interaction among the silicate platelets or larger units forming during drying in the organophilization process, as well as during the preparation of the composites.

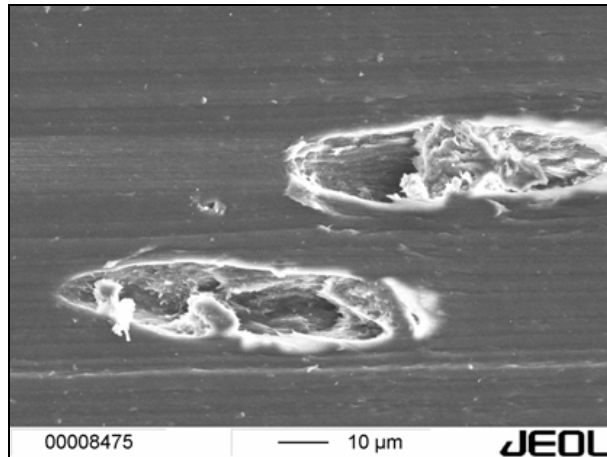


Fig. 3.16a

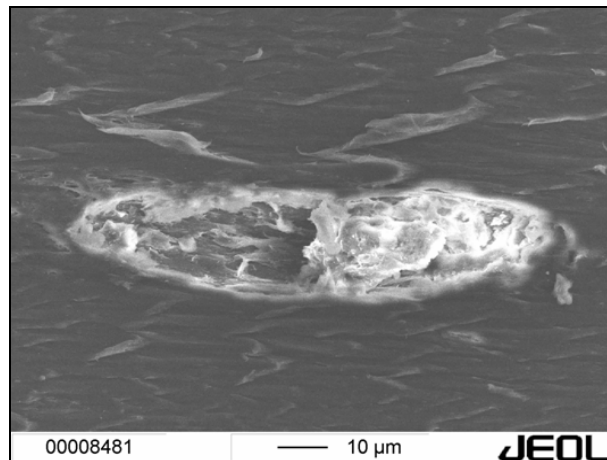


Fig. 3.16b

Fig. 3.16 Mechanism of deformation in PA6/OMMT nanocomposites. a) 1 vol% N784 (amino acid), b) 1 vol% N948 (aliphatic amine).

3.4. Conclusions

The results obtained in the study of PA6/NaMMT composites and PA/OMMT nanocomposites prepared from silicates with drastically differing organophilization showed that the structure of the composites is more complicated than usually stated. They contain various structural entities; besides individual silicate platelets, tactoids with different degree of intercalation and larger particles can be also found in them. Volume strain measurements and the analysis of the deformation process showed that elastic deformation and shear yielding dominates during the elongation of the specimens. The matrix polymer and the composites deform according to different mechanisms. Sound is emitted by cavitation in the former, while sound emitting processes are related to larger structural entities, i.e. to tactoids and non-exfoliated particles in the composites. Acoustic events are generated mainly by the fracture of the particles. Matrix/silicate adhesion seems to be strong, debonding rarely takes place, and volume increase is initiated primarily by particle failure. The type and amount of the surfactant used for organophilization plays an important role in the determination of deformation processes and properties, since it influences both matrix/filler interaction and the internal adhesion of silicate particles.

3.5. References

1. Kim, G. K., Lee, D. H., Hoffmann, B., Kressel, J., Stöppelmann, G.: *Polymer* **42**, 1095-1100 (2001)
2. Gloaguen, J. M., Lefebvre, J. M.: *Polymer* **42**, 5841-5847 (2001)
3. Rácz, L., Pukánszky Jr., B., Pozsgay, A., Pukánszky, B.: *Progr Colloid Polym Sci* **125**, 96-102 (2004)
4. Varlot, K., Reynaud, E., Kloppfer, M. H., Vigier, G., Varlet, J.: *J Polym Sci Part B, Phys.* **39**, 1360-1370 (2001)
5. Lan, T., Pinnavaia, T. J.: *J Chem Mater* **6**, 2216-2219 (1994)
6. Vu, Y. T., Rajan, G. S., Mark, J. E., Myers, C. L.: *Polym Int* **53**, 1071-1077 (2004)
7. Fornes, T. D., Paul, D. R.: *Polymer* **44**, 493-5013 (2003)
8. Wang, Z. M., Nakajima, H., Manias, E., Chung, T. C.: *Macromolecules* **36**, 8919-8922 (2003)
9. Liu, L. X., Wu, Q. J., Zhang, Q. X., Mo, Z. S.: *Polym Bull* **48**, 381-387 (2002)
10. Fornes, T. D., Yoon, P. J., Hunter, D. L., Keskkula, H., Paul, D. R.: *Polymer* **43**, 5915-5933 (2002)
11. Ellis, T. S., D'Angelo, J. S.: *J Appl Polym Sci* **90**, 1639-1647 (2003)
12. Kawasumi, M., Hasegawa, N., Kato, M., Usuki, A., Okada, A.: *Macromolecules* **30**, 6333-6338 (1997)
13. Hasegawa, N., Okamoto, H., Kawasumi, M., Kato, M., Tsukigase, A., Usuki, A.: *Macromol Mater Eng* **280**, 76-79 (2000)
14. Hasegawa, N., Usuki, A.: *J Appl Polym Sci* **93**, 464-470 (2004)
15. Kaempfer, D., Thomann, R., Mühlaupt, R.: *Polymer* **43**, 2909-2916 (2002)
16. Reichert, P., Hoffmann, B., Bock, T., Thomann, R., Mühlaupt, R., Friedrich, C.:

-
17. Százdi, L., Ábrányi, Á., Pukánszky Jr., B., Vancso, G. J., Pukánszky, B.: *Macromol Rapid Commun* **22**, 519-523 (2001)
 18. Százdi, L., Ábrányi, Á., Pukánszky Jr., B., Vancso, G. J., Pukánszky, B.: *Macromol Mater Eng* **291**, 858-868 (2006)
 19. Osman, M. A., Rupp, J. E. P., Suter, U. W.: *Polymer* **46**, 1653-1660 (2005)
 20. Giannelis, E. P., *Appl Organomet Chem* **12**, 675-680 (1998)
 21. Wang, H., Zeng, C. C., Elkovitch, M., Lee, L. J., Koelling, K. W.: *Polym Eng Sci* **41**, 2036-2046 (2001)
 22. Kádár, F., Százdi, L., Fekete, E., Pukánszky, B.: *Langmuir* **22**, 7848-7854 (2006)
 23. Galeski, A.: *Prog Polym Sci* **28**, 1643-1699 (2003)
 24. Karger-Kocsis, J., Harmia, T., Czigány, T.: *Compos Sci Technol* **54**, 287-298 (1995)
 25. Haselbach, W., Lauke, B.: *Compos Sc. Techno.* **63**, 2155-2162 (2003)

Chapter 4

Deformation and failure of wood flour reinforced composites: effect of inherent strength of wood particles⁶

4.1. Introduction

A previous study on wood flour filled PP composites showed that four micro-mechanical deformation processes occur during the deformation of such materials [1]. The matrix polymer deforms mainly by shear yielding which does not emit much sound. The presence of wood flour initiates particle related processes. Debonding dominates in the absence of coupling agent, which is initiated at very small deformations and stresses. The pull-out of fibers may follow the debonding of large particles at an intermediate stress level. The introduction of a functionalized polymer increases interfacial adhesion considerably and completely changes the deformation mechanism. Although debonding of very large particles may take place at intermediate stress levels, the dominating deformation process is the fracture of wood particles. We concluded from these results that further improvement of composite strength is possible only by the increase of the inherent strength of wood particles. One way to do that might be the decrease of their size. Accordingly, the goal of this study was the investigation of the effect of interfacial adhesion and wood particle size on the deformation mechanism and failure of PP/wood composites, to identify the main factors determining macroscopic properties and to find ways to improve composite performance, if possible.

4.2. Experimental

The polymer used as matrix in the experiments was the Tipplon R 359 grade random copolymer (MFR = 10 g/10 min at 230 °C and 2.16 N) produced by TVK, Hungary. Two wood flours with different particle sizes (Filtracel EFC 1000, $d = 210 \mu\text{m}$ and Arbocel CW 630 PU, $d = 30 \mu\text{m}$) were obtained from Rettenmaier GmbH, Germany. The two fillers are abbreviated as W68 and W35 in further discussion. Two maleinated polypropylenes with different properties were added to the composites in order to improve interfacial adhesion (Licomont AR 504, Clariant, $M_n = 3500 \text{ g/mol}$, MA = 3.5 wt% and Orevac CA 100, Atofina, $M_n = 25000 \text{ g/mol}$, MA = 1.0 wt%). The wood flour content of the composites changed between 0 and 80 wt% at a MAPP/wood ratio of 0.1. The components were homogenized in a Werner and Pfleiderer LDUK IKRPV internal mixer for 15 min at 180 °C then compression molded into 4 mm thick plates. Molding was carried out at 190 °C using a Wickert WLP 800/4/2.5 machine.

Mechanical properties were characterized by tensile testing using an Instron 5566 apparatus. Stiffness (E) was determined at 0.5 mm/min cross-head speed and 80

⁶Renner, K., Móczó, J., Pukánszky, B: *Compos Sci Technol* **69**, 1653-1659 (2009)

mm gauge length. Tensile strength (σ), and elongation-at-break (ϵ) were calculated from force vs. deformation traces measured on the same specimens at 5 mm/min cross-head speed. Acoustic emission signals were recorded with a Sensophone AED 40/4 apparatus. Volume strain was determined by measuring the change also in one lateral dimension of the specimen by a strain transducer. We assumed that dimensional changes are the same in both lateral directions. Particle characteristics of the wood flour and the structure, as well as deformation mechanism of the composites were studied by SEM on fracture surfaces created at liquid nitrogen temperature. Micrographs were taken from broken surfaces using a JEOL JSM 6380 LV equipment.

4.3. Results and discussion

Earlier experience and results obtained in the present study showed that the characteristics of the MAPP used as coupling agent have only a small influence on the deformation mechanism and properties of the composites. As a consequence, we focus our attention mainly on the effect of particle size and adhesion generally during the discussion of the results and do not emphasize the type of MAPP used. Most of the results presented were obtained with the Orevac CA 100 coupling agents having smaller functionality and larger molecular weight. The results are presented in several sections. First we discuss the particle characteristics of the wood flours, and then show the composition dependence of tensile properties. The results of micromechanical testing are presented subsequently and deformation mechanism is discussed in the final section.

4.3.1. Particle characteristics

As mentioned above, one of our goals was to study the effect of the particle size of the wood flour on the deformation mechanism and properties of PP/wood composites. Two wood flours with different particle characteristics were selected for this purpose. The particle size distribution of the two fillers is shown in Fig. 4.1. The difference in the particle size and size distribution of the two wood flours is clear. The most frequent particle size of the W68 grade is around 210 μm , while that of the W35 is approximately 30 μm . Their particle size distribution also differs somewhat, the W68 grade has a considerably broader distribution with some very large, several mm long particles. We must call attention here to the fact that in spite of the one order of magnitude difference in the size of the particles, both sizes are large, such particles debond very easily in composites put under external load.

The particles have anisotropic geometry; their aspect ratio differs from 1 as shown in Fig. 4.2. The average aspect ratio is approximately 6.8 for the W68 grade, i.e. for the large particles, and 3.5 for the W35 filler. The abbreviation for the two fillers is based on their aspect ratio. As a consequence, besides size the aspect ratio and the orientation of the particles also may influence composite properties. During the evaluation of the results we assumed that average orientation is practically the same, since the samples were prepared under the same conditions by the same technology.

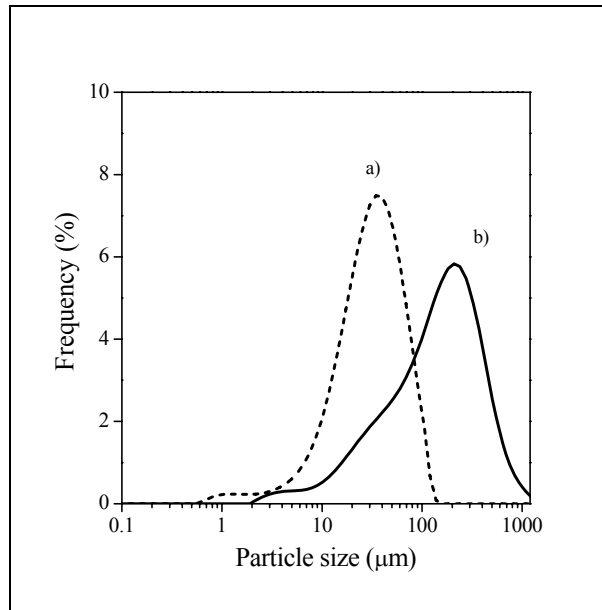


Fig. 4.1 Particle size distribution of the two wood flours used in the experiments; a) W35 (small), b) W68 (large).

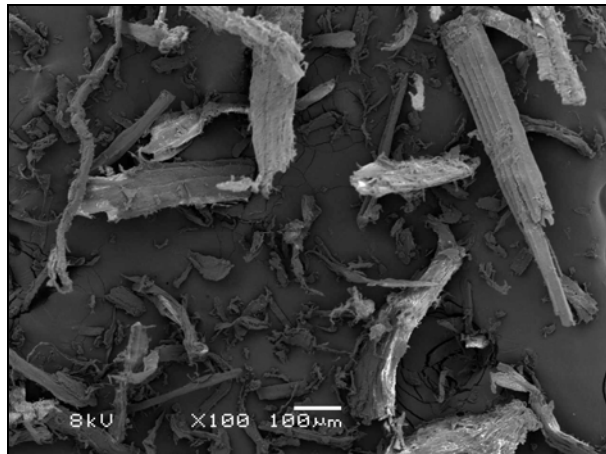


Fig. 4.2a

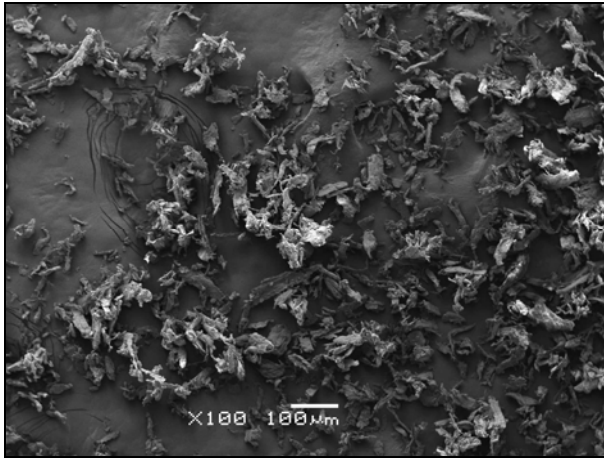


Fig. 4.2b

Fig. 4.2 SEM micrographs showing the particle characteristics of the wood flours; aspect ratio is ~ 3.5 for W35 and ~ 6.8 for W68.

4.3.2. Composite properties, reinforcement

Since PP/wood composites are mainly used in structural applications, the effect of wood flour on stiffness and strength are very important. The Young's modulus of the composites is plotted against wood flour content in Fig. 4.3. Stiffness increases considerably with increasing wood content, but neither particle characteristic nor interfacial adhesion influence modulus very strongly. The lack of any effect of size or adhesion is not very surprising, since earlier studies proved that interfacial adhesion and structure influence stiffness much less than properties determined at larger deformations, i.e. tensile yield stress or tensile strength both in particulate filled and short fiber reinforced composites [2-4]. At larger filler content, a few points deviate from the general tendency indicated by the solid line. We assume that the deviation is caused by the aggregation of the particles, which is caused by simple geometrical reasons, since the maximum packing fraction of the reinforcement is reached in the upper range of studied compositions [5].

Our previous study carried out with the W68 grade filler proved that the dominating deformation mechanism is the fracture of wood particles in the presence of both functionalized polymers used in this study [1]. We assumed that small particles have larger inherent strength and they do not break under the effect of external load, thus we expected better reinforcement and larger composite strength for the small particles. The strength of the composites containing the two fillers is plotted as a function of wood content in Figure 4.4. Composite strength is small and decreases with increasing wood content in the absence of the functionalized polymer. At large filler content the deviation from the general tendency indicated by the solid line is caused again by the aggregation of the particles. Particle size does not influence composite strength at all when interfacial interaction is weak. The introduction of MAPP results in considerable rein-

forcement, in a large increase of strength due to improved adhesion. Particle size has a slight influence in this case, which contradicts all our expectations and requires further considerations.

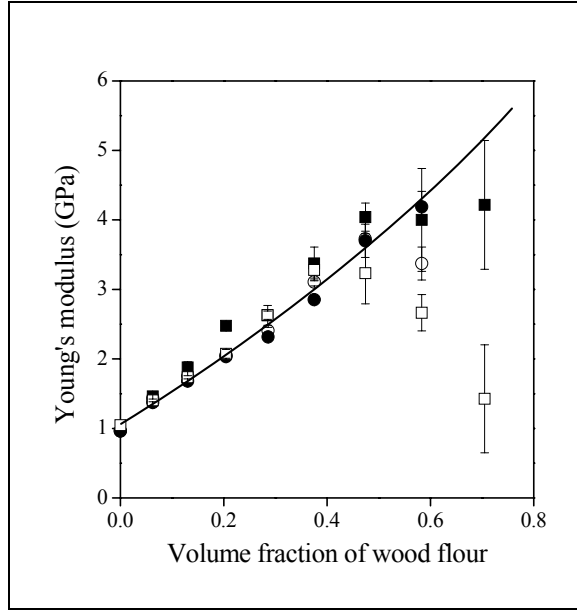


Fig. 4.3 Effect of wood content, particle size and adhesion on the Young's modulus of PP/wood flour composites. (\square) W68, no MAPP, (\blacksquare) W68 with MAPP, (\circ) W35, no MAPP, (\bullet) W35 with MAPP.

The reinforcing effect of a filler or fiber can be expressed quantitatively with the help of a simple model developed earlier [1,6] (see Chapter 2). The model presented there for yield stress can be modified to describe also the composition dependence of tensile strength. The modified model takes into account the effect of the decreasing load-bearing cross-section of the polymer as an effect of filling, while changing interaction is expressed by an exponential term, i.e.

$$\sigma_T = \sigma_{T0} \lambda^n \frac{1-\varphi}{1+2.5\varphi} \exp(B\varphi) \quad (4.1)$$

where σ_T and σ_{T0} are the true tensile strength ($\sigma_T = \sigma\lambda$ and $\lambda = L/L_0$) of the composite and the matrix, respectively, n is a parameter expressing the strain hardening tendency of the matrix, φ is the volume fraction of the wood flour in the composite and B is related to the relative load-bearing capacity of the filler, i.e. to the extent of reinforcement, which depends on interfacial interaction. The relationship of B with the size of the interface and the properties of the interphase are reflected by Eq. 4.2

$$B = (1 + A_f \rho_f \ell) \ln \frac{\sigma_{Ti}}{\sigma_{T0}} \quad (4.2)$$

where A_f and ρ_f are the specific surface area and density of the filler, while ℓ and σ_{Ti} the thickness and strength of the interphase. We can write Eq. 4.1 in linear form

$$\ln \sigma_{Tred} = \ln \frac{\sigma_T (1 + 2.5 \varphi)}{\lambda^n (1 - \varphi)} = \ln \sigma_{T0} + B \varphi \quad (4.3)$$

and plotting the reduced tensile strength of the composite against wood flour content should result in a linear correlation, the slope of which is proportional to the reinforcing effect of the fiber. The reduced tensile strength of some of the studied composites is plotted in Fig. 4.5 in the form indicated by Eq. 4.3. We obtain straight lines, indeed, with some deviation at large filler content due to structural effects, i.e. aggregation. The slope of the straight lines is also shown in Table 4.1.

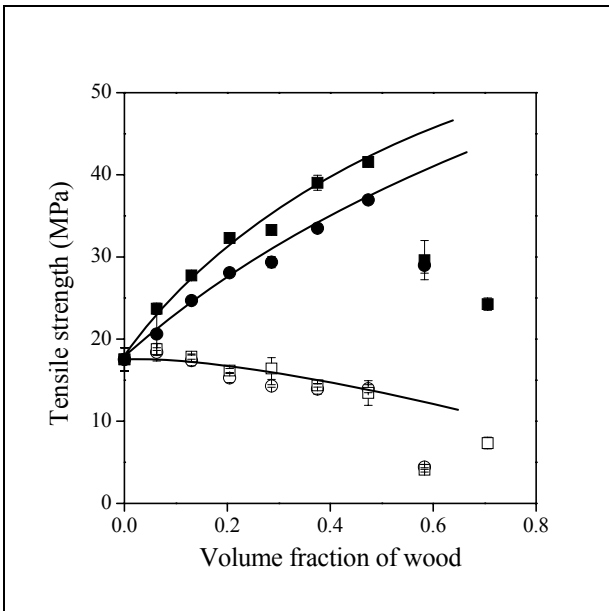


Fig. 4.4 Effect of wood content, particle size and adhesion on the tensile strength of PP/wood flour composites. Symbols are the same as in Fig. 4.3.

We can see that the effect of particle size on reinforcement is even less than estimated qualitatively from Fig. 4.4. However, we must call attention here to the fact that we expected considerable improvement in strength with decreasing particle size and just the opposite occurred. The composites containing the small particles are slightly weaker than those prepared with the W68 grade. The reason for the lack of reinforcement is unclear, either the deformation mechanism did not change and the fracture of

particles dominates also at the small size or some other, uncontrolled factor also influences properties. The answer might be given by the results of micromechanical testing.

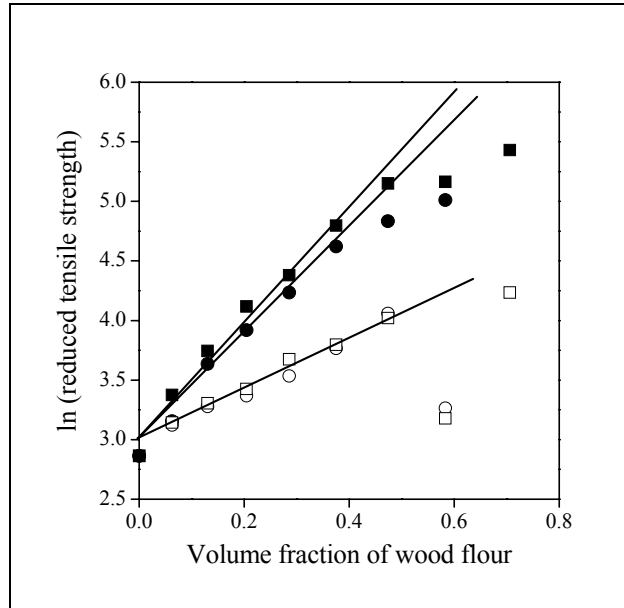


Fig. 4.5 Relative tensile strength of PP/wood flour composites plotted against composition in the linear representation of Eq. 4.3. See the change in reinforcement with increased adhesion. Symbols are the same as in Fig. 4.3.

Table 4.1 Effect of particle size and the type of functionalized polymer on the reinforcing effect of wood flour in PP composites

Wood flour	Parameter B		
	neat	Orevac	Licomont
W68	2.32	4.94	4.70
W35	2.33	4.67	4.67

4.3.3. Micromechanical deformations

We plot the stress vs. strain correlation of the composite containing 20 vol% of the large particles in the absence of MAPP, i.e. when the adhesion is poor between the components in Fig. 4.6. The small circles indicate the acoustic events detected, which

were assigned mainly to debonding and to fiber pull out before [1]. We can see that a considerable number of such events occur during the deformation of the composite up to the failure of the specimen. Changing particle size leads to a significant decrease in the number of acoustic events and also the amplitude of the signals becomes smaller (Fig. 4.7). Moreover, not only the number and the amplitude of the signals is different for the composites containing the smaller particles, but their distribution, as well. Comparison of Figures 4.6 and 4.7 clearly prove that changing particle size leads to an important modification in the micromechanical deformation behavior of the composites. This change, however, does not appear in the macroscopic properties, the smaller number of micromechanical events is not accompanied by an increase in composite strength, which is rather surprising.

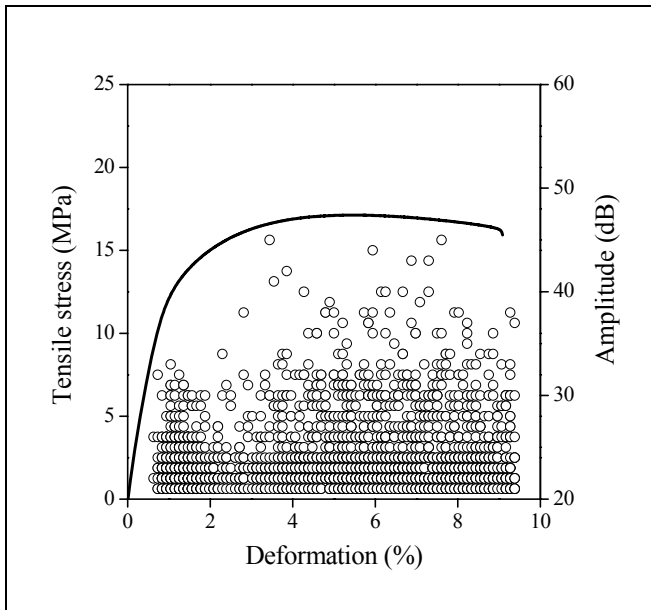


Fig. 4.6 *Acoustic emission signals detected during the tensile testing of PP/wood composites containing the large particles (W68) in 20 wt%. No MAPP, poor adhesion. Symbols: ——— stress vs. strain trace; (O) acoustic events.*

The evaluation of individual acoustic events is difficult and it is almost impossible to draw far reaching conclusions from the results presented in Figs. 4.6 and 4.7. In order to facilitate evaluation, we plotted the cumulative number of acoustic events as a function of deformation in the case of poor adhesion, i.e. in the absence of MAPP, for composites containing 20 wt% wood in Fig. 4.8. The corresponding stress vs. strain traces of the composites are also presented in the figure for reference. Individual acoustic signals are not plotted in order to simplify the figure and facilitate understanding [1,7]. The deformation and failure behavior of the two composites differ considerably from each other. Although tensile yield stress and strength are more or less the same,

the ultimate deformation of the composite containing the large particles is much smaller than that of the material prepared with the CW35 grade filler. Contrary to deformation behavior, rather large differences exist in the number of acoustic hits detected during deformation. Both the character of the cumulative number of hits vs. deformation traces and the actual values differ considerably. The correlation obtained for the composites containing the large particles exhibits two steps. The first was assigned to the debonding of wood particles, while the second to fiber pull out. Small particles debond at larger deformation and stress as predicted by theory [8,9]. The total number of debonding events is somewhat larger in the composite containing the small particles, but it is even more important that only one process takes place during deformation in this case. Pull-out does not occur almost at all in the composite containing the small particles, the cumulative total number of hits remains practically constant after the debonding of larger particles is completed, it does not increase with increasing deformation. It is obvious that the deformation of the composite containing the small particles differs from that prepared with the W68 filler, but the differences correspond to the expectation. In the absence of MAPP debonding starts at larger deformation and stress due to the smaller size of the particles [6,10] and because of the relatively narrow particle size distribution of this filler, it is completed in a very narrow deformation range (see Chapter 2).

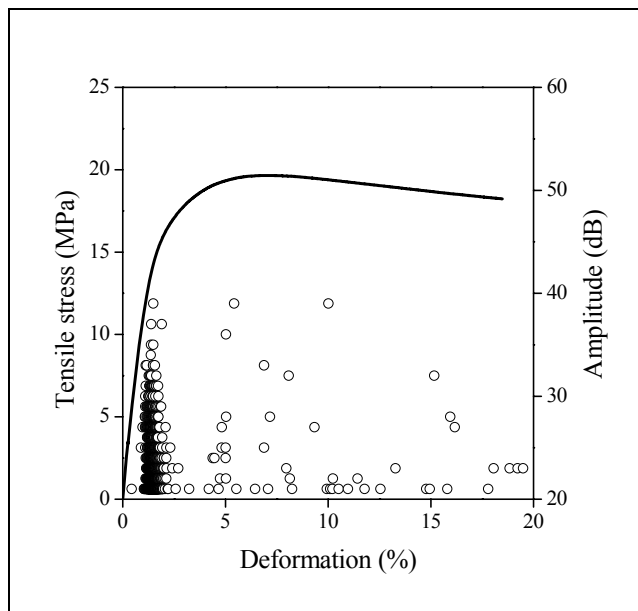


Fig. 4.7 *Acoustic emission signals detected during the tensile testing of PP/wood composites containing the small particles (W35) in 20 wt%. No MAPP, poor adhesion. Symbols are the same as in Fig. 4.6. See also the definition of characteristic deformation values (ϵ_{AE1} , ϵ_{AE2}).*

Deformation behavior and the corresponding acoustic emission results are plotted in Fig. 4.9 for composites containing also a functionalized polymer. Improved adhesion is shown by the considerably increased yield stress and tensile strength of the composites. The relative deformability of the two materials remained the same. The really drastic change is observed in the cumulative number of acoustic events. Only one process takes place during deformation and this was identified as the fracture of wood particles in composites prepared with the W68 filler [1]. The dependence of the cumulative number of hits changes drastically for the composite containing the small particles. Hardly any events are picked up during the entire deformation process. Most probably limited extent of debonding and the fracture of a few larger wood particles result in the few acoustic events detected. Figs. 4.8 and 4.9 clearly prove that the mechanism of deformation changes with particle size as assumed originally, particles do not break and do not debond in the presence of an appropriate coupling agent.

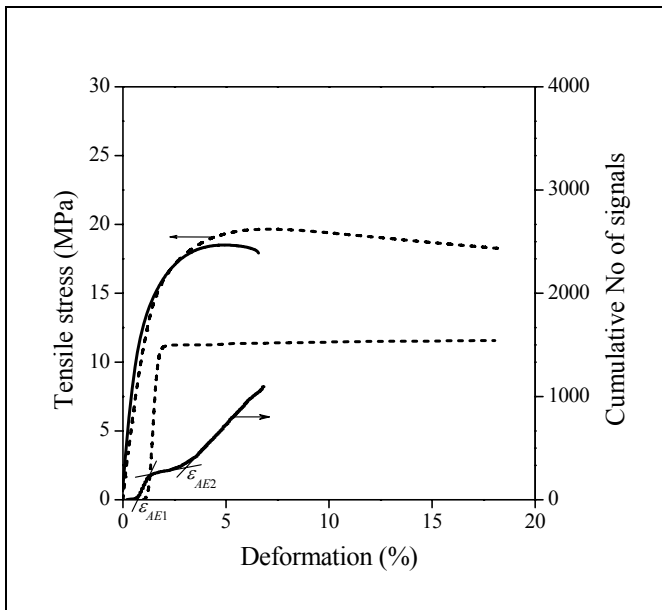


Fig. 4.8 Stress vs. deformation and cumulative number of acoustic events vs. deformation traces for PP/wood composites containing 20 wt% wood flour without MAPP (weak adhesion); ——— W68, ----- W35.

Based on Fig. 4.9, it is very difficult to define the dominating mechanism during the deformation of the composites containing the small particles in the case of good adhesion. Both fiber fracture and debonding is accompanied by the emission of sound, but practically no events were detected during the deformation of the specimens. On the other hand, both processes are accompanied also by a volume increase. As a consequence, volume strain measurements might give us some indication about the dominating process. Since the mechanism of failure was unambiguously identified in compos-

ites containing the large particles, only the volume strain traces recorded on specimens containing the small particles are shown in Fig. 4.10.

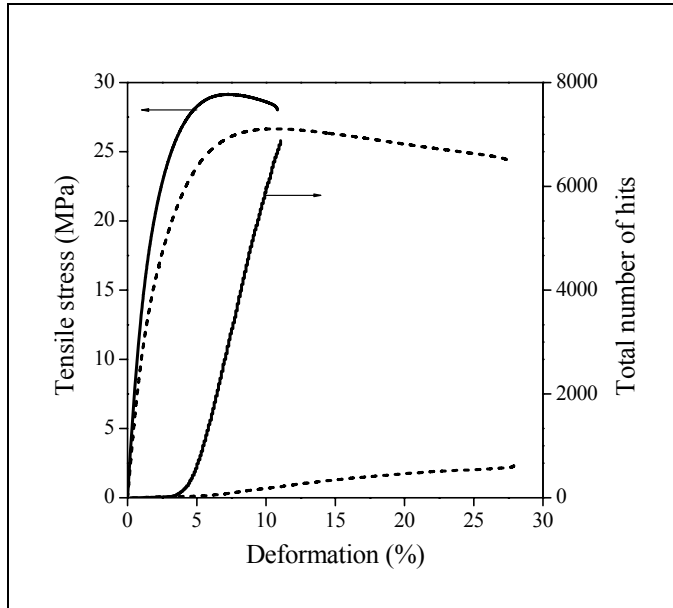


Fig. 4.9 Stress vs. deformation and cumulative total number of acoustic events vs. deformation traces for PP/wood composites containing 20 wt% wood flour at 0.1 MAPP/wood ratio (strong adhesion); ——— W68, - - - - - W35.

The corresponding stress vs. strain correlations are also presented to help evaluation. The effect of changing adhesion was discussed in the previous section and can be clearly seen in the figure. Larger strength and smaller deformability is the result of improved adhesion. However, it is also clear that although debonding starts at larger deformation, considerable volume increase is measured also in composites containing MAPP, in spite of the almost complete lack of sound. Taking into consideration the results of acoustic emission and volume strain measurements we can conclude that the dominating deformation mechanism in composites containing the small particles is debonding. One may argue that debonding should give sound and acoustic events should be detected also in this case. However, our experience with particulate fillers shows that no sound is emitted by debonding at small particle sizes. Obviously the same effect, which needs further study and explanation, is observed here.

Further proof for this explanation is supplied by SEM micrographs. Large particles break during the failure of the composites indeed as shown by Fig. 4.11a for the composite prepared with the W68 wood flour. We can also see that practically no debonding can be detected on the fracture surface of the specimen studied. On the other hand, the fracture of particles does not occur in composites containing the wood flour with the smaller particle size, but a few debonded particles can be observed instead (Fig.

4.11b). Unfortunately the identification of any mechanism is rather difficult on these micrographs because of the poor contrast between the phases. Further analysis is needed to confirm our hypotheses and to identify the dominating processes.

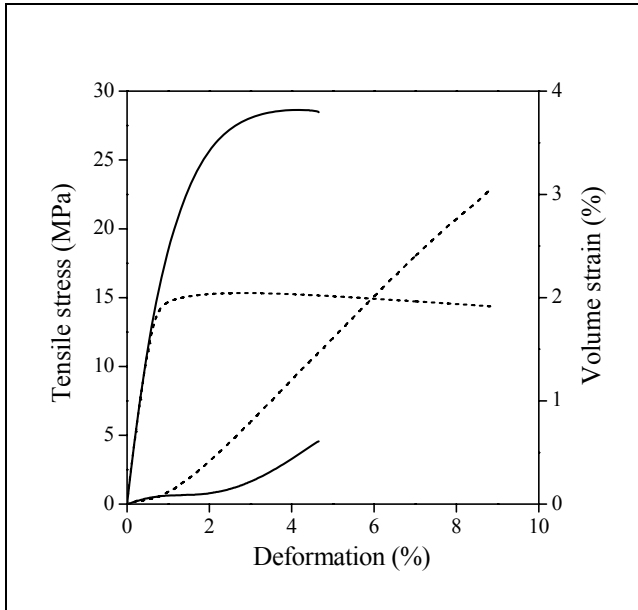


Fig. 4.10 Volume strain traces of PP/wood composites containing the small particles (W35) in 40 wt% at poor (no MAPP) and good adhesion (with MAPP).

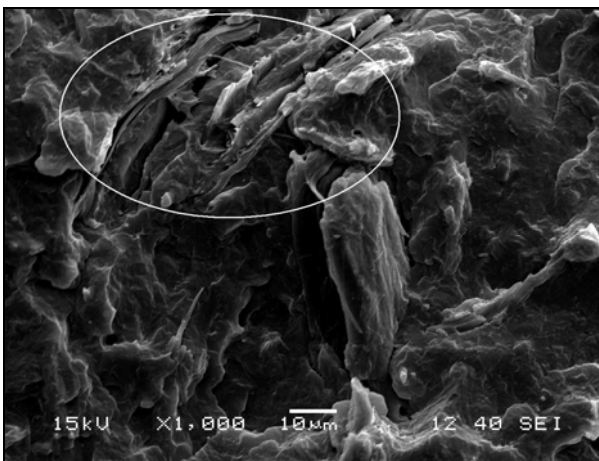


Fig. 4.11a

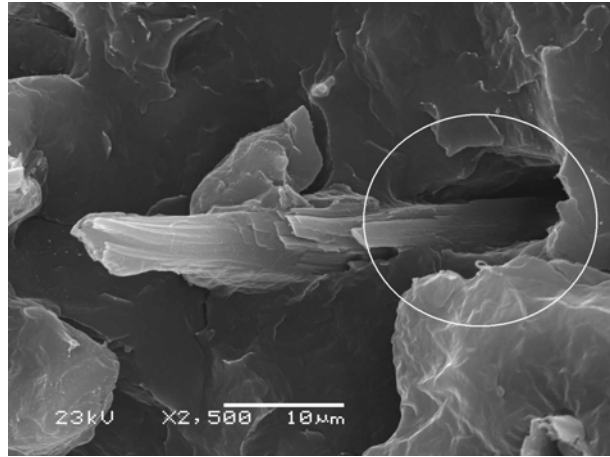


Fig. 4.11b

Fig. 4.11 SEM micrographs taken from the fracture surface of specimens broken during tensile testing; the composites contained MAPP in both cases (good adhesion); a) 30 wt% W68, fiber fracture; b) 20 wt% W35, debonding.

4.3.4. Discussion

The analysis of characteristic deformation and stress values derived from micromechanical measurements helps to identify the mechanism of these deformations and the determination of the dominating one. The number and amplitude of the signals also offers additionally information. In this section we discuss only the composition dependence of characteristic stresses derived from acoustic emission testing. The initiation of a process can be determined fairly well and the corresponding deformation and stress values can be derived from them as shown in Fig. 4.8. Characteristic stresses are determined from the deformation values by using the stress vs. strain trace.

The values are plotted in Fig. 4.12 as a function of composition. Very few signals are detected in the neat polymer, which were assigned to crystal cracking and cavitation [11]. Two processes can be identified in composites containing the large particles, but always only one in those prepared with the wood flour of small particle size. The dominating micromechanical deformation process of the composites not containing MAPP is debonding independently of particle size (\square , \circ). Debonding stress is very small and the difference between the two fillers cannot be seen on the scale of the graph. The second process observed in composites containing the W68 filler was identified as fiber pull-out (∇). The stress initiating this process is somewhat larger, but has practically the same dependence on composition as debonding stress. The addition of MAPP and increased adhesion result in the change of the mechanism of the micromechanical processes and in the increases of the stress necessary to initiate them. In composites containing the large particles, two processes can be identified again, although the second clearly dominates deformation and failure. The first, small step with a very limited number of events was assigned to the debonding of large particles (\blacktriangle). The

majority of events was generated by the fracture of large particles (■) in these composites. This process occurs at considerably higher stress levels than debonding or fiber pull-out. In the case of good adhesion, only one process was detected again in composites containing the small particles. According to the considerations presented in the previous section, this process was identified not as the fracture, but as the debonding of small particles (●), in spite of the fact that initiation of debonding occurs at the same stress level in these composites as fiber fracture in the other set containing W68. The different mechanism is confirmed by the lack of sound, the relatively small amplitudes and the increase in specimen volume. The lack of fiber fracture and debonding is confirmed also by the analysis of SEM micrographs.

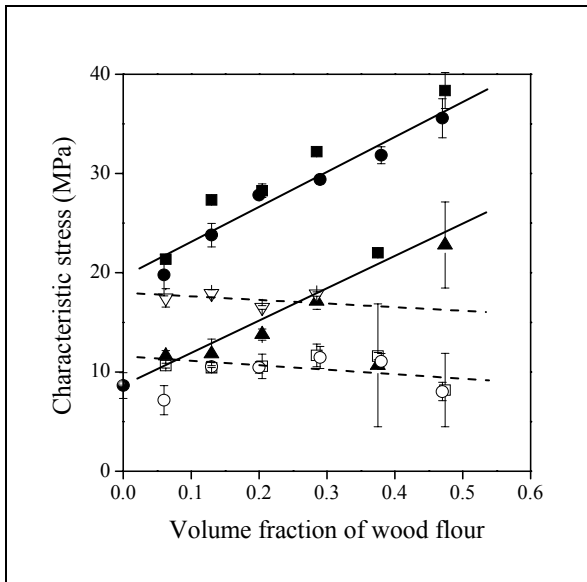


Fig. 4.12 Characteristic stress values derived from acoustic emission traces indicating the competitive deformation mechanisms occurring in the composites during deformation. Symbols: (●) PP, (□) W68, no MAPP, σ_{AE1} ; (▽) W68, no MAPP, σ_{AE2} ; (▲) W68, MAPP, σ_{AE1} ; (■) W68, MAPP, σ_{AE2} ; (○) W35, no MAPP, σ_{AE1} ; (●) W35, MAPP, σ_{AE1} .

Finally the question remains, why reinforcement does not improve with decreasing particle size (see Figs. 4.4 and 4.5), with the increase of the inherent strength of individual particles. As mentioned earlier, besides particle size the aspect ratio of the two fillers is also different, much smaller for the small than for the large particles. Aspect ratio and orientation are important factors determining the strength of fiber reinforced composites. Obviously, the change in aspect ratio has approximately the same effect on strength as particle size. The improvement in strength gained by decreased particle size was lost by the decrease in aspect ratio. The two factors must be optimized in order to achieve further improvement in composite strength.

4.4. Conclusions

The study of the deformation and failure of PP/wood composites containing wood particles of different sizes proves that micromechanical deformations change drastically with decreasing particle size. Less debonding, fiber pull out and fiber fracture occur in composites containing small particles. The apparently slight influence of particle size on composite strength results from the smaller aspect ratio of the small particles, which indicates that orientation and orientation distribution must have a strong effect on reinforcement. Further improvement in composite strength is possible only through the optimization of particle size, aspect ratio and the inherent strength of wood.

4.5. References

1. Dányádi, L., Renner, K., Móczó J., Pukánszky, B.: *Polym Eng Sci* **47**, 1246-1255 (2007)
2. Pukánszky, B.: Particulate filled polypropylene: structure and properties. In: Karger-Kocsis J, editor. *Polypropylene: Structure Blends and Composites*, vol. 3. London: Chapman and Hall, 1995. p. 1-70.
3. Jancar, J., Kummer, M., Kolarik, J.: In: Ishida H, editor. *Interfaces in Polymer, Ceramic, and Metal Matrix. Composites*. Elsevier, New York, 1988, p. 705.
4. Demjén, Z., Pukánszky, B., Nagy, J.: *Composites* **29A**,323-329 (1998)
5. Nielsen, L. E.: *Particulate-filled polymers. Mechanical properties of polymers and composites*, Marcel Dekker, New York 1975. p. 379-452.
6. Pukánszky, B.: *Composites* **21**, 255-262 (1990)
7. Renner, K., Yang, M. S., Móczó, J., Choi, H. J., Pukánszky, B.: *Eur Polym J* **41**, 2520-2529 2005
8. Vollenberg, P., Heikens, D., Ladan, H. C. B.: *Polym Compos* **9**, 382-388 (1988)
9. Pukánszky, B., Vörös, G.: *Compos Interfaces* **1**, 411-427 (1993)
10. Vollenberg, P. H. T.: Ph.D. Thesis, Eindhoven University of Technology, Eindhoven, (1987)
11. Henning, S., Michler, G. H., Ania, F., Balta-Calleja, F. J.: *Colloid Polym Sci* **283**, 486-95 (2005)

Chapter 5

Micromechanical deformation processes in PP/wood composites: particle characteristics, adhesion, mechanisms⁷

5.1. Introduction

Considerably number of papers are published on the improvement of interfacial interactions [1-6], surprisingly limited information is available about the effect of particle characteristics on composite properties [7-9]. Some of these may even be misleading because only a part of the information is supplied that is necessary for the interpretation of composite properties [10]. Even less attention is paid to micromechanical deformation processes taking place during the loading of composite parts. As a consequence, the goal of this part of the Thesis was to study the effect of particle characteristics and interfacial adhesion on the micromechanical deformation processes taking place in PP/wood composites. Besides an analysis of deformation mechanisms, a failure map is presented, and the consequences for practice are also discussed at the end of the chapter.

5.2. Experimental

The Tipplen R 359 ethylene-propylene random copolymer produced by TVK was used as matrix (MFI = 10 g/10 min at 230 °C, 21.6 N) in the study. Four different natural fillers were studied as reinforcement, a grinded corn cob GM200 (Hódmarket Kft, Hungary) and three lignocellulosic fibers (Rettenmaier GmbH). The reinforcements were characterized by various methods. Their chemical characterization indicated somewhat smaller lignin and larger wax content for the corn cob than for the wood fibers. Particle characteristics were determined using a Malvern Mastersizer 2000 and also with the help of SEM micrographs. Specific surface area was determined using an Autosorb 1 (Quantachrome, USA) apparatus. The particle characteristics of the reinforcements studied are analyzed in detail in a separate section. The Orevac CA 100 MAPP (MA content 1.0 wt%, $M_n = 25000$ g/mol, Arkema) was used to improve interfacial adhesion. MAPP/wood ratio was kept constant at 0.1 in all composites with good adhesion. Filler content was changed from 0 to 60 wt% in 10 wt% steps.

Composites were homogenized in a Brabender W 50 EH internal mixer at 180 °C, 50 rpm for 10 min. The homogenized material was compression molded into 1 mm thick plates at 180 °C using a Fontijne SRA 100 machine. Dog-bone type specimens were cut from the plates for mechanical testing. Mechanical properties were characterized by tensile testing using an Instron 5566 apparatus. Tensile modulus was determined at 0.5 mm/min cross head speed and 115 mm gauge length, while other tensile characteristics were measured at 5 mm/min speed. Acoustic emission measurements were

⁷Renner, K., Móczó, J., Pukánszky, B: Micromechanical deformation processes in PP/Wood composites: particle characteristics, adhesion, mechanisms *Composites Part A*. submitted

done with a Sensophone AED 40/4 apparatus. Threshold limit of detection was set to 20 dB. The mechanism of failure was studied on fracture surfaces generated during the tensile test. SEM micrographs were taken by a Jeol JSM 6380 LA apparatus.

5.3. Results

The results of the study are discussed in several sections. Although the chemical composition of the fillers was also determined, we pay our attention mainly to particle characteristics discussed in the first section. Composite properties and micromechanical deformation processes are presented in the following two sections, while the consequences of these processes on composite performance are discussed briefly in the last section.

5.3.1. Particle characteristics

The particle size distribution of the four fillers is shown in Fig. 5.1. The distributions cover 3-4 orders of magnitudes in particle size and both the width and the most frequent size differ for the four fibers. Average size, i.e. the $D[4,3]$ value can be determined for the fillers, but its meaning and significance are quite unclear, since the particles have anisotropic geometry. This is demonstrated quite well by Fig. 5.2 presenting SEM micrographs of the fillers. The relatively large size and small anisotropy of corn cob is clearly seen in Fig. 5.2a. The Arbocel CW 630 (W35) filler is significantly smaller than the rest of the reinforcements and its aspect ratio is not very large either. The Filtracel EFC 1000 wood fiber (W68) has the largest size and the particles are more anisotropic than those of the two fillers discussed previously. The last reinforcement, Arbocel FT 400 (W126) has fibrous character; it consists of long and thin fibers. The meaning of sizes determined by laser light scattering are especially questionable in this case.

For a better comparison of particle characteristics, fiber dimensions were determined quantitatively by the analysis of SEM micrographs. The average thickness and length of the fiber was determined and average aspect ratio was calculated as well. The results of particle characterization measurements, including specific surface area determination are collected in Table 5.1. The table contains also the name of the fibers and an abbreviation used in the further part of the chapter. Since aspect ratio proved to be one of the most important characteristics of the fibers, abbreviations are created which contain this value. Accordingly CC23 means corn cob with an aspect ratio of 2.3, while W126 is the abbreviation of the Arbocel FT 400 wood fiber with an aspect ratio of 12.6.

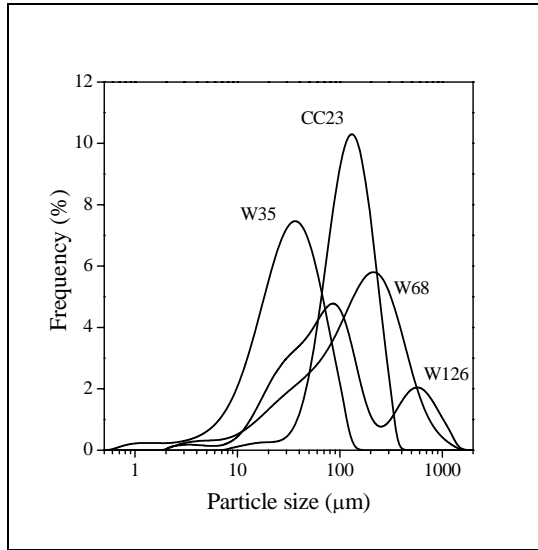


Fig. 5.1 Particle size distribution of the studied fibers determined by light scattering.

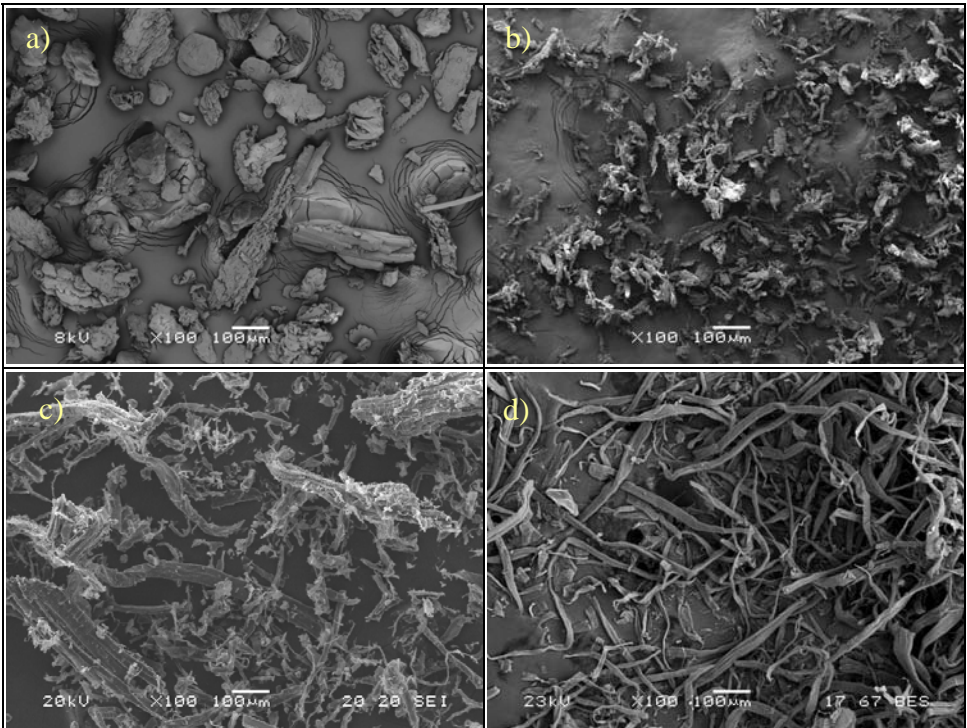


Fig. 5.2 Particle geometry of the investigated fibers. SEM micrographs. a) corn cob (CC23), b) Arbocel CW 630 (W35), Filtracel EFC 1000 (W68), Arbocel FT 400 (W126).

The analysis of the results of Table 5.1 allows making several important observations. The table proves that the average particle size of all four fibers is large corroborated also by their small specific surface area. The comparison of results obtained by light scattering and SEM, respectively shows some correlation between the D[4,3] value and the length of the fibers, but much less between D[4,3] and diameter. Practically no correlation exists between size represented by the D[4,3] value and aspect ratio. This latter characteristic differs significantly for the four reinforcements; it changes almost one order of magnitude from the CC23 to the W126 filler. As a consequence, we use the values determined by SEM in the further evaluation of the results. The question remains, which is or are the most important particle characteristics determining reinforcement and composite properties.

Table 1 *Particle characteristics of the natural fiber reinforcements studied*

Fiber		D[4,3] (μm)	Length ^{a)} (μm)	Diameter ^{a)} (μm)	Aspect ratio ^{a)}	Specific surface area (m^2/g)
Name	Abbrev.					
Corn cob	CC23	143.4	108.1	55.7	2.3	0.89
Arbocel CW 630	W35	39.6	93.5	33.3	3.5	1.44
Filtracel EFC 1000	W68	213.1	363.4	63.9	6.8	1.50
Arbocel FT 400	W126	171.2	235.2	21.8	12.6	3.50

a) average values determined from SEM micrographs

5.3.2. Properties, reinforcement

Aspect ratio is claimed to be the main factor determining the mechanical properties of composites. Accordingly size should be of secondary importance and interfacial adhesion supposed to play a minor role in the determination of stiffness [11-13]. The Young's modulus of the composites is plotted as a function of fiber content in Fig. 5.3 and the considerations presented above seem to be valid at least for the wood reinforcements. In this and in all subsequent figures empty symbols indicate composites with poor adhesion, i.e. prepared without MAPP and full symbols relate to materials with good interfacial adhesion. Only two lines are drawn in the figure, which encompass the entire range of properties measured. In this and in most other figures, the lines are not best fits, but are drawn only to show tendencies and guide the eye. We must call the attention here to the role of particle orientation, which is of the utmost importance for anisotropic particles. In the present case we assume that the fibers are oriented parallel to the plane of the compression molded plates, but randomly within the plates. This random orientation should be the same for all four reinforcements. Accordingly, the role of orientation is excluded from further evaluation.

As mentioned above, the effect of fiber characteristics on composite stiffness corresponds to the expectations, modulus increases with increasing aspect ratio. Adhe-

sion does not influence stiffness for the wood fibers, but relative large difference is observed in the modulus of composites containing corn cob with good or bad adhesion, respectively. The difference can be tentatively explained by the large size of the particles, which facilitates debonding already at the small deformations of the modulus measurement and results in small stiffness. Decreasing modulus at large filler content must result from the physical contact of the particles, as mentioned above.

The strength of all composites is presented in Fig. 5.4 as a function of fiber content. Adhesion has a very large effect on this property as expected, but particle characteristics seem to have also larger effect on strength than on stiffness. Due to its large size and small aspect ratio corn cob clearly decreases strength, while the larger anisotropy of the wood particles results in some moderate reinforcement. However, the effect of aspect ratio and size is quite unclear in the case of poor adhesion. Improved adhesion results in considerable reinforcement in all cases. The effect of the large aspect ratio of the W126 fiber is clear, but differences are small in the case of the other three fibers. This result indicates that aspect ratio alone does not determine reinforcement and properties, but some other factor also plays a role.

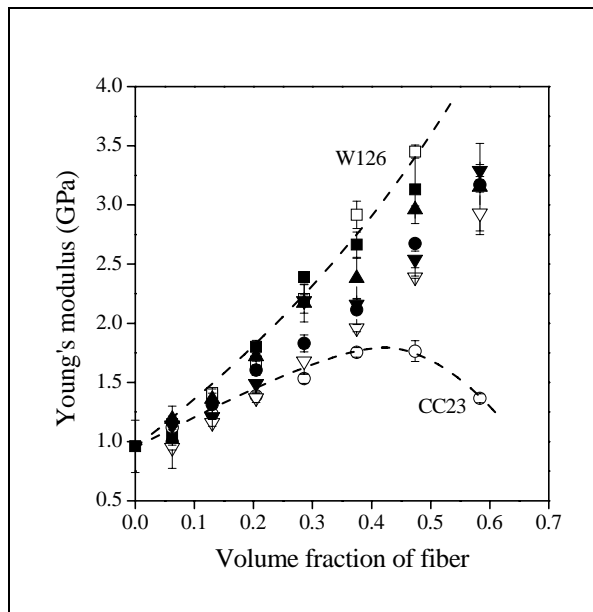


Fig. 5.3 Composition dependence of the stiffness of PP/natural fiber composites; effect of fiber characteristics and interfacial adhesion. Empty symbols indicate poor adhesion (no MAPP), full symbols good adhesion (MAPP); (○) CC23, (▽) W35, (▲) W68, (□) W126.

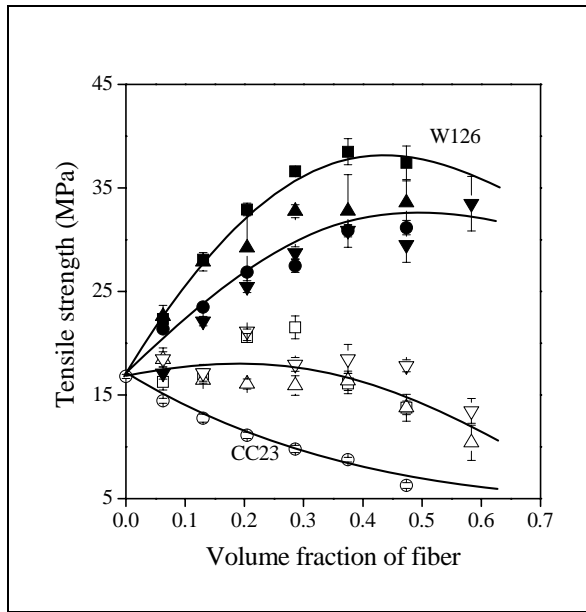


Fig. 5.4 Tensile strength of PP composites reinforced with natural fibers; effect of particle characteristics and adhesion. Symbols are the same as in Fig. 5.3.

The reduced tensile strength of some of the studied composites is plotted in Fig. 5.5 in the form indicated by Eq. 4.1. Only four composites are plotted for better clarity. The correlations are reasonably linear with a few points deviating at large filler content. Such deviations were shown to indicate structural effects: aggregation or changing orientation may be the main reasons in our case. The effect of adhesion and aspect ratio is clear from the figure. We may also conclude that the coupling agent has a much larger effect for the filler with the small aspect ratio, i.e. usual wood flours with an average aspect ratio of 3-5 need MAPP to achieve reasonable reinforcement. The extent of reinforcement, i.e. Parameter B is collected in Table 5.2 for all four fibers. We can see that reinforcement increases both with adhesion and aspect ratio; within the range of variables studied we could increase reinforcement approximately five times. However, we must call attention here to the fact that the B value for the small W35 fiber is larger than that for the W68 wood flour with twice as large anisotropy. The correlation between reinforcement and aspect ratio is shown much better by Fig. 5.6. The deviation of the W35 fiber from the general tendency can be explained only with its small size, since every other parameter is the same as for the other fillers. Size seems to influence also deformation and failure mechanism, thus reinforcement and composite properties.

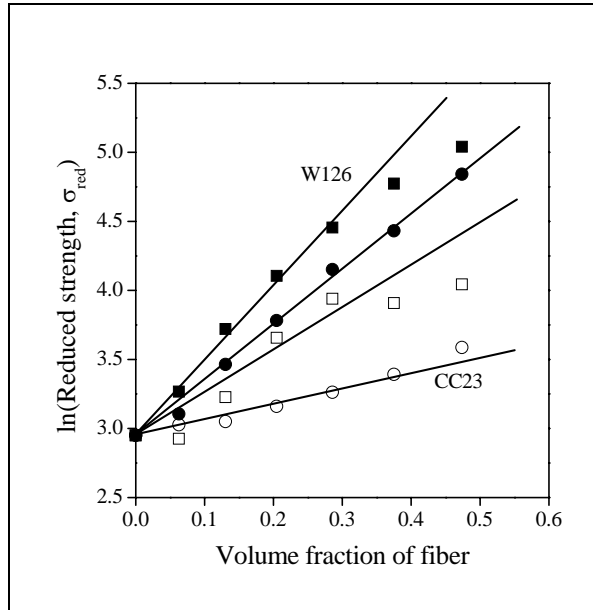


Fig. 5.5 *Reduced tensile strength of selected composites plotted in the linear form (see Eq. 4.3). The slope of the straight line expresses the extent of reinforcement. Symbols: (●) CC23, good adhesion, (○) CC23 poor adhesion, (■) W126, good adhesion, (□) poor adhesion.*

Table 5.2 *Extent of reinforcement (Parameter B) determined for the various fibers in composites with poor (no MAPP) and good (MAPP) adhesion.*

Fiber	Parameter B	
	poor adhesion	good adhesion
CC23	1.16	3.97
W35	3.07	4.66
W68	2.59	4.57
W126	3.83	5.37

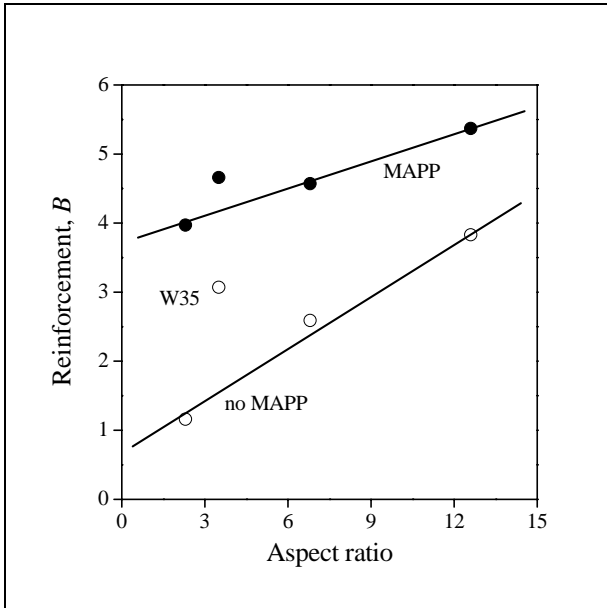


Fig. 5.6 Influence of aspect ratio on the reinforcing effect of the fibers studied. (●) good adhesion, (○) poor adhesion.

5.3.3. Micromechanical deformation processes

Micromechanical deformation processes were studied again by acoustic emission. The result of a representative measurement is shown in Fig. 7. The stress vs. deformation correlation measured in a tensile test is plotted in the figure as continuous line. The small circles indicate individual acoustic events (signals, hits) with the corresponding amplitude. We can see that acoustic activity starts at small deformation and the events can be divided into two groups: those occurring below $\sim 3\%$ deformation and the rest above. The detection of two groups of signals indicates the occurrence of two consecutive deformation processes.

The evaluation and interpretation of the results is rather difficult in the form presented in Fig. 5.7. Instead of individual hits, the cumulative number of signals is plotted in Fig. 5.8 as a function of deformation for the same composite. The corresponding correlations of the neat matrix PP are also presented as reference. We can see that the acoustic activity of PP is very small, deformation occurs with a mechanism not giving any sound possibly by shear yielding. The two sets of signals of Fig. 5.7 translate into two steps in the cumulative signal correlation corresponding to two mechanisms. The two steps allow the determination of characteristic deformation values as indicated in Fig. 5.8 and the corresponding stress values can be derived from these deformations. We will use mainly the σ_{AE1} value derived from ϵ_{AE1} since occasionally only one process takes place during the deformation of the composites, or only one can be distin-

guished reliably. The σ_{AE1} value corresponds to the initiation stress of the first or the dominating micromechanical deformation process occurring during the deformation of the composite.

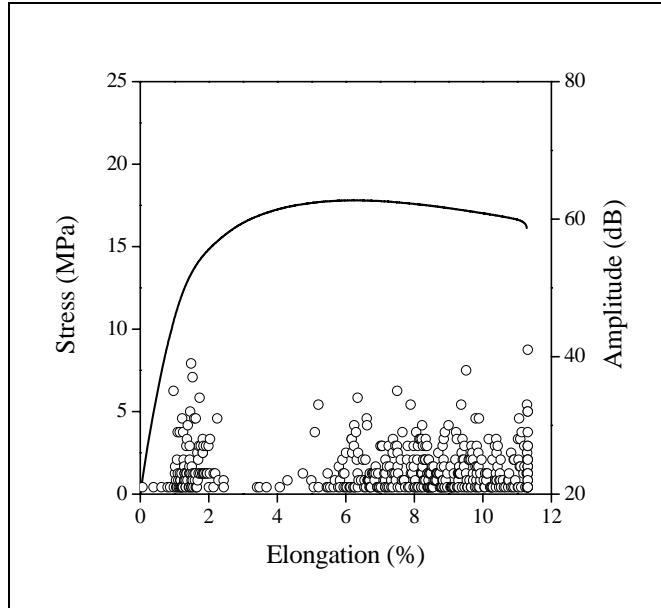


Fig. 5.7 The results of acoustic emission measurement on a PP/W68 composite prepared without MAPP (poor adhesion). Fiber content: 20 wt%. — stress vs. deformation correlation, (O) individual acoustic signals.

It is impossible to present the cumulative hit vs. deformation traces for all the composites studied thus we compare only two sets of correlations determined at 20 wt% fiber content. The traces measured in composites not containing MAPP, i.e. at poor adhesion, are presented in Fig. 5.9. The total number of signals is large for the corn cob and only a single step can be detected on the trace which corresponds to the debonding of the particles. Debonding is very easy at this large particle size, it occurs at a small stress, results in the development of many voids which lead to failure at small deformation and stress. The result explains the dependence of stiffness on fiber content, but also the weak reinforcing effect of this filler. The rest of the correlations are more or less similar and exhibit two steps. The first was identified as debonding and the second as fiber pull-out. The role of the second process becomes more pronounced with increasing aspect ratio as expected.

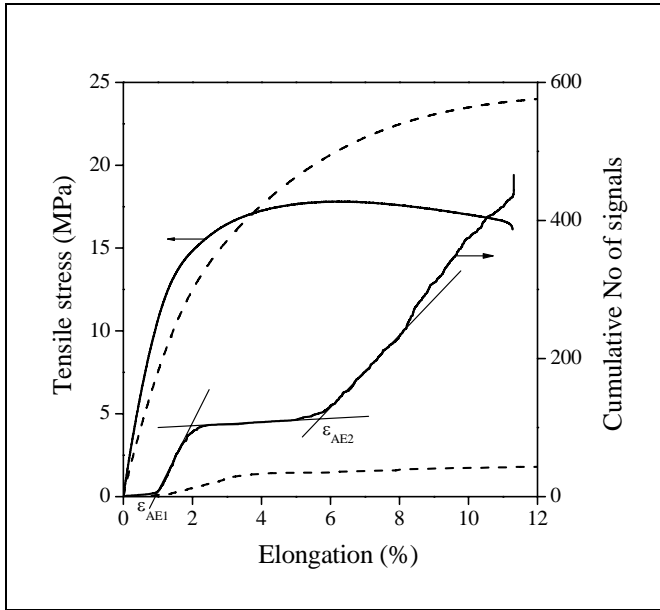


Fig. 5.8 Dependence of the cumulative number of signals on deformation for the composite of Fig. 5.7. The stress and cumulative number of signals vs. deformation traces of the neat PP are also plotted for reference. ----- PP, ——— PP/20 wt% W68 wood flour.

Improved adhesion changes the cumulative hit traces significantly (Fig. 5.10). The four fibers show three different behaviors corresponding to different combinations of micromechanical processes. CC23 and W35 behave more or less similarly. After initiation, the number of signals gradually increases and approaches a saturation value. The dominating deformation mechanism must be debonding here, which occurs at a larger stress due to the stronger adhesion between the fiber and the polymer. The difference in initiation deformation and the corresponding stress is the result of different particle size, which is much larger for the CC23 sample. Accordingly debonding occurs at much smaller deformation and stress for this filler. Only one process takes place, but definitely dominates in the composite containing the W68 fiber. This process was identified as fiber fracture [14]; large particles break parallel to their axis. The most signals can be detected in composites reinforced with the W126 fiber and at least two processes take place consecutively during deformation. Debonding could be the first process for fibers oriented parallel to the direction of the load and fiber fracture could be the second resulting in a large number of signals with larger amplitudes. However, we need further evidence to support this tentative explanation.

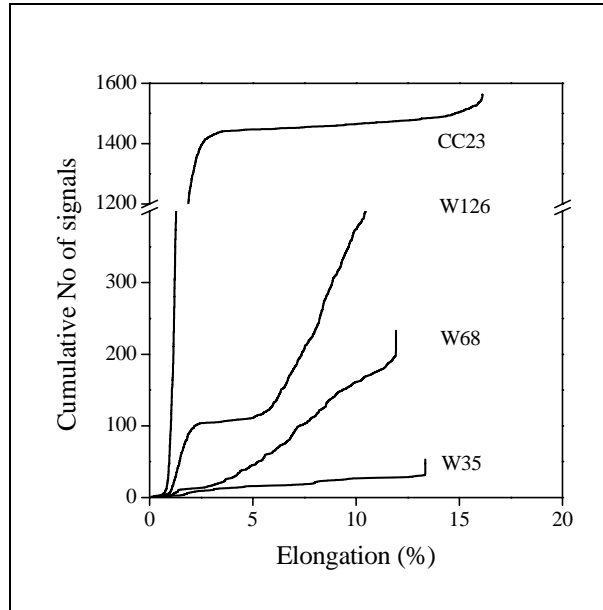


Fig. 5.9 Comparison of the evolution of the cumulative number of signals during the deformation of composites containing the four fibers in 20 wt% in the absence of MAPP.

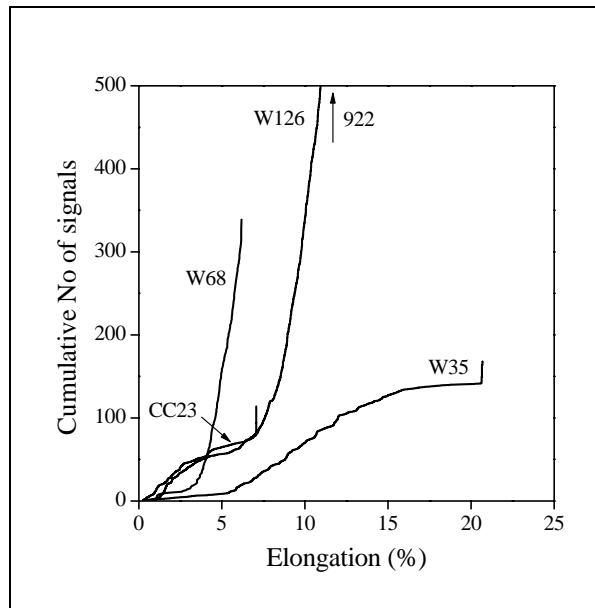


Fig. 5.10 Cumulative number of signals plotted against deformation for PP composites containing the four natural fibers in 20 wt% in the presence of MAPP.

The characteristic stress derived from the cumulative signal traces is plotted against fiber content in Fig. 5.11. The effect of the main variables is clear. The σ_{AE1} value is related invariably to debonding in the case of poor adhesion and it is determined mainly by the combined effect of particle diameter, aspect ratio and orientation. Improved adhesion increases the characteristic stress considerably and results in much better reinforcement expressed quantitatively by the B values listed in Table 2. The dominating deformation mechanism can be either debonding or fiber fracture in this case. The similar values obtained for the W35 and W68 fibers show very well the effect of particle size and aspect ratio. Similar values, i.e. similar reinforcements are obtained in spite of the fact that deformation and failure occur according to different mechanisms. Because of the small particle size and aspect ratio of the W35 filler, the dominating mechanism is debonding in its composites. Due to the larger aspect ratio, better reinforcement could be obtained with the W68 fiber; however, the large size of the particles leads to fiber fracture which limits reinforcement. The thin long fibers of the W126 filler offer the maximum reinforcement.

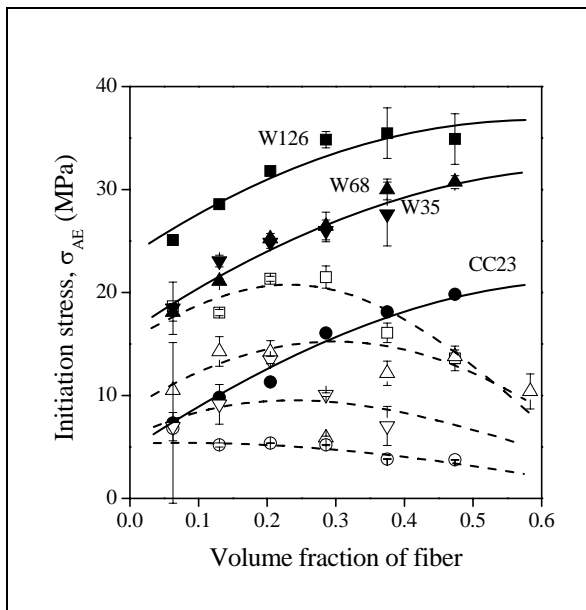


Fig. 5.11 Composition dependence of the characteristic stress values determined from acoustic emission measurements for the various composites. Effect of particle characteristics and adhesion. Symbols are the same as in Fig. 5.3.

Naturally, acoustic emission testing cannot reveal the exact mechanism of deformation; further evidence is needed, which might be supplied by SEM analysis. Only a few micrographs are presented here to save space, but they sufficiently demonstrate the main deformation mechanisms and support our analysis presented above. In the case of poor adhesion, the dominating deformation mechanism is debonding especially for large particles as shown by Fig. 12a. However, debonding occurs also in composites

containing the thin long fibers (see Fig. 12b). Fiber pull-out takes place as well in these composites as shown by the same micrograph. If the adhesion is good, the large and relatively long particles break parallel with their axis in composites containing the W68 wood flour (Fig. 12c), while the long fibers of W126 fracture mainly perpendicularly to their axis (Fig. 12d).

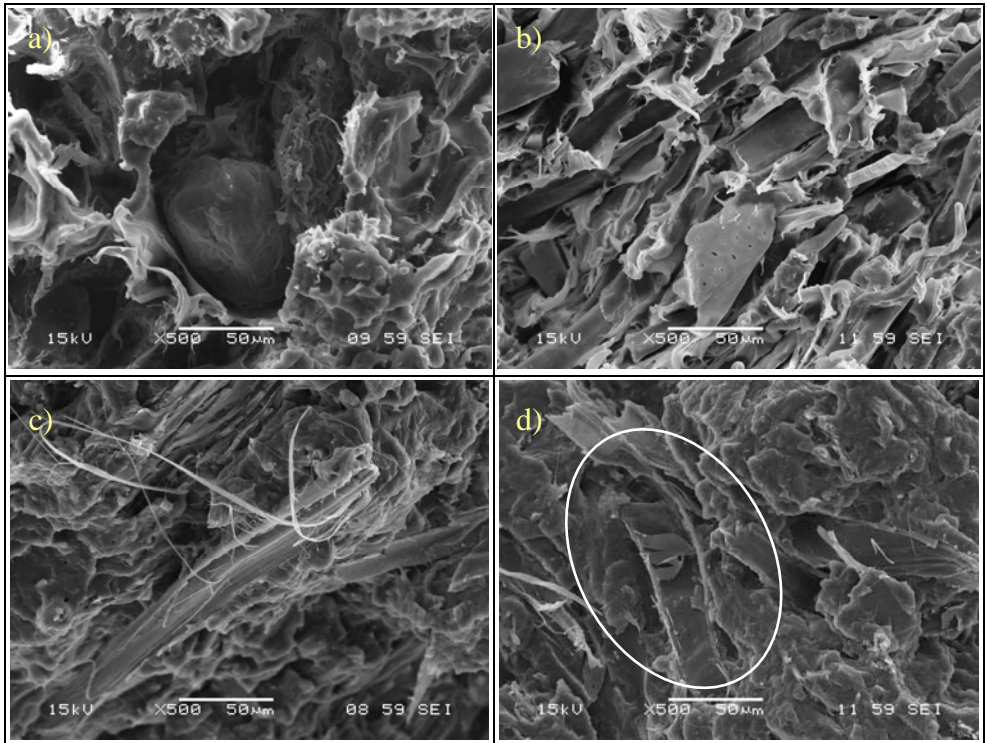


Fig. 5.12 SEM micrographs taken from the fracture surface of specimens broken during the tensile test; examples of various failure mechanisms. a) debonding, CC23; b) debonding and pull-out; W126; c) fracture parallel to the axis of the fiber, W68, MAPP; d) fracture perpendicularly to the axis of the fiber, W126, MAPP. All composites contained the fibers in 30 wt%.

All deformation mechanisms can be distinguished on the SEM micrographs, which also prove that they are competitive and occur simultaneously and/or consecutively during deformation. The detailed analysis of acoustic emission traces and SEM micrographs allowed us to construct a failure map which is presented in Table 3. The table clearly proves that debonding is the dominating deformation mechanism at poor adhesion and it can be accompanied by fiber pull-out at larger aspect ratios. Debonding dominates also at strong adhesion for large particles with small aspect ratio, while mainly fiber fracture occurs at large aspect ratio. According to the table, failure mechanism depends very much on interfacial adhesion and particle characteristics.

Table 5.3 *Map of deformation and failure mechanisms in the studied PP composites prepared with various fibers at poor and good adhesion, respectively*

Fiber	AR ^{a)}	Deformation mechanism					
		Poor adhesion			Good adhesion		
		Debonding	Pull-out	Fracture	Debonding	Pull-out	Fracture
CC23	2.3	+	–	–	+	–	–
W35	3.5	+	–	–	+	–	–
W68	6.8	+	+	–	(+)	–	+
W126	12.6	(+)	+	(+)	(+)	(+)	+

a) aspect ratio

(+) possible mechanism

5.4. Consequences

One may question the importance of local processes occurring around heterogeneities on a very small, micrometer scale. However, these processes determine the final properties, failure and performance of the entire composite. This statement is strongly supported by Fig. 5.13 in which parameter B related to the reinforcing efficiency of the fiber is plotted against the characteristic stress value determined from acoustic emission analysis. A very close correlation exists between the two quantities proving that larger characteristic stress results in better reinforcement.

Further and even more direct evidence is supplied for the close relationship of micro- and macromechanical deformation processes by Fig. 5.14. The tensile strength of all composites prepared is plotted against the characteristic stress derived from the acoustic analysis (see Fig. 5.8). The correlation is surprisingly close for most composites indicating that local processes determine the strength of the composites. Controlling these processes and increasing the initiation stress of the dominating process would lead to stronger composites. The results obtained for corn cob deviate also in this correlation from the general tendency both for poor and good adhesion. Composites are stronger than predicted by acoustic emission. One possible reason for this behavior may be the very large size and small aspect ratio of this filler, leading to easy debonding of the largest particles, which then determines initiation stress. The few debonding events might not lead to the catastrophic failure of the composites and strength is dominated by the debonding of the majority of smaller particles occurring at a larger stress. Further analysis and probably also experiments are needed to prove the validity of this tentative explanation.

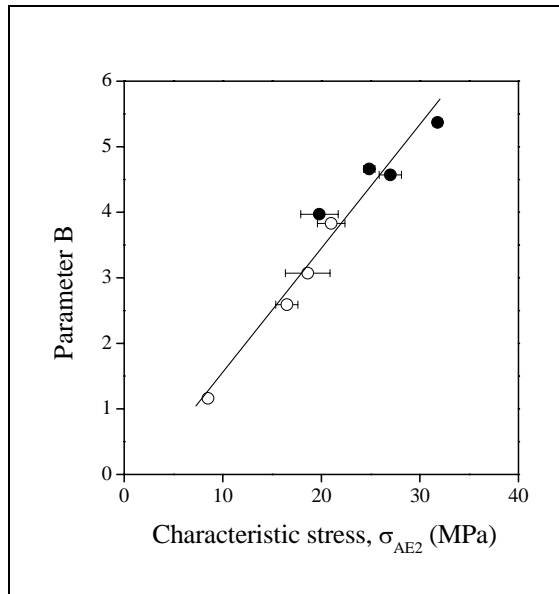


Fig. 5.13 Correlation between the reinforcing effect of fibers (Parameter B) and the characteristic stress (σ_{AE2}) determined from acoustic emission measurements. (●) good adhesion, (○) poor adhesion.

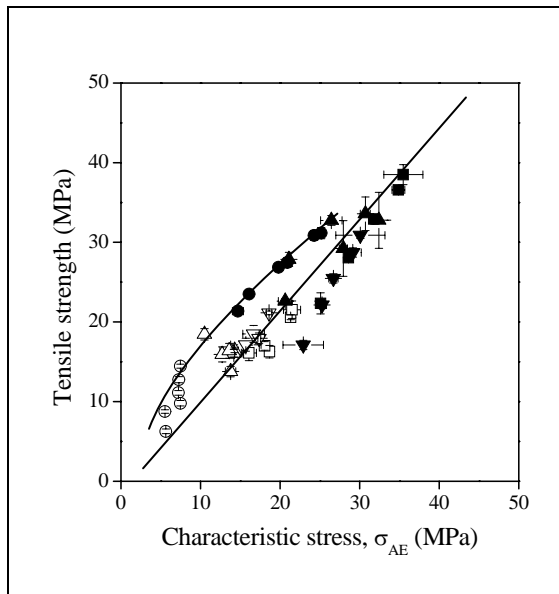


Fig. 5.14 Correlation between the tensile strength of PP/wood composites and the characteristic stress (σ_{AE}) determined from acoustic emission measurements. Symbols are the same as in Fig. 5.3.

5.5. Conclusions

The properties of PP/wood composites depend strongly on interfacial adhesion and on the particle characteristics of the wood. Coupling with functionalized polymer is necessary for the preparation of composites with acceptable properties if the size of the particles is large and their aspect ratio is small. The effect of adhesion is smaller for particles with large aspect ratio. Large aspect ratio and small fiber diameter result in better reinforcement. Several micromechanical deformation processes may occur in PP/wood composites including matrix yielding, debonding, fiber pull-out and fiber fracture both parallel and perpendicular to the fiber axis. The processes are competitive and may take place simultaneously and/or consecutively. The inherent properties of the reinforcement may limit the improvement of composite strength. Micromechanical deformation processes determine composite properties irrespectively of their mechanism as shown by the close correlation between the characteristic stress derived from acoustic emission measurements and composite strength.

5.6. References

1. Nunez, A. J., Sturm, P. C., Kenny, J. M., Aranguren, M. I., Marcovich, N.E., Re-boredo, M. M.: *J Appl Polym Sci* **88**, 1420–1428 (2003)
2. Li, Q., Matuana, L. M.: *J Appl Polym Sci* **88**, 278–286 (2003)
3. Kazayawoko, M., Balatinecz, J. J., Matuana, L. M.: *J Mater Sci* **34**, 6189–6199 (1999)
4. Cantero, G., Arbelaiz, A., Mugika, F., Valea, A., Mondragon, I.: *J Reinf Plast Compos* **22**, 37–50 (2003)
5. Lu, J. Z., Wu, Q., Negulescu, I. I.: *J Appl Polym Sci* **96**, 93–102 (2005)
6. Liu, X. Y., Dai, G. C., *Express Polym Lett* **1**, 299–307 (2007)
7. Coutinho, F. M. B., Costa, T. H. S., Suarez J. C. M., Melo, D. P.: *Polym Test* **19**, 625–633 (2000)
8. Bledzki, A., Faruk, O.: *App Compos Mater* **10**, 365–379 (2003)
9. Stark, N. M., Rowland R.E.: *Wood Fiber Sci* **35**; 167–174 (2003)
10. Clemons, C. M., Caufield, D. F.: Natural fibers. Chapter 11. in Functional fillers for plastics, ed. Xanthos, M., Wiley-VCH, Weinheim, 2005, p. 249.
11. Pukánszky, B.: Particulate filled polypropylene: Structure and properties. in Polypropylene: Structure, Blends and Composites, Vol. 3, Chapman and Hall, London, 1995, p. 1–70.
12. Jancar, J., Kummer, M., Kolarik, J.: Interfaces in Polymer, Ceramic, and Metal Matrix Composites, Elsevier, New York, 1988, p. 705.
13. Demjén, Z., Pukánszky, B., Nagy, J.: *Composites* **29A**, 323–329 (1998)
14. Dányádi, L., Renner, K., Móczó, J., Pukánszky, B.: *Polym Eng Sci* **47**, 1246–1255 (2007)

Chapter 6

Micromechanical deformations in PP/lignocellulosic filler composites: effect of matrix properties⁸

6.1. Introduction

Many attempts have been made to improve the properties of natural fiber reinforced composites. Several reports are available on the effect of wood type [1-3], but it is still unclear if the use of soft or hard wood results in composites with better properties. Somewhat clearer picture is obtained on the effect of fiber characteristics on properties [4-6]. The extent of reinforcement increases with anisotropy, but the effect of coupling becomes less pronounced as the aspect ratio of the filler increases. Although the effect of wood characteristics and interfacial adhesion on composite properties has been studied extensively [7-12], much less attention has been paid to the influence of matrix characteristics [13,14]. As a consequence, the goal of this study was to investigate the influence of matrix characteristics on deformation and failure in PP/natural fiber composites. A homopolymer, a random and a heterophase polypropylene copolymer were used as matrix, while corn cob (CC) was applied as reinforcement in the study. An attempt was made to identify the dominating deformation mechanism during the failure of the composites and the possible effect of the matrix on it. The consequences of the observations to practice are also briefly discussed at the end of the chapter.

6.2. Experimental

The most important characteristics of the matrix polymers used are listed in Table 6.1. All polymers were supplied by TVK, Hungary. The MFI of the polymers changes in a wide range, which might influence composite properties. However, at large filler contents the deformability of the composites decreases drastically thus molecular weight has only small effect on properties, and micromechanical deformations dominate. The GM 200 corn cob was produced by Hodmarket Kft, Hungary. It has an average particle size of 140 μm and an aspect ratio of 2.3. Because of the small aspect ratio, orientation has limited effect on properties, thus uniform and random orientation is assumed during the evaluation of the results. Interfacial adhesion was modified by the application of the maleated polypropylene (MAPP) Orevac CA 100 produced by Arkema, France. The maleic anhydride content of the polymer was approximately 1.0 wt% and its number average molecular weight 25000 g/mol. MAPP/wood ratio was kept constant at 0.1 throughout the experiments. Sample preparation and measurement conditions were the same as in Chapter 5.

⁸Renner, K., Kenyó, Cs., Móczó, J., Pukánszky, B.: accepted in *Compos Sci Technol*

6.3. Results and discussion

The results are discussed in several sections. The composition dependence of properties and reinforcement are presented first, and then the effect of matrix properties on micromechanical deformations is shown. Deformation and failure mechanisms are analyzed in the next section, followed by the discussion of their influence on composite properties. We do not present all primary results here in order to save space, typical correlations and figures will be shown only to support our statements.

Table 6.1 *Characteristics of the PP polymers used as matrices in the study*

Polymer type	M_n (g/mol)	M_w (g/mol)	M_w/M_n	Ethylene content (wt%)	MFR ^{a)} (g/10 min)	Modulus (GPa)
homo	68 700	285 650	4.16	-	4	1.42 ± 0.01
heterophase	38 450	146 250	3.80	9	45	1.31 ± 0.03
random	56 600	195 700	3.46	3	12	0.97 ± 0.03

a) 230 °C, 2.16 kg

6.3.1. Properties

One of the main goals of the use of natural reinforcements is to improve the stiffness of the polymer. Young's modulus of all three polymers increases with increasing filler content, but in different extent. The effect depends very much on the initial modulus of the matrix polymer (see Table 6.1), the smallest increase is observed in the homopolymer, while the largest in the random copolymer, as expected. The direct comparison of the results is difficult because of inherent differences in matrix properties. In accordance with earlier experience, an increase can be observed in modulus as an effect of improved adhesion, but the effect is slight. The composition dependence of stiffness is not presented here, because it does not offer any new information compared to that published in the literature before [1,7,8,15-18].

The effect of filler content on the tensile yield stress of the polymer is shown in Fig. 6.1. The differences due to the inherent properties of the matrix can be clearly seen in the figure. Based on the figure we can conclude that the introduction of the MAPP coupling agent increases yield stress considerably in all three polymers. Comparison is much easier on a relative basis. The tensile yield stress of the composites is related to that of the matrix and the resulting values are plotted against filler content in Fig. 6.2. The very strong effect of adhesion is clearly seen in the figure. Yield stress decreases with increasing corn cob content in the absence of MAPP, i.e. at poor adhesion, while it increases when the coupling agent is used. The effect of the matrix polymer is also different in the two cases. The smallest relative yield stress is obtained for the homopolymer in both cases, but the order of the two copolymers is different when adhesion is poor and good, respectively.

Based on Fig. 6.2 we might assume two different deformation mechanisms, one for poor and one for good adhesion. We may assume that in the absence of MAPP, i.e. at poor adhesion, the dominating deformation mechanism is debonding. This assumption is strongly justified by our previous results proving that the large size of the reinforcing particles and poor interaction leads to easy debonding during deformation [17-19]. Debonding stress depends on matrix modulus [20,21], which might result in the differences among the composites prepared with dissimilar matrices. The identification of the dominating mechanism is much more difficult in the case of good adhesion. Stronger adhesion leads to larger debonding stress [20], thus debonding might be the dominating mechanism in this case too. However, other mechanisms might be also initiated, like the fracture of the particles or the yielding of the matrix. Fiber pull-out can be eliminated as a possible mechanism [17,18] because of the small aspect ratio of the fibers. The mechanism of deformation and failure cannot be determined from the primary data; further measurements and analysis are needed.

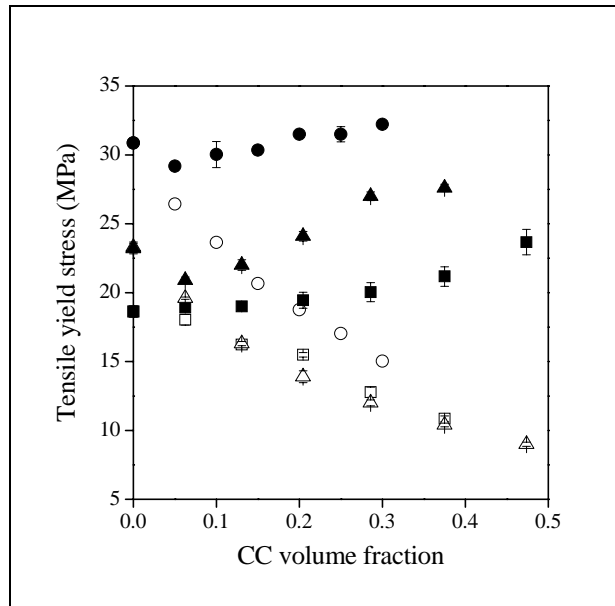


Fig. 6.1 Effect of corn cob content and matrix type on the tensile yield stress of PP composites; (○) homo, (□) heterophase, (△) random; empty symbols: poor adhesion (without MAPP), full symbols: good adhesion (with MAPP).

Reinforcement can be expressed quantitatively by using simple models describing the composition dependence of properties [17,22]. A model which takes into account also the effect of adhesion describes reinforcement by a parameter (B) expressing the load-bearing capacity of the filler (see Chapter 2 and 4, Eqs. 2.1 and 4.1 - 4.3). B parameters calculated from the yield stress of the composites are listed in Table 6.2. The

effect of matrix properties and adhesion are reflected well by changes in B . Unfortunately neither the changes in parameter B or the consideration of modified debonding stress with changing matrix modulus can explain the different order of the composites either at poor or at good adhesion.

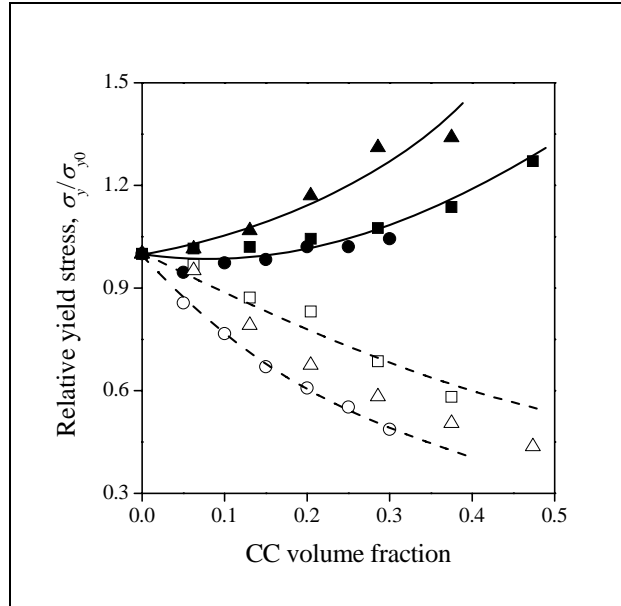


Fig. 6.2 Relative yield stress (σ_y/σ_{y0}) of PP composites plotted against their corn cob content; effect of matrix properties. Symbols are the same as in Fig. 6.1.

Table 6.2 Extent of reinforcement (parameter B) determined in composites prepared from the three matrices with poor (no MAPP) and good (MAPP) adhesion.

Polymer	Parameter B	
	poor adhesion	good adhesion
homo	0.71	3.27
heterophase	2.16	3.32
random	1.16	3.97

Tensile strength, i.e. the stress measured at the failure of the specimens, changes very similarly to yield stress with increasing filler content (Fig. 6.3). The effect of the two parameters studied, i.e. adhesion and matrix properties, are similar as in the

previous case. Apparently matrix characteristics influence strength less than yield stress. In spite of the consistent results, several questions remain open including the mechanism of deformation and failure, as well as the reason for the different effect of the matrix on the final properties of the composites.

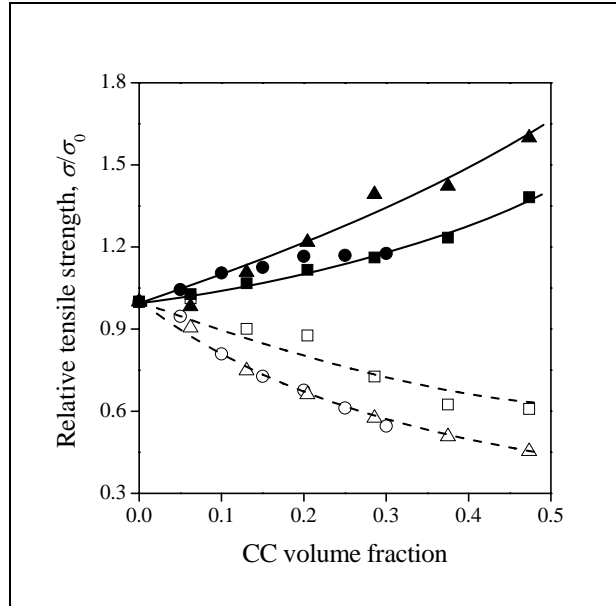


Fig. 6.3 *Dependence of relative tensile strength of PP/corn cob composites on filler content and the on the type of the matrix. Symbols are the same as in Fig. 6.1.*

6.3.2. Micromechanical deformations

The loading of the specimens initiates the local deformations mentioned in the previous section, which can be detected by microphones. The individual events (signals, hits) detected in the composite prepared from the homopolymer and 20 wt% corn cob are presented in Fig. 6.4. The stress vs. strain trace of the composite is also shown as reference. Most of the events occur at very small deformations, much below yield level. Very few signals develop at larger deformations. The number of events is much larger in the composite containing MAPP, i.e. at good adhesion, and the signals are spread in a much wider deformation range (Fig. 6.5). It is also worth to note that micromechanical deformations start only at a larger deformation at around 1.5 % compared to 0.5 % when adhesion was poor (compare to Fig. 6.4). The comparison of the two figures clearly indicates significant differences in the deformation behavior of the two composites as deduced already from the composition dependence of primary results (see Figs. 6.1-3).

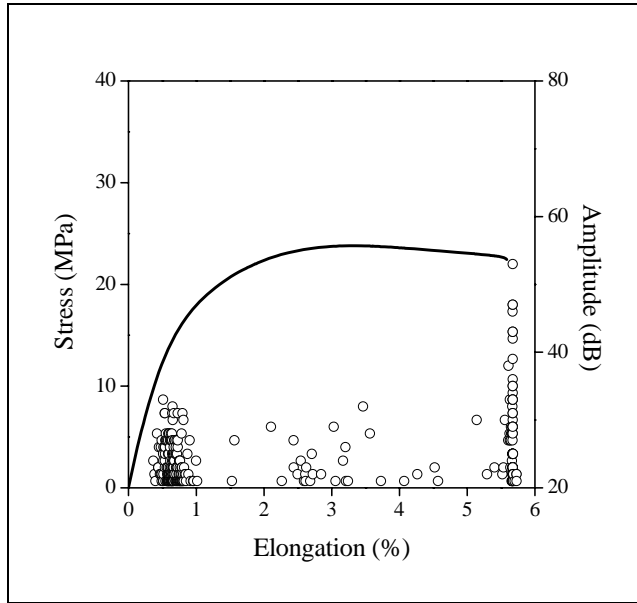


Fig. 6.4 *Development of acoustic events during the deformation of a PP/corn cob composite: CC content: 20 wt%, matrix: homo, no MAPP. (○) individual acoustic signals, ——— stress vs. strain trace.*

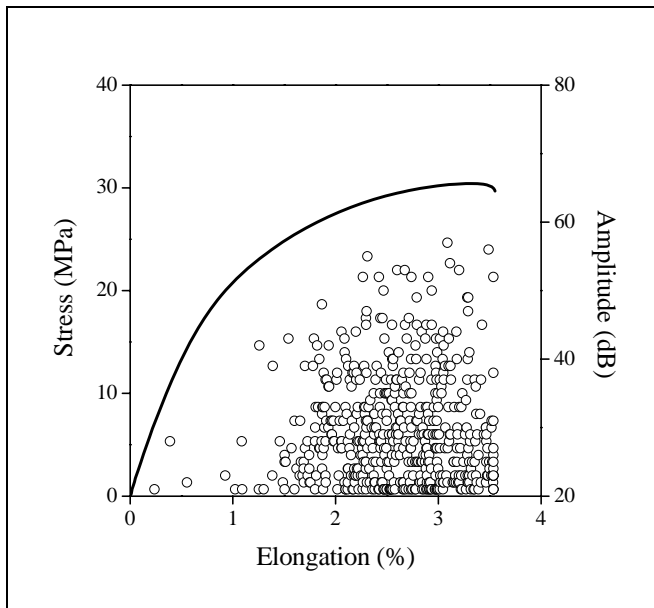


Fig. 6.5 *Distribution of acoustic events during the deformation of a PP/CC composite with good adhesion. Conditions: 20 wt%, homo, MAPP. Symbols are the same as in Fig. 6.4.*

Evaluation and drawing conclusions are rather difficult from results presented in the form of Figs. 6.4 and 6.5. More information can be obtained if the cumulative number of events is plotted against deformation. The behavior of the two composites discussed above is compared in such a representation in Fig. 6.6. The stress vs. strain traces are included again as reference. The effect of improved adhesion on mechanical properties is clear; strength increases and deformation decreases as an effect of MAPP addition. The difference in the shape of the cumulative hit vs. deformation traces is striking. A step is observed in the correlation when adhesion is poor, while the number of hits increases continuously starting from a larger deformation value when adhesion is improved with MAPP. The two different correlations indicate different mechanisms. Earlier experience shows that the stepwise change is characteristic for debonding, while the cumulative number of signals increases continuously when the fracture of the reinforcement is the dominating process. A stepwise change was observed in the absence of MAPP for the homo and the random copolymer, while a very small number of signals were detected in the composite prepared from the heterophase copolymer (not shown). The cumulative signal vs. deformation traces are compared in Fig. 6.7 in the presence of MAPP. We can see stepwise increase in the number of cumulative hits for the two copolymers, while a continuous, steep increase is recorded for the homopolymer. We can conclude from these results that although yield stress and strength increased for all three polymers in the presence of MAPP, the mechanism of deformation is different for composites prepared from the homo- and the two copolymers.

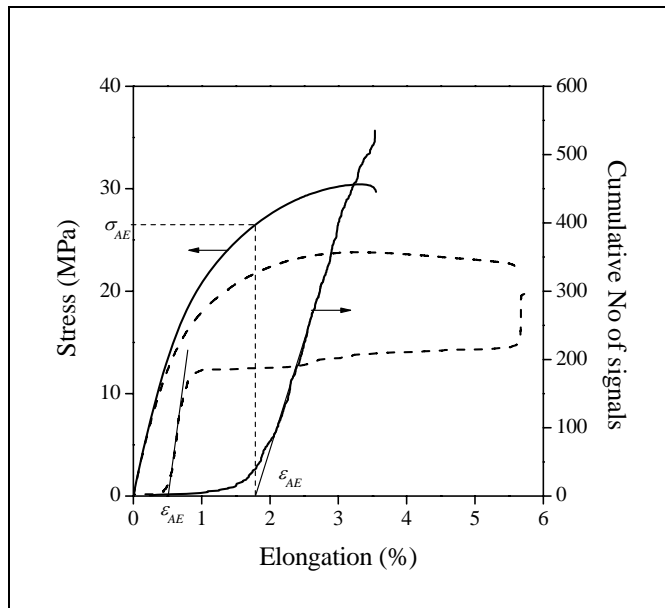


Fig. 6.6 Effect of adhesion on the acoustic activity of PP/corn cob composites. Left axis: stress; right axis: cumulative number of signals. Conditions: 20 wt%, homo, ----- poor adhesion, ——— good adhesion.

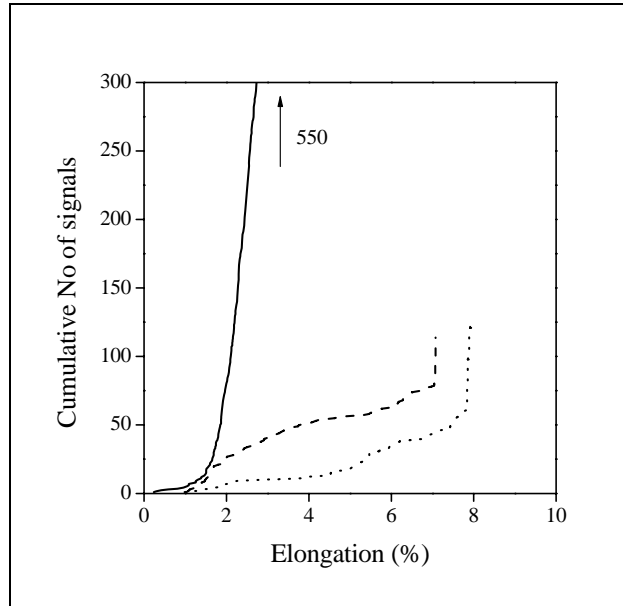


Fig. 6.7 Comparison of the acoustic activity of the three PP polymers in the case of good adhesion. — homo, - - - - random, ····· heterophase.

Characteristic, initiation stress can be derived from the acoustic emission traces in the way indicated in Fig. 6.6. It is plotted against filler content in Fig. 6.8. The six series of composites can be divided into three groups. Initiation stresses are small and slightly decrease with filler content in the case of poor adhesion. The differences among the polymers can be related to matrix properties, mainly to changing stiffness. In the presence of MAPP signals are initiated at larger stresses for the two copolymers, while the homopolymer is a separate class in itself with even larger debonding stresses. The influence of the two mechanisms indicated by the different shape of the cumulative hit vs. deformation traces is manifested also in the different initiation stresses. Unfortunately we still do not know the exact mechanism of deformation.

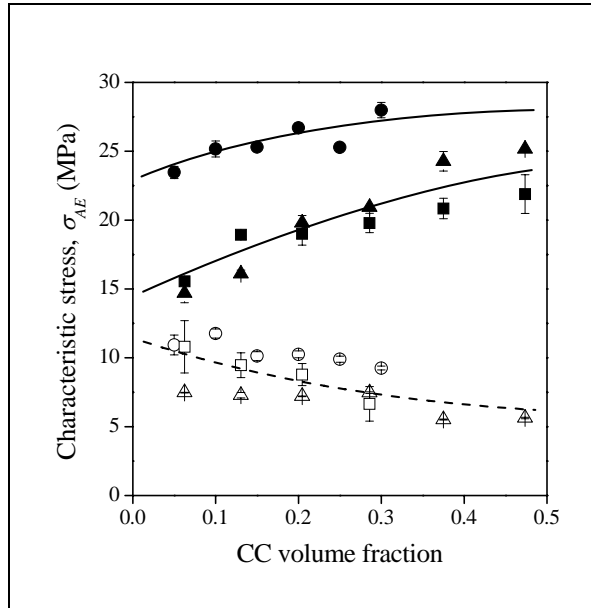


Fig. 6.8 *Effect of filler content on the stress value characterizing the initiation of the dominating micromechanical deformation process in PP/CC composites. Symbols are the same as in Fig. 6.1.*

6.3.3. Deformation and failure mechanisms

The characteristic stress, σ_{AE} , determined from the acoustic emission measurements (see Fig. 6.6) is related to the dominating deformation process. Accordingly debonding stress can be determined experimentally from such measurements. The characteristic stress is plotted against the square root of matrix modulus in Fig. 6.9. As we mentioned earlier, debonding stress must depend linearly on the square root of matrix modulus if debonding is the dominating process (see Eq. 1.2). We can see that a very good linear correlation is obtained in the absence of MAPP, i.e. at poor adhesion, indicating that in this case debonding dominates indeed. On the other hand, no correlation is obtained between the characteristic stress and modulus when adhesion is good, proving that other mechanisms than debonding must occur during the deformation of the composites.

These other mechanisms might be the fracture of the reinforcing particles or the yielding of the matrix. If any of these processes dominate, the characteristic stress should correlate with the yield stress of the matrix instead of modulus. σ_{AE} is plotted against matrix yield stress in Fig. 6.10. The obtained correlations are almost the exact opposite of those seen in Fig. 6.9. A linear correlation exists between σ_{AE} and yield stress in the case of good adhesion, while no such correlation can be observed in the absence of the coupling agent. These results strongly support our assumption that yielding is the dominating process in the case of good adhesion. The question remains open

whether particles fracture in any of the matrices as observed earlier [17,18], and in the case of a positive answer, why is the correlation of σ_{AE} and yield stress is linear.

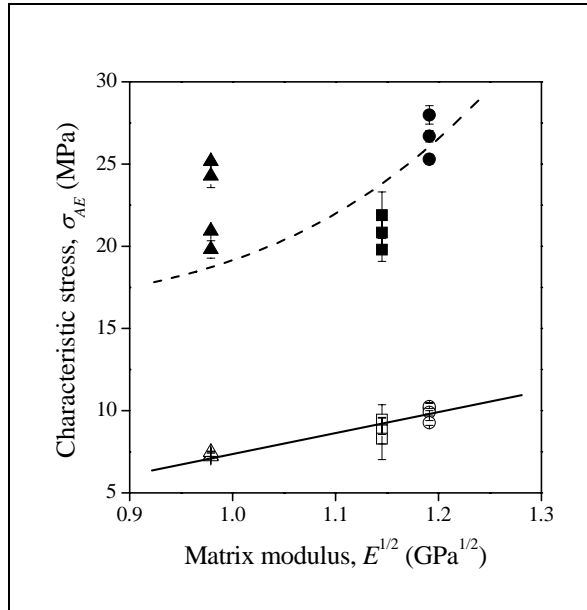


Fig. 6.9 Correlation between characteristic stress and the square root of matrix modulus (see Eq. 1.2) for PP/corn cob composites at various filler contents. Symbols are the same as in Fig. 6.1.

Additional information about the mechanism of failure was obtained from the SEM micrographs taken from the surface of specimens broken during tensile testing. Only three micrographs are presented here in order to save space. The fracture surface of the composite prepared from the homopolymer and 20 wt% corn cob is shown in Fig. 6.11a. The micrograph does not leave any doubt that debonding is the dominating deformation process in this case. Just the opposite is seen in Fig. 6.11b showing the surface of a similar composite but also containing MAPP. Besides, the fracture of a large, anisotropic particle, we see also the ragged, broken surface of an almost spherical particle (indicated by the white circle) adhering well to the matrix. In the micrographs of the composites prepared from the two copolymers mainly extensive yielding and some debonding can be observed. An example is shown in Fig. 6.11c.

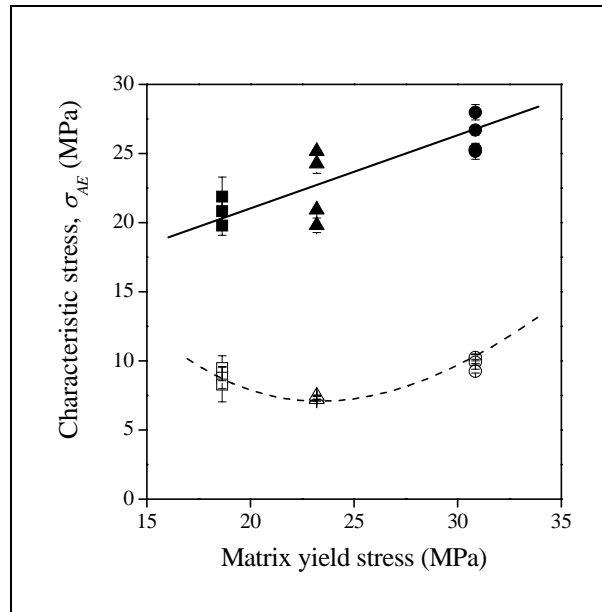


Fig. 6.10 Correlation of characteristic stress and matrix yield stress in PP/CC composites with different corn cob contents. Symbols are the same as in Fig. 6.1.

Table 6.3 Map of deformation and failure mechanisms in the studied PP composites prepared in various matrices at poor and good adhesion, respectively

Polymer	Deformation mechanism					
	Poor adhesion			Good adhesion		
	Debonding	Yielding	Fracture ^{a)}	Debonding	Yielding	Fracture ^{a)}
homo	+	-	-	-	-	+
heterophase	+	-	-	(+)	+	-
random	+	-	-	(+)	+	-

a) fracture of the corn cob particles

(+) possible mechanism

Based on the analysis presented above and the study of a large number of SEM micrographs a failure map was created for the composites prepared from the three matrices (Table 6.3). The dominating deformation is debonding for all three matrices when adhesion is poor, no other mechanism could be detected in these materials. Shear yielding of the matrix and limited debonding takes place in the two copolymers while the fracture of the corn cob particles dominates in the homopolymer. Particle fracture initiates the shear yielding of the matrix thus resulting in the linear correlation of Fig. 6.10.

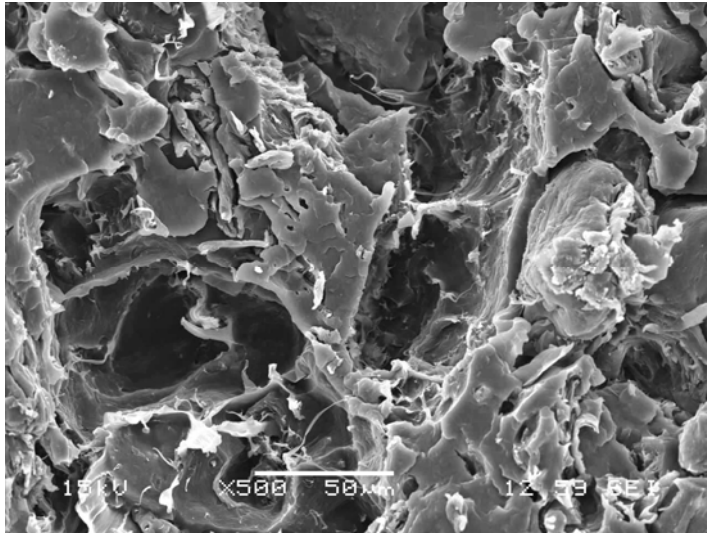


Fig. 6.11a

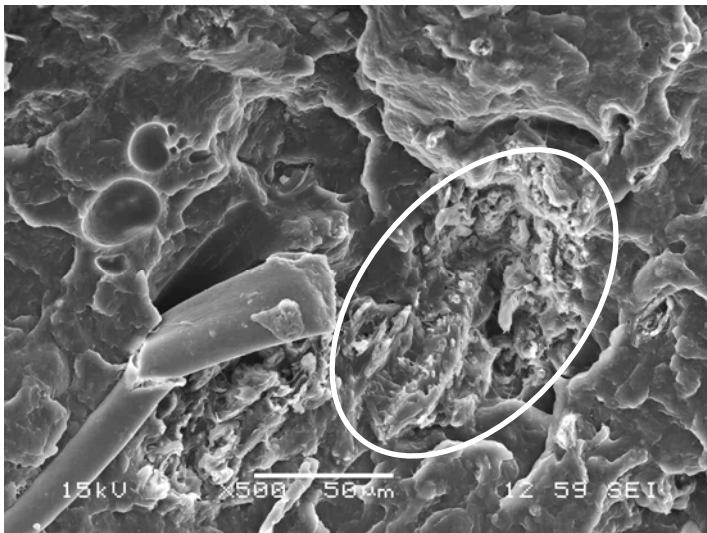


Fig. 6.11b

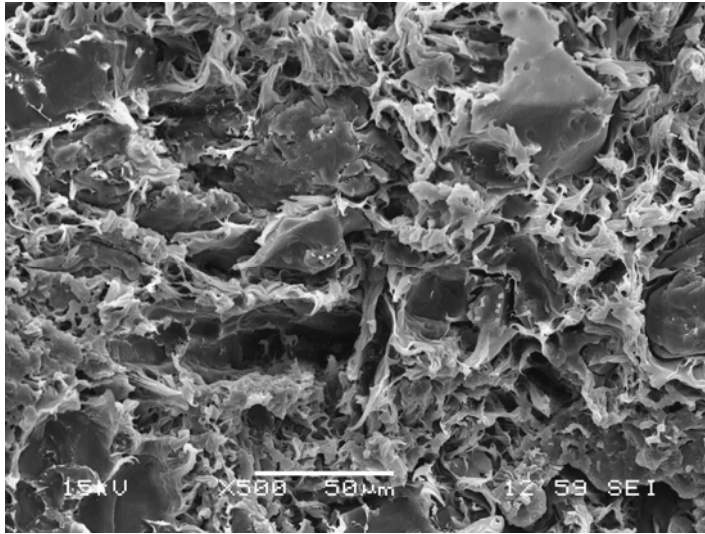


Fig. 6.11c

Fig. 6.11 *Characteristic SEM micrographs revealing different deformation mechanisms in PP/corn cob composites. CC content: 20 wt%, a) homo, no MAPP, debonding, b) homo, MAPP, fracture of CC, c) heterophase, MAPP, shear yielding and debonding.*

6.3.4. Consequences

The importance of the micromechanical deformation processes in the application of the composites is emphasized strongly by Fig. 6.12 in which tensile strength of the composites is plotted against the characteristic stress determined by acoustic emission measurements. Very close correlation exists between the two quantities showing that strength is determined by the dominating micromechanical deformation irrespective of its mechanism. The deviations from the general tendency can be assigned to structural effects. Orientation, probable geometrical interaction of the particles and even their embedding into the elastomeric phase in the case of the heterophasic copolymer may result in positive or negative deviations.

The identification of the dominating mechanism also allows us to consider the ways to achieve further improvement in properties. The yield stress of the matrix limits the improvement of stiffness and strength in the copolymers, further increase is possible only by the proper selection of the reinforcement. Different particle geometry with larger aspect ratio and orientation results in stiffer and stronger composites. These factors have the same effect in the homopolymer as well. However, the limiting factor is the inherent strength of the particles in this polymer. Improvement is possible by the chemical modification of the filler or by the selection of another type of reinforcement with larger inherent strength. The determination of micromechanical deformation processes clearly identifies the limits of property improvement with a certain set of components and allows the optimization of price and performance.

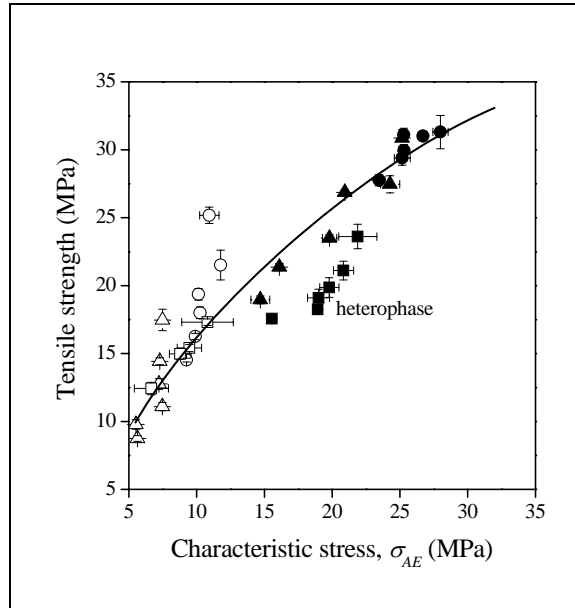


Fig. 6.12 Correlation between the characteristic stress of the dominating micromechanical deformation process and the tensile strength of PP/CC composites. Symbols are the same as in Fig. 6.1.

6.4. Conclusions

The experiments carried out with three different PP matrices, a homopolymer, a random and a heterophase copolymer, proved that the dominating micromechanical deformation process may change with matrix properties. Yield stress determined from the stress vs. strain traces may cover widely differing processes. Debonding is the dominating process when the adhesion of the components is poor, while matrix yielding and/or filler fracture dominate when adhesion is improved by the introduction of a functionalized polymer. The dominating deformation mechanism is determined by component properties (matrix characteristics, particle strength and geometry) and adhesion. Interfacial adhesion, matrix yield stress and the inherent strength of the reinforcement can be limiting factors in the improvement of composite strength. The properties of polymer composites reinforced with lignocellulosic fibers are determined by micromechanical deformation processes, but they are independent of the mechanism of these processes.

6.5. References

1. Bledzki, A. K., Letman, M., Viksne, A., Rence, L.: *Composites* **A36**, 789–797 (2005)
2. Maldas, D., Kokta, B. V.: *Compos Interf* **1**, 87–108 (1993)
3. Neagu, R. C., Gamstedt, E. K., Berthold, F.: *J Compos Mater* **40**, 663–699 (2000)
4. Coutinho, F. M. B., Costa, T. H. S., Suarez, J. C. M., Melo, D. P.: *Polym Test* **19**, 625–633 (2000)
5. Bledzki, A., Faruk, O.: *App Compos Mater* **10**, 365–379 (2003)
6. Stark, N. M., Rowland, R.E.: *Wood Fiber Sci* **35**, 167- (2003)
7. Ichazo, M. N., Albano, C., Gonzalez, J., Perera, R., Candal, M.V.: *Compos Struct* **54**, 207–214 (2001)
8. Cantero, G., Arbelaz, A., Mugika, F., Valea, A., Mondragon, I.: *J Reinf Plast Compos* **22**, 37–50 (2003)
9. Demir, H., Atikler, U., Balköse, D., Tihminlioglu, F.: *Composites* **A37**, 447–456 (2006)
10. Zhang, C., Li, K., Simonsen, J.: *J Adhesion Sci Technol* **18**, 1603–1612 (2004)
11. Zhang, C., Li, K., Simonsen, J.: *Polym Eng Sci* **46**, 108–113 (2006)
12. Joly, C., Gauthier, R., Escoubes, M.: *J Appl Polym Sci* **61**, 57–69 (1996)
13. Bledzki, A. K., Gassan, J.: *Prog Polym Sci* **24**, 221–74 (1999)
14. Doan, T. T. L., Gao, S.L., Mader, E.: *Compos Sci Technol* **66**, 952–963 (2006)
15. Bledzki, A. K., Faruk, O., Huque, M.: *Polym Plast Techn Eng* **41**, 435–451 (2002)
16. Cantero, G., Arbelaz, A., Mugika, F., Valea, A., Mondragon, I.: *J Reinf Plast Compos* **22**, 37–50 (2003)
17. Dányádi, L., Renner, K., Móczó, J., Pukánszky, B.: *Polym Eng Sci* **47**.1246–55 (2007)
18. Renner, K., Móczó, J., Pukánszky, B.: *Compos Sci Technol* **69**, 1653–1659. (2009)
19. Dominkovics, Z., Dányádi, L., Pukánszky, B.: *Compos Part A-Appl* **38**, 1893–1901 (2007)
20. Pukánszky, B., Vörös, G.: *Compos Interf* **1**, 411–427 (1993)
21. Renner, K., Yang, M. S., Móczó, J., Choi, H. J., Pukánszky B. *Eur Polym J* **41**, 2520–2529 (2005)
22. Pukánszky, B.: *Composites* **21**, 255–262 (1990)

Chapter 7

Quantitative determination of interfacial adhesion in composites with strong bonding⁹

7.1. Introduction

According to some authors interfacial adhesion is the decisive factor determining the properties of composites and appropriate adjustment of interphase properties and adhesion strength is the most important condition of achieving acceptable properties [1,2]. The debate continues also on the most proper adhesion strength in composites. Very strong adhesion is claimed to lead to stiff and brittle composites, while in the case of weak adhesion the components debond under the effect of external load with the consequences mentioned above. Medium or appropriate strength is claimed to be the most advantageous, however a quantitative value is never assigned to this claim.

The strength of interfacial adhesion can be estimated reasonably well by the determination of the reversible work of adhesion. This quantity can be calculated from the surface tension of the components and/or acid base interactions when interfacial adhesion is created by secondary, van der Waals forces [3]. Very good correlations were found between interfacial adhesion and various mechanical properties, mostly yield stress and ultimate strength, in several composites [4,5]. Often functionalized polymers are added to polyolefin composites to create the necessary adhesion. Maleated polypropylene (MAPP) or polyethylene (MAPE) is used in wood reinforced composites or layered silicate composites. In glass fiber reinforced PP the fibers are treated with an aminosilane coupling agent and MAPP is added to the matrix to improve adhesion. Covalent bonding and interdiffusion of the functionalized polymer with the matrix result in strong adhesion in these cases. The concept of reversible work of adhesion cannot be used in such cases for the estimation of the strength of adhesion. Interfacial adhesion can be determined by single fiber tests in long fiber reinforced composites [6,7], but no method exists for particulate filled, short fiber reinforced or nanocomposites.

The goal of this chapter is to present an approach which makes possible the determination of the strength of interfacial adhesion in cases when debonding is the dominating micromechanical deformation process. Debonding stress is determined by acoustic emission and an appropriate model is used for the calculation of interfacial adhesion. The approach is validated with known values of interfacial adhesion and the strength of adhesion is determined for composites containing various fillers and for different surface modifications.

7.2. Experimental

The polymer used as matrix in the experiments was the Tipplen H 543 F grade

⁹ Renner, K., Móczó, J., Vörös, G., Pukánszky, B.: *Macromol Rapid Comm* (submitted)

polymer (MFR 4 g/10 min at 230 °C and 2.16 N) produced by TVK, Hungary. Two types of filler were used in the experiments both with different particle sizes. The CaCO₃ fillers were supplied by Omya, Switzerland and the average particle size of the samples was 260, 36, 21, and 5 μm. Glass beads were purchased from Potters Inc., USA with average particle sizes of 73, 60, 25 and 10 μm. CaCO₃ fillers were used without any coating, with stearic acid treatment, and MAPP was added to increase adhesion. Glass beads were added to the polymer as received, stearic acid was used to decrease, while MAPP (Orevac CA 100, Arkema, France), 3-aminopropyl-triethoxy-silane as well as the combination of MAPP and the silane were used to increase interfacial adhesion. Composites were prepared as a function of composition; filler content changed between 0 and 0.30 volume fraction in 0.05 volume fraction steps. The components were homogenized in a Brabender W 50 EH internal mixer at 190 °C, 50 rpm for 10 minutes. The composites were compression molded into 1 mm thick plates at 190 °C using a Fontijne SRA 100 machine. Tensile characteristics were determined at 5 mm/min cross-head speed and 80 mm gauge length using an Instron 5566 apparatus. Acoustic emission signals were recorded with a Sensophone AED 40/4 apparatus. The structure of the composites and the mechanism of failure were studied by SEM (JEOL JSM-6380 LA) on fracture surfaces created during tensile testing.

7.3. Result and discussion

7.3.1. Approach

As described earlier (see Chapter 1) models were developed by Vollenberg and Heikens as well as by Vörös and Pukánszky to predict the stress necessary to initiate debonding [8, 9]. As emphasized in the introduction the exact values of the geometric constant are unknown in Eq. 1.2 at the moment and cannot be determined in a simple way, thus the absolute value of debonding stress cannot be predicted. However, if we can determine debonding stress by an appropriate method for composites with known interfacial adhesion, C_1 and C_2 can be calculated from Eq. 1.2, and then interfacial adhesion, W_a , can be derived quantitatively for composites in which interaction is created by other mechanisms than secondary forces.

One of the key elements of the approach is the determination of debonding stress and acoustic emission seems to be an appropriate method for this purpose. Acoustic emission measurements were carried out on various composites and the results proved that signals develop during deformation and the mechanism of micromechanical deformation processes can be often determined by proper analysis [10,11]. The results of such an acoustic emission experiment are presented in Fig. 7.1 for demonstration. The small circles are the individual signals (events, hits) picked up by the microphone. Their amplitude (scale not shown) is characteristic for the deformation process [11]. We can see that considerable number of signals is detected only after a certain deformation, i.e. above a certain stress value. The cumulative number of signals is determined and used in further evaluation. The shape of the trace depends on the mechanism of deformation; usually a trace approaching a saturation value is obtained when debonding is

the dominating deformation process. The corresponding stress vs. strain correlation is also plotted in the figure partly for comparison and to demonstrate the determination of a characteristic stress value, σ_{AE} , which is assigned to the initiation of debonding. In further treatment we assume that $\sigma^D = \sigma_{AE}$. Fig. 7.1 calls attention also to the difficulty and weak point of the approach. Individual signals are very much spread along the deformation axis. Commercial fillers usually have a broad particle size distribution and according to Eq. 1 debonding stress depends on particle size. As a consequence, the assignment of the proper particle size to the corresponding σ_{AE} value is difficult. Since debonding starts on large particles first, we used the largest particle size determined by extrapolation from the upper leg of the particle size distribution trace for the determination of the constants and adhesion strength.

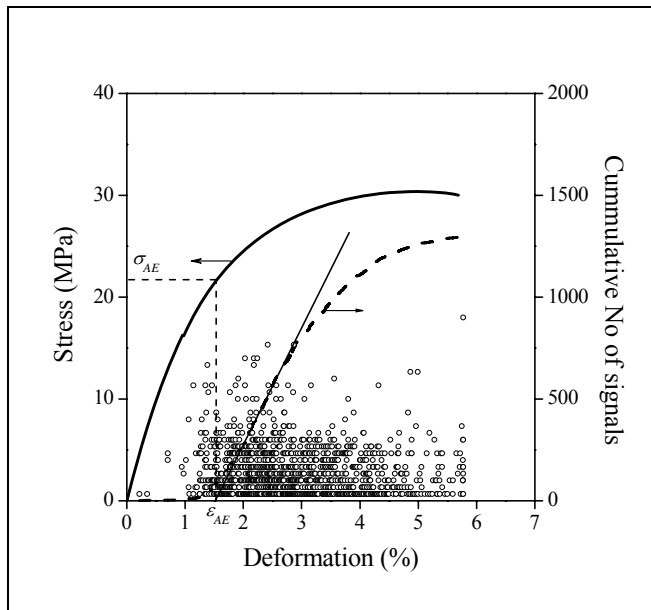


Fig. 7.1 Determination of debonding stress by acoustic emission experiments. PP/CaCO₃/MAPP composite; average size of the filler: 36 μm ; filler content: 15 vol%; \circ individual acoustic signals, ——— stress vs. strain and - - - - - cumulative number of signals vs. strain traces.

7.3.2. Determination of constants C_1, C_2

Acoustic emission gives debonding stress and particle size is determined from the distribution curve as described above. The reversible work of adhesion can be calculated from the surface tension of the components for composites in which secondary forces create adhesion. We determined the values of the constants C_1 and C_2 using results obtained on PP/CaCO₃ composites. For uncoated CaCO₃ particles the reversible work of adhesion is 107 mJ/m^2 [12]. Plotting the characteristic stress, σ_{AE} , against $(1/R)^{1/2}$ or $(EW_{AB}/R)^{1/2}$ we should obtain straight lines which yield C_1 and C_2 as the slope

and the intersection. Thermal stress, σ_T , was estimated to be 10 MPa [13,14] and the modulus of the matrix was 1.5 GPa. The correlation is plotted in Fig. 7.2 for PP/CaCO₃ composites containing a fillers with different particle sizes in 20 vol%. We obtain a straight line as predicted with a determination coefficient (goodness of the fit) of 1.000. Similar lines were obtained for other filler contents as well, although the goodness of the fit was somewhat worse in the other cases the smallest value being 0.9013. Averaging all values determined with various filler contents we obtain $C_1 = 0.23 \pm 0.08$ and $C_2 = 4.31 \pm 0.5$. The knowledge of the constants of Eq. 1.2 allows us the calculation of interfacial adhesion for any composite, if we can determine debonding stress by acoustic emission or any other technique.

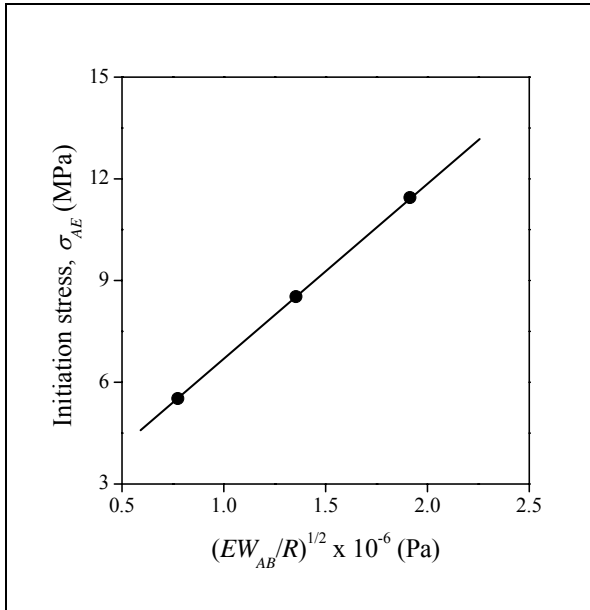


Fig. 7.2 Determination of the C_1 and C_2 parameters of Eq. 1.2 from initiation stresses derived from acoustic emission experiments in PP/CaCO₃ composites; uncoated filler; 20 vol%.

The major condition of using the approach presented here is that debonding must be the dominating deformation mechanism and the signals detected by acoustic emission must originate in this process. SEM micrographs were taken from the fractured surface of composites to verify the mechanism of deformation. Debonding is undoubtedly the dominating process in composites containing uncoated or stearic acid coated fillers [15,16]. However, the mechanism is less unambiguous when other surface modification techniques are used, like MAPP or silane treatment. Two micrographs are presented in Fig. 7.3 in order to justify the approach. The fracture surface of a PP/CaCO₃ composite with MAPP modification is shown in Fig. 7.3a. Debonding and subsequent plastic deformation is clearly seen in the figure. Debonding is even more obvious in composites containing silane treated glass particles (Fig. 7.3b). Clean sur-

faces and separation of even small particles from the matrix clearly prove that the mechanism is debonding also in this case. Another proof for the validity of the approach is supplied by its application to PP/CaCO₃ composites containing particles coated with stearic acid. Non-reactive treatment of the filler should decrease matrix/filler interaction in this case, on the one hand, and reversible work of adhesion can be easily calculated in such composites, on the other. We obtained a value of 65 mJ/m² for W_{AB} by calculation and we arrived to $W_a = 51$ mJ/m² by using the approach. Both SEM and the comparison to values obtained by direct determination of the strength of interaction verified the approach.

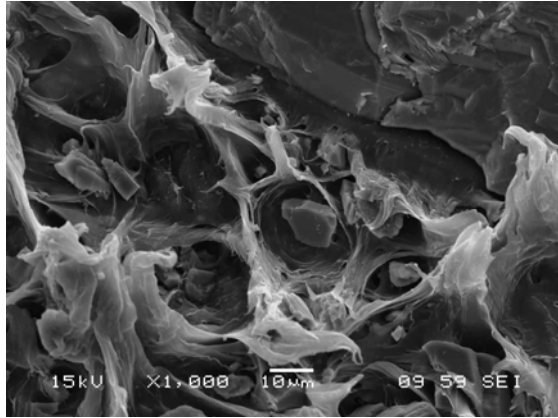


Fig. 7.3a

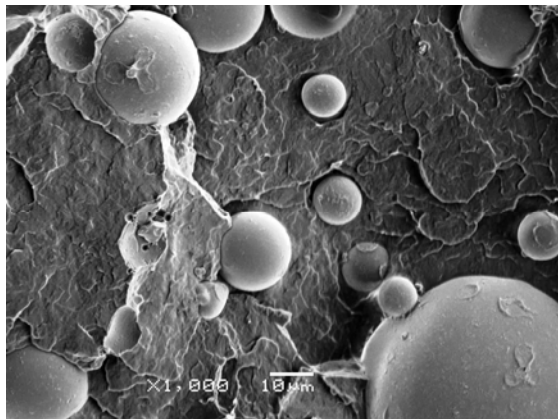


Fig. 7.3b

Fig. 7.3 SEM micrographs showing the debonding of particles during tensile testing; a) PP/CaCO₃/MAPP, average size of the filler: 21 μm, filler content: 15 vol%; b) PP/glass beads/silane, filler size: 60 μm, filler content: 15 vol%.

7.3.3. Strength of adhesion, surface modification

The method was applied to composites in which interfacial adhesion is created by other mechanisms than secondary forces. These included MAPP modification in PP/CaCO₃ and various treatments in PP/glass bead composites. The results of the measurements and the calculated interfacial adhesion values are summarized in Table 7.1. Interfacial adhesion values obtained by direct calculation are also included as reference. Some of the results correspond to expectations, but others need explanation. The strongest adhesion was obtained in the PP/CaCO₃ composites containing MAPP. This is not surprising, since MAPP can attach to the surface of CaCO₃ by ionic bonds after hydrolysis or by strong dipole like interaction in its absence. We assume the formation of ionic bonds in this case. However, the strength of adhesion could be determined quantitatively by our method and it proves to be one order of magnitude larger than adhesion created by simple secondary forces in the case of the uncoated or stearic acid coated filler.

Table 7.1 Adhesion strengths determined in PP composites at various surface modifications by the proposed approach

Filler	Surface modification	Adhesion strength, W (mJ/m ²)	
		Calculated, W_{AB}	Measured, W_a
CaCO ₃	–	105	99
CaCO ₃	stearic acid	65	51
CaCO ₃	MAPP		861
glass beads	–		487
glass beads	stearic acid		80
glass beads	MAPP		650
glass beads	aminosilane		584
glass beads	MAPP + silane		648

The explanation of the values obtained for PP/glass bead composites is more difficult. The effect of stearic acid is clear and corresponds to expectations. The adsorption and effect of stearic acid is slightly surprising though, because of the lack of specific interactions between the glass surface and stearic acid. On the other hand, the larger value of 80 mJ/m² compared to the PP/CaCO₃ case might be explained with incomplete coverage of the surface. The relatively large value obtained for the uncoted glass may be assigned to the high surface energy of this specific glass. Unfortunately we could not measure surface tension by IGC because of the large size of the particles,

which made column preparation impossible. Silanes are believed and often claimed to improve adhesion in all systems even in the lack of reactive groups [17,18]. We could not expect coupling in PP, but earlier experiments proved that limited oxidation of the matrix during processing may lead to coupling reactions [19]. The proof of these reactions is the relatively large adhesion of 590 mJ/m² obtained upon silane treatment. MAPP has the strongest effect, which is practically the same as that of the combination of MAPP and aminosilane. The strength of adhesion is only marginally larger than that obtained for the uncoated filler. The limited improvement in adhesion might result from inefficient and/or insufficient treatment with the silane compound, or can be a real effect showing the limitations of these surface modification techniques in the studied composites. Obviously further experiments are needed to answer the question. Nevertheless, expressing the strength of adhesion in numbers makes possible further analysis. The results also call attention to the fact that silane treatment does not always work and that careful considerations and thorough experimentation are needed before the selection of a certain surface modification technique.

7.4. Conclusions

An approach was proposed for the quantitative determination of adhesion strength in composites, in which adhesion is created by other mechanisms than secondary interactions. The approach is based upon a model, which gives debonding stress as a function of interfacial adhesion. Debonding stress is determined by acoustic emission experiments. The mechanism of deformation was checked by SEM experiments and the approach was verified on composites with known interfacial adhesion. The results obtained showed that the use of functionalized polymer in PP/CaCO₃ composites resulted in adhesion strength one order of magnitude larger than without the coupling agent. The application of various surface modification techniques in PP/glass bead composites yielded different adhesion values covering a range of about one order of magnitude. The quantitative determination of interfacial adhesion makes possible the design and optimization of most surface modification techniques in particulate filled and short fiber reinforced composites.

7.5. References

1. Kardos, J.L.: The role of the interface in polymer composites - some myths, mechanisms, and modifications, in H. Ishida and G. Kumar (Eds.), *Molecular Characterization of Composite Interfaces*, Plenum, 1985, pp. 1-11
2. Eirich, F.R.: Some mechanical and molecular aspects of the performance of composites, *J. Appl. Polym. Sci., Appl Polym. Symp.*, **39** 93-102 (1984)
3. Pukánszky, B., Fekete, E.: Adhesion and Surface Modification in Mineral Fillers in Thermoplastics. Raw Materials and Processing, ed. Jancar, J., *Adv. Polym. Sci.* **139**, 109-153 (1999)
4. Móczó, J., Fekete, E., Pukánszky, B.: *J. Adhesion* **78**, 861-875 (2002)
5. Vörös, Gy., Fekete, E. and Pukánszky, B., *J. Adhesion*, **64**, 229 (1997).
6. Herrerafranco, P. J., Drzal, L. T.: *Composites* **23**, 2-27 (1992)

7. Piggott, MR Interfaces in composites Elsevier London
8. Vollenberg, P. The mechanical behaviour of particle filled thermo-plastics. PhD Thesis, Eindhoven University of Technology, Eindhoven, 1987.
9. Pukánszky, B., Vörös, Gy.: *Compos. Interfaces* **1**(5), 411-427 (1993)
10. Dányádi, L., Renner, K., Móczó, J., Pukánszky, B: *Polym. Eng. Sci.* **47** 1246-1255 (2007)
11. Renner, K., Móczó, J., Pukánszky, B: *Compos. Sci. Technol.* **69**, 1653-1659 (2009)
12. Pukánszky, B., Fekete, E., Tüdös, F.: *Makromol. Chem., Macromol. Symp.* **28**, 165-186 (1989)
13. Vollenberg, P., Heikens, D., Ladan, H. C. B.: *Polym Compos;* **9** 382-388 (1988)
14. Beck, R. H., Gratch, S., Newman, S., Rausch, K. C.: *J. Polym. Sci., Polym. Lett.*, **6**, 707 (1968)
15. Lazzeri, A., Zebarjad, S. M., Pracella, M., Cavalier, K., Rosa, R.: *Polymer* **46**, 827-844 (2005)
16. Osman, M. A., Atallah, A.: *Marcomol Chem Phys* **208**, 87-93 (2007)
17. Trotignon, J., P., Verdu, J., Boissard, R., Vallois, A., in *Polymer Composites*, ed. Sedlacek, B., Walter de Gruyter, Berlin, 1986, p.191
18. Han, C. D., Van Den Weghe, T., Shete, P., Haw, J.R.: *Polym Eng. Sci.*, **21**, 196 (1981)
19. Demjén, Z., Pukánszky, B., Nagy, J.Jr.: *Polymer* **40**, 1763-1773 (1998)

Chapter 8

Summary

Polymers reinforced with natural fibers are used in large quantities; the production of such materials is a mature technology now. Intensive research continues in the field with the goal of improving composite properties, and to produce better and cheaper materials. Particulate filled and natural fiber reinforced composites are usually applied in load-bearing applications, thus the goal of most development work is to produce stiffer and stronger composites. Under the effect of external load stress concentration develops around the inclusions in these heterogeneous materials. Local stress maxima induce local deformation processes which determine the mechanism of failure and the final properties of the composites. Improvement of composite properties is possible only if we know and control the local micromechanical deformations processes. This Thesis started on the investigation of particulate filled PP composites. The observation made on these systems helped to understand the basics of micromechanical deformation processes and to get acquainted with the limitation of acoustic emission measurements. These preliminary experiments provided useful information about debonding so we tried to extend our investigations onto other heterogeneous polymer systems. In recent years the interest of the scientific community turned towards new fields. Much research is done on nanocomposites, but considerable interest is focused on bio-related materials derived from renewable resources. Since our research group was working on these fields for a while it was an obvious choice to focus our attention onto natural reinforced and nanocomposites. Accordingly, this Thesis was dedicated to the study micromechanical deformations and failure mechanisms in heterogeneous polymers and specifically to the determination of factors limiting the effect of reinforcement in the studied composites. Although we summarized the most important results of the research at the end of each chapter, we briefly repeat them here to give a concise overview of our achievements. At the end of this chapter we compile the most important new findings of this work in a few thesis points.

Particle filled polymers were studied in the first stage of the research. PP/PMMA model composites containing particles with narrow particle size distribution were compared to composites made from PP and commercial CaCO_3 filler. Measurements of acoustic emission signals during the elongation of PP/PMMA composites allowed us to assign the debonding process, including its initiation, unambiguously to a well defined range of the stress vs. strain curve. The number and intensity of the signals detected in the matrix and the composite, respectively, differed considerably, which made possible the separation of the various micromechanical deformation processes occurring in them. At small particle content debonding occurs at relatively low stresses, which differ considerably from yield stress. Considerable plastic deformation of the matrix starts at the yield point. At larger filler content debonding and shear yielding occur simultaneously. Micromechanical deformation processes cannot be separated as clearly in composites prepared from the commercial CaCO_3 filler with a broad particle size distribution. The debonding of particles with different sizes occurs in a wide deformation range because of the particle size dependence of debonding stress. The analysis of characteristic values derived from acoustic emission experiments proved that the

interacting stress fields of neighboring particles influence deformation and that even large particles may aggregate or at least associate at large filler content.

Nanocomposites were prepared from polyamide and silicates with and without organophilization. The goal of the study was to investigate the effect of filler content and adhesion on the structure and properties of the composites. With the help of acoustic emission and volume strain measurements supplemented by microscopy we tried to obtain as much information about the mechanism of deformation as possible. The results showed that the structure of the composites is more complicated than usually stated. They contain various structural entities; besides individual silicate platelets, tactoids with different degree of intercalation and larger particles can be also found in them. The matrix polymer and the composites deform according to different mechanisms. Sound is emitted by cavitation in the former, while sound emitting processes are related to larger structural entities, i.e. to tactoids and non-exfoliated particles in the composites. Acoustic events are generated mainly by the fracture of the particles. Matrix/silicate adhesion seems to be strong, debonding rarely takes place, and volume increase is initiated primarily by particle failure. The type and amount of the surfactant used for organophilization plays an important role in the determination of deformation processes and properties, since it influences both matrix/filler interaction and the internal adhesion of silicate particles.

Experiments carried out on PP/wood composites proved that several processes take place during the deformation of failure of these composites. The matrix deforms mainly by shear yielding, debonding and fiber pull out occurs when interfacial adhesion is poor, and fiber fracture dominates in the presence of coupling agent. We concluded from these results that further improvement of composite strength is possible only by the increase of the inherent strength of wood particles. One way to do that was assumed to be the decrease of their size. The study of the deformation and failure of PP/wood composites containing wood particles of different sizes proved that micromechanical deformations change drastically with decreasing particle size. Less debonding, fiber pull out and fiber fracture occur in composites containing small particles. The apparently slight influence of particle size on composite strength results from the smaller aspect ratio of the small particles, which indicates that orientation and orientation distribution must have a strong effect on reinforcement. Further improvement in composite strength is possible only through the optimization of particle size, aspect ratio and the inherent strength of wood.

A more detailed study on the factors determining the reinforcing efficiency was carried out subsequently. PP/lignocellulosic composites were prepared from four different fillers. The results proved that the properties of the composites depend strongly on interfacial adhesion and on the particle characteristics of the wood. Coupling with functionalized polymer is necessary for the preparation of composites with acceptable properties if the size of the particles is large and their aspect ratio is small. The effect of adhesion is smaller for particles with large aspect ratio. Large aspect ratio and small fiber diameter result in better reinforcement. The inherent properties of the reinforcement may limit the improvement of composite strength. A failure map was presented to show the effect of particle characteristics and adhesion on the dominating deformation process.

While the effect of wood characteristics and interfacial adhesion on composite properties were studied extensively, much less attention has been paid to the influence of matrix characteristics. As a consequence, the goal of another subproject was to investigate the influence of matrix characteristics on deformation and failure in PP/natural fiber composites. The experiments carried out with three different PP matrices, a homopolymer, a random and a heterophase copolymer, proved that the dominating micromechanical deformation process may change with matrix properties. Yield stress determined from the stress vs. strain traces may cover widely differing processes. Debonding is the dominating process when the adhesion of the components is poor, while matrix yielding and/or filler fracture dominate when adhesion is improved by the introduction of a functionalized polymer. The dominating deformation mechanism is determined by component properties (matrix characteristics, particle strength and geometry) and adhesion. Interfacial adhesion, matrix yield stress and the inherent strength of the reinforcement can be limiting factors in the improvement of composite strength. The properties of polymer composites reinforced with lignocellulosic fibers are determined by micromechanical deformation processes, but they are independent of the mechanism of these processes.

Various models and methods were introduced in this thesis to characterize interfacial interaction and the effect of reinforcement. In the final part of the study an approach was proposed for the quantitative determination of adhesion strength in composites, in which adhesion is created by other mechanisms than secondary interactions. The approach is based upon a model, which gives debonding stress as a function of interfacial adhesion. Debonding stress is determined by acoustic emission experiments. The mechanism of deformation was checked by SEM experiments and the approach was verified on composites with known interfacial adhesion. The results obtained showed that the use of functionalized polymer in PP/CaCO₃ composites resulted in adhesion strength one order of magnitude larger than without the coupling agent. The application of various surface modification techniques in PP/glass bead composites yielded different adhesion values covering a range of about one order of magnitude. Consequently the quantitative determination of interfacial adhesion makes possible the design and optimization of most surface modification techniques in particulate filled and short fiber reinforced composites.

The most important conclusions of this thesis can be briefly summarized in the following points:

1. We proved by the analysis of micromechanical deformation processes in PP composites containing model and commercial fillers that debonding stress can be determined with the help of acoustic emission measurements. We pointed out that debonding occurs in a deformation range depending on the size distribution of the filler. The interacting stress fields of neighboring particles influence deformation, and even large particles may aggregate or associate at large filler content.
2. We showed by the analysis of PA6/layered silicate composites that they contain various structural entities; besides individual silicate platelets, tactoids with different degree of intercalation and larger particles can be also found in them. We proved by acoustic emission and volume strain measurements that

deformation processes are related to larger structural entities, i.e. to tactoids and non-exfoliated particles in the composites, and the dominant deformation process is mainly the fracture of particles.

3. We analyzed the micromechanical processes taking place during the deformation of PP/wood composites containing wood particles of different sizes and showed that micromechanical deformations change drastically with decreasing particle size. Less debonding and fiber fracture occurred in composites containing the filler with smaller particle size, but thus influenced composite strength only slightly. We predicted that further improvement in composite strength is possible only through the optimization of particle size, aspect ratio and the inherent strength of wood.
4. We predicted by the study of deformation processes in different PP/lignocellulosic composites that micromechanical deformation processes determine composite properties irrespectively of their mechanism. We proved this statement by the close correlation between the characteristic stress derived from acoustic emission measurements and composite strength.
5. We could confirm by the study of PP/lignocellulosic composites with three different PP matrices that interfacial adhesion, matrix yield stress and the inherent strength of the reinforcement can be limiting factors in the improvement of composite strength. We proved that in the case of strong adhesion the dominating deformation process change with matrix properties, yielding occurs if the inherent strength of the filler is larger than the yield stress of the matrix, but for matrices with larger yield stress the fracture of filler particles becomes the dominant deformation process limiting the reinforcing effect.
6. We developed a method for the quantitative determination of adhesion strength in composites, in which adhesion is created by other mechanisms than secondary interactions. We pointed out for the first time that the use of functionalized polymer in PP/CaCO₃ composites results in adhesion strength of one order of magnitude larger than without the coupling agent.

List of symbols and abbreviations

ε	elongation-at-break (%)
γ_s^d	dispersion component of the surface tension of fillers (mJ/m ²)
φ	volume fraction of the filler in the composite
λ	relative elongation
ρ_f	density of the filler (g/cm ³)
σ	tensile strength (MPa)
$\sigma_{AE1}, \sigma_{AE2}$	characteristic stress derived from acoustic emission measurements (MPa)
σ^D	debonding stress (MPa)
σ^T	thermal stress (MPa)
σ_T	true tensile strength of the composite (MPa)
σ_{T0}	true tensile strength of the matrix (MPa)
σ_{Tred}	reduced tensile strength
σ_{VOLS}	characteristic stress derived from volume strain measurements
σ_y	yield stress of the composite
σ_{y0}	yield stress of the matrix
σ_{yi}	yield stress of the interphase
σ_{yred}	reduced yield stress of the composite
AE	acoustic emission
A_f	specific surface area of fillers (m ² /g)
B	load bearing capacity of fillers
C_1, C_2	constant for the determination of debonding stress
E	Young's modulus (GPa)
IGC	inverse gas chromatography
MAPE	maleic anhydride modified polyethylene
MAPP	maleic anhydride modified polypropylene
MFR	melt flow rate (g/10 min)
n	parameter characterizing the strain hardening of the matrix
PA	polyamide
PE	polyethylene
PP	polypropylene
SEM	scanning electron microscopy
StAc	stearic acid
R	radius of particle (μm)
VOLS	volume strain
vol %	volume percent
W_{AB}	work of adhesion (mJ/m ²)
W_a	measured work of adhesion (mJ/m ²)
wt %	weight percent
WPC	wood plastic composites
XPS	X-ray photoelectron spectroscopy
XRD	X-ray diffraction

Acknowledgements

First of all I would like to thank my supervisor, Béla Pukánszky for his attention and relentless support of my studies. I appreciate very much his guidance towards a more scientific way of thinking. I should also thank to my colleague and friend János Móczó for his support and patience during my Ph.D work. I am grateful for my friends and colleagues at the Laboratory of Plastics and Rubber Technology of the Budapest University of Technology and Economics, as well as at the Institute of Materials and Environmental Chemistry, Chemical Research Center, Hungarian Academy of Sciences for their help and for the pleasant atmosphere they created. And at last but not the least, I should like to thank my family and my friends for their continuous support in reaching my goals.

List of publications

Papers used for the preparation of the Thesis

1. Renner, K., Yang, M-S., Móczó J., Choi, H-J., Pukánszky, B.: Analysis of the debonding process in polypropylene model composites, *Eur. Polym. J.* **41**, 2520-2529 (2005)
2. Renner, K., Henning, S., Móczó, J., Yang, M-S., Choi, H-J., Pukánszky, B: Micromechanical deformation processes in PA/layered silicate nanocomposites: correlation of structure and properties, *Polym. Eng. Sci.* **47**, 1235-1245 (2007)
3. Renner, K., Móczó, J., Pukánszky, B: Deformation and failure of PP composites reinforced with lignocellulosic fibers: Effect of inherent strength of the particles, *Compos. Sci. Technol.* **69**, 1653-1659 (2009)
4. Renner, K., Móczó, J., Suba, P., Pukánszky, B: Micromechanical deformations in PP/Lignocellulosic filler composites: effect of matrix properties *Compos Sci Technol* (accepted).
5. Renner, K., Kenyó, Cs., Móczó, J., Pukánszky, B: Micromechanical deformation processes in PP/wood composites: particle characteristics, adhesion, mechanisms, *Composites Part A* (submitted)
6. Renner, K., Móczó, J., Vörös, G., Pukánszky, B: Quantitative determination of interfacial adhesion in composites with strong bonding *Macromol Rapid Comm* (submitted)
7. Renner, K., Móczó, J., Pukánszky, B: Micromechanical Deformations in Particulate filled Polymers: *The Effect of Adhesion, Conference proceedings of the 17th International Conference on Composite Materials*, (2009)
8. Renner, K., Móczó, J., Pukánszky, B.: Mikromechanikai deformációs folyamatok akusztikus emissziós vizsgálata poliamid nanokompozitokban, *Műanyag Gumi*, **42**, 443-448 (2005)

Other publications

1. Dányádi, L., Renner, K., Szabó, Z., Nagy, G., Móczó, J., Pukánszky, B: Wood flour filled PP composites: adhesion, deformation, failure. *Polym. Advan. Technol.* **17**, 967-974 (2006)
2. Dányádi, L., Renner, K., Móczó, J., Pukánszky, B: Wood flour filled PP composites: interfacial adhesion and micromechanical deformations, *Polym. Eng. Sci.* **47**, 1246-1255 (2007)
3. Dominkovics, Z., Renner, K., Pukánszky, B. Jr., Pukánszky, B.: Quantitative characterization of the structure of PP/layered silicate nanocomposites at various length scales, *Macromol. Symposia*: 267, 52-56 (2008)

4. Jerabek, M., Major, Z., Renner, K., Móczó, J., Pukánszky, B.: Particle filled polypropylene composites - micromechanical deformations and interfacial failure, *Polymer* (submitted)
5. Sudár, A.; Renner, K.; Móczó, J.; Pukánszky, B.: PP/üvegyöngy kompozitok: deformációs jellemzők és határfelületi kölcsönhatások, *Műanyag Gumi* **44**, 305-310 (2007)
6. Renner, K., Móczó, J., Pukánszky, B.: Mikromechanikai deformációs folyamatok társított polimerekben, *Magyar Kémiai folyóirat*
7. Gábor, Á., Faludi, G., Imre, B., Renner, K., Móczó, J., Pukánszky, B.: Mikromechanikai deformációs folyamatok politejsav alapú biokompozitokban, *Műanyag és Gumi* **46**, 445-448 (2009)
8. Renner, K.: Heterogén polimer rendszerek akusztikus emissziós vizsgálata, *Műanyagipari szemle*, (2006)
9. Renner, K., Móczó, J., Pukánszky, B.: Mikropórusos filmek alapanyagának fejlesztése, *Műanyag és Gumiipari Évkönyv*, 11-14 (2005)

Conference presentations

1. Pozsgay, A., Móczó, J., Renner, K., Pukánszky, B.: Deformation mechanism of layered silicate polyamide nanocomposites: effect of interfacial interactions, *NanoPol04*, Smolenice, 13. – 14. December 2005.
2. Renner, K., Yang, M-S., Móczó J., Choi, H-J., Pukánszky, B.: Debonding in PP model composites containing particles of uniform size. Eurofillers 2005, Brugges, 9. – 12. May 2005.
3. Renner, K., Móczó J., Choi, H-J., Pukánszky, B.: Mikromechanikai deformációs folyamatok kontrollált szemcseméretű töltőanyagot tartalmazó PP modell kompozitokban. MTA *Természetes Polimerek és Műanyag Munkabizottsági Ülés*, Budapest, 26. April 2005.
4. Renner, K., Móczó J., Choi, H-J., Pukánszky, B.: A határfelületek elválásának vizsgálata polipropilén modell kompozitokban. MTA *Kutatóközponti Tudományos Napok*, Budapest, 1. June 2005.
5. Renner, K., Móczó J., Hennig, S., Pukánszky, B.: Particulate morphology and exfoliation in PA6/Layered silicate nanocomposites; effect on micromechanical deformation processes. *Polymeric Materials 2005*, Halle, 1. June 2005.
6. Renner, K., Yang, M-S., Móczó J., Choi, H-J., Pukánszky, B.: Debonding in PP model composites containing particles of uniform size. *Workshop on Composite on the base of PP with difference type and size of CaCO₃, possibilities of control their physical-mechanical properties with emphasis on fracture toughness*. Brno, 2. June 2005.

-
7. Renner, K., Yang, M-S., Móczó J., Choi, H-J., Pukánszky, B.: Határfelületek elválásának vizsgálata polipropilén modell kompozitokban. Doktoráns Konferencia 2006, Budapest 7. February 2006.
 8. Renner, K., Móczó, J., Pukánszky, B.: Mikormechanikai deformációs folyamatok poliamid nanokompozitokban. MTA *KK Anyag- és Környezetkémiai Intézet szemináriuma*, Budapest, 11. April 2006.
 9. Renner, K., Móczó, J., Pukánszky, B.: Mikromechanikai deformációs folyamatok poliamid rétegszilikát nanokompozitokban. *IX. Doktori Iskola*, Tahi, 24. – 25. April 2006.
 10. Móczó, J., Dányádi, L., Renner, K., Pukánszky, B.: Mikromechanikai deformációs folyamatok faliszt töltőanyagot tartalmazó polimer kompozitokban. MTA *Kutatóközponti Tudományos Napok*, Budapest, 18. May 2006.
 11. Klébert, Sz., Dányádi, L., Renner, K., Móczó, J., Pukánszky, B.: Wood flour reinforced PP composites, *International Scientific Advisory Board*, MTA KK AKI, Budapest, 7. – 8. June 2006.
 12. Renner, K., Százdí, L., Móczó, J., Pukánszky, B.: Structure and deformation of layered silicate polymer nanocomposites. *Advanced Polymeric Materials*, Bratislava, 11. – 15. June 2006.
 13. Renner, K., Dányádi, L., Móczó, J., Pukánszky, B.: Wood flour filled polypropylene composites: interfacial interactions and micromechanical deformations. *Advanced Polymeric Materials*, Bratislava, 11. – 15. June 2006.
 14. Renner, K., Móczó, J., Pukánszky, B.: Micromechanical deformation processes in PP-based composites. *8th Austrian Polymer Meeting 2006 „The Chain of Knowledge –From Catalyst to Application“*, Linz, 20. – 22. September 2006.
 15. Dányádi, L., Renner, K., Móczó, J., Pukánszky, B.: Mikromechanikai deformációk faliszt erősítésű PP kompozitokban, MTA *Természetes Polimerek Munkabizottsága*, Budapest, 3. November 2006.
 16. Fekete, E., Kovács, J., Móczó, J., Renner, K., Pukánszky, B.: Surface characterization of coated and uncoated fillers, *Eurofillers 2007*, August. 26-30, 2007. Zalakaros, Hungary
 17. Renner, K., Móczó, J., Pukánszky, B.: Effect of component properties and adhesion on the deformation behavior of heterogeneous polymers, *Eurofillers 2007*, August. 26-30, 2007. Zalakaros, Hungary
 18. Xiao, H., Liu, H., Yi, W., Pukánszky, B., Móczó, J., Renner, K.: Investigation of nanoparticles modification and mechanical properties of polypropylene/nanoparticles composites, *Eurofillers 2007*, August. 26-30, 2007. Zalakaros, Hungary
 19. Renner, K., Móczó, J., Pukánszky, B.: Comparison of the micromechanical deformations of wood and wood flour filled composites, *Eurofillers 2007*, August. 26-30, 2007. Zalakaros, Hungary

20. Renner, K., Móczó, J., Kabe, K., Pukánszky, B.: Micromechanical deformation processes in particulate filled elastomers, *Eurofillers 2007*, August. 26-30, 2007. Zalakaros, Hungary
21. Fekete, E., Móczó, J., Kovács, J., Renner, K., Pukánszky, B.: Surface characterization of coated and uncoated fillers, *Eurofiller' 2007 Conference*, August 26-30, 2007. Zalakaros, Hungary
22. Renner, K., Móczó, J., Pukánszky, B.: Micromechanical deformation processes in wood flour filled PP composites, *3rd China-Europe Symposium Processing and Properties of Reinforced Polymers*, Budapest, 11-15 June, 2007, Hungary
23. Renner Károly, Móczó János, Pukánszky Béla: Heterogén polimer rendszerek mikromechanikai deformációs folyamatainak vizsgálata, *VII. Téli iskola*, Balatonfüred, 27. January 2007.
24. Renner, K., Yang, M-S., Móczó J., Choi, H-J., Pukánszky, B.: Mikromechanikai deformációs folyamatok faliszt töltőanyagot tartalmazó PP kompozitokban. *Doktoráns Konferencia 2007*, Budapest 7. February 2007.
25. Sudár András, Dányádi Livia, Renner Károly, Móczó János, Pukánszky Béla: Faliszt erősítésű PP kompozitok, *MTA Műanyag és Természetes Polimerek Munkabizottsági ülés*, Budapest 12. April 2007.
26. Renner Károly, Móczó János, Pukánszky Béla: Mikromechanikai deformációs folyamatok heterogén polimer rendszerekben, *Matematikai és Természettudományi Kuratórium Fiatal kutatók meghallgatása*, 6. June 2007.
27. Sudár András, Renner Károly, Móczó János, Pukánszky Béla: A komponens tulajdonságok és az adhézió hatása PP/üveggyöngy kompozitok deformációjára, *MTA Anyagtudományi és Technológiai Komplex Bizottsági ülés*, 28. November 2008.
28. Móczó J., Sudár A., Renner K., Dányádi L., Pukánszky B.: A komponenstulajdonságok és az adhézió hatása heterogén polimer rendszerek deformációs folyamataira, *MTA Anyagtudományi Nap*, 11. May 2007.
29. Renner K., Móczó J., Pukánszky B.: Szerkezet-tulajdonság összefüggések faliszt töltőanyagot tartalmazó PP kompozitokban *Doktoráns Konferencia 2008*, Budapest 8. February 2008.
30. Renner K., Móczó J., Pukánszky B.: Micromechanical deformation processes in polypropylene composites *Austrian Slovenien Polymer Meeting 2008*, Graz, Austria 26-28, March 2008.
31. Renner, K., Móczó, J., Pukánszky, B.: Szerkezet-tulajdonság összefüggések faliszt töltőanyagot tartalmazó PP kompozitokban *XI. Doktori Iskola*, Mátrafüred, 21. – 22. April 2008. (invited lecture)
32. Renner, K., Móczó, J., Pukánszky, B.: Deformation and failure of natural fiber reinforced composites; effect of particle characteristics and adhesion, *7th Global WPC and Natural Fibre Composites Congress and Exhibition*, June 18 - 19, 2008, Kassel, Germany.

-
33. Renner, K., Móczó, J., Pukánszky, B.: Debonding in particulate filled polymers: effect of specific surface area and adhesion, *Polymeric Materials P2008*, 24. - 26. September 2008, Halle, Germany.
 34. Renner K., Móczó J., Pukánszky B.: Határfelületek elválása töltött polimer rendszerek-ben; a fajlagos felület és az adhézió hatása. *MTA KK AKI Szeminárium 2008*, Budapest 30. October 2008.
 35. Móczó J., Renner K., Pukánszky B.: Kompozitok mikromechanikai deformációs folyamatainak vizsgálata akusztikus emisszióval. *MTA Anyagtudományi és Technológiai Komplex Bizottság, Anyagtudományi Nap*, Budapest, 15. May 2009.
 36. Renner, K., Móczó, J., Pukánszky, B.: Micromechanical Deformation Processes in Polymer Composites: Measurement and Practical Consequences, *Advances in Polymer Science and Technology (APST) 1*, 8. - 10. July 2009, Linz, Austria.
 37. Renner, K., Móczó, J., Pukánszky, B.: Wood Flour Reinforced Thermoplastics: Structure, Micromechanical Deformations, Properties, *Eurofillers 2009*, 21. - 25. July 2009, Alessandria, Italy.
 38. Móczó, J., Kenyó, Cs., Renner, K., Pukánszky, B.: PVC/natural fiber reinforced composites: interfacial interactions and micromechanical deformations, *Eurofillers 2009*, 21. - 25. July 2009, Alessandria, Italy.
 39. Renner, K., Móczó, J., Pukánszky, B.: Deformation and failure of PP/wood composites, effect of inherent strength of wood, *Eurofillers 2009*, 21. - 25. July 2009, Alessandria, Italy. (poster award)
 40. Renner, K., Móczó, J., Pukánszky, B.: Micromechanical Deformations in Particulate filled Polymers: The Effect of Interfacial Adhesion, *17th International Conference on Composite Materials*, 27. - 31. July 2009, Edinburgh, UK.
 41. Renner, K., Móczó, J., Pukánszky, B.: Természetes szálak szilárdságának hatása kompozitok deformációs folyamataira, *MTA Kutatóközponti Tudományos Napok*, Budapest, 24 - 26. November 2009. (Young scientist award)

Nyilatkozat

Alulírott Renner Károly kijelentem, hogy ezt a doktori értekezést magam készítettem és abban csak a megadott forrásokat használtam fel. Minden olyan részt, amelyet szó szerint, vagy azonos tartalomban, de átfogalmazva más forrásból átvettem, egyértelműen, a forrás megadásával megjelöltem.

Budapest, 2010. február 21.

Renner Károly